SOURCE APPORTIONMENT OF THE AIR QUALITY ON SABLE ISLAND

by

Alex Hayes

Submitted in partial fulfilment of the requirements
for the degree of Master of Applied Science

at

Dalhousie University
Halifax, Nova Scotia
March 2014

TABLE OF CONTENTS

LIST OF TABLES

LIST OF FIGURES

ABSTRACT

Air pollution can have varying health and environmental impacts which are not limited to the point of release, making it important to identify and quantify sources of air pollution and their fate and transport globally. Most studies are conducted in urban areas with few studies taking place at sea or near oil and gas (O&G) production facilities, resulting in a paucity of data. This study aims to examine the different sources of air pollution affecting the air quality on Sable Island, a remote marine site, with the aim of better understanding the impacts of emissions from nearby offshore O&G activities and continental outflow. Air pollution data obtained from Sable Island between May 7th and October 30th of 2013 was used to perform statistical analysis, source apportionment, and meteorological analysis. The models used to identify and quantify sources of air pollution included the National Oceanic and Atmospheric Administration (NOAA) HYbrid Single-Particle Lagrangian Integrated Trajectory (HYSPLIT) model and the United States Environmental Protection Agency (USEPA) Positive Matrix Factorization (PMF) model v 3.0.2.2. The air pollutants measured and their temporal resolution were non-methane hydrocarbons (NMHCs), black carbon (BC), hydrogen sulfide (H_2S), mono-nitrogen oxides (NO_x), nitrogen oxide (NO), nitrogen dioxide (NO_2), ozone (O_3), particulate matter with a median aerodynamic diamer less than or equal to 2.5 microns ($PM_{2.5}$), and sulphur dioxide (SO_2). NMHCs and BC measurements were averaged every 5 minutes while the remaining data was averaged hourly. The average concentration of O_3 (30.4 ppb) was below the annual average concentration of O_3 in ambient air in Canada which was 33 ppb in 2011 (Environment Canada, 2013) while all of the average and maximum concentrations for pollutants governed by The Air Quality Regulations from Nova Scotia Environment (including O_3) fell below maximum permissible levels. The mean values (min:max) for NMHC, BC, $PM_{2.5}$, SO_2, H_2S, O_3, NO, NO_x, and NO_2 were 0.034 ppm (0.0 : 1.13), 0.092 $\mu g/m^3$ (0.0 : 13), 14.1 $\mu g/m^3$ (0 : 43), 0.168 ppb (0.0 : 3), 0.361ppb (0.0 : 13.7), 30.4 ppb (8.24 : 61.1), 2.17 ppb (0.0 : 3.5), 1.12 ppb (0.0 : 28.7), 0.998 ppb (0.0 : 14.6). During this study, a new gas production facility came on line on July 22nd 2013. Significant differences ($P<0.05$) between concentrations of BC, $PM_{2.5}$, SO_2, H_2S, O3, NO, NO_x, and NO_2 were seen after July 22nd 2013. The median values and upper percentiles for BC, $PM_{2.5}$, NO, and NO_x show decreases after July 22nd, while those for SO_2, H_2S, and NO_2 show increases. Due to the strong correlation of SO_2 and H_2S with offshore oil and gas activities found through PMF modelling and a spearman rank order correlation this implies the new off-shore gas production did have an impact on the air quality on Sable Island. The PMF model run identified 4 factors contributing to the air quality on Sable Island but source contributions could not be determined due to insufficient $PM_{2.5}$ and VOC speciation data. Long range transport, off-gassing from offshore O&G activities (with contributions from phytoplankton blooms), flaring, and on-site combustion were the sources associated with these 4 factors. It was recommended that sampling on Sable Island continue as further characterization of the air quality would be beneficial to more fully understanding sources and sinks of air pollution on the island and the surrounding Scotian Shelf.

LIST OF ABBREVIATIONS USED

CH – Hydrocarbons

CH_4 – Methane

Cl – Chloride

CNSOPB - Canada-Nova Scotia Offshore Petroleum Board

CO – Carbon monoxide

CO_2 – Carbon dioxide

CMB – Chemical Mass Balance

$d^{13}C$ – Carbon 13

$d^{18}O$ – Delta-O-18

EA – Environmental Assessment

EC – Environment Canada

H_2 – Hydrogen

H_2S – Hydrogen Sulfide

H_2SO_4 – Sulphuric acid

HNO_3 – Nitric acid

HO_x – Hydroxy radicals (HO, RO2 and HO2)

HYSPLIT – HYbrid Single-Particle Lagrangian Integrated Trajectory

NASA - National Aeronautics and Space Administration

Na – Sodium

Ni - Nickel

NO – Nitrogen oxide

NO_x – Mono-nitrogen oxides (including NO and NO_2)

NO_2 – Nitrogen dioxide

NO_3 - Nitrates

N_2O – Nitrous oxide

NOAA – National Oceanic and Atmospheric Administration

NSE – Nova Scotia Environment

O_3 – Ozone

OC – Organic Carbon

OH – Hydroxide

O&G – Oil and gas

PCA/APCS – Principal Component Analysis/Absolute Principle Component Scores

ppb – Parts per billion

pphm – Parts per hundred million

PM – Particulate matter

$PM_{2.5}$ – Particulate matter with a median aerodynamic diamer less than or equal to 2.5 microns

PM_{10} – Particulate matter with a mean aerodynamic diameter of less than or equal to 10 μm

PMF – Positive Matrix Factorization

ppm – Parts per million

RO_2 – Peroxyl radical

RH – Used to denote a hydroxy radical

Rn – Radon

SF_6 – Sulphur Hexafluoride

SOA – Secondary organic aerosols

SO_2 – Sulphur dioxide

SO_4 – Sulphates

SOM – Seconary organic matter

USDA - United States Department of Agriculture

USEPA – United States Environmental Protection Agency

UV – Ultraviolet

V – Vanadium

VOC – Volatile organic compound

ACKNOWLEDGEMENTS

I would like to say a big thank you to my supervisor Dr. Mark Gibson for his support, expertise, and the opportunity to be a part of the Sable Island study. I would also like to thank the current and past members of the AFRG research group who have helped me along the way, my supervisory committee members Dr. Susanne Craig and Dr. Rob Jamieson, Graduate Programs Administrative Secretary Paula McKenna, the Environmental Studies Research Fund, Nova Scotia Environment, and Environment/Parks Canada for making this study possible, as well as the many others who have lent a hand along the way. You all made this process much easier and more enjoyable.

CHAPTER 1 INTRODUCTION

1.1 Structure of the Thesis

There are 6 sections or chapters outlining the study. Chapter 1 outlines the rationale and objectives of the study. Chapter 2 consists of a literature review covering background on Sable Island, particulate matter, volatile organic compounds (VOCs), oil and gas (O&G) emissions, source apportionment (receptor modelling), the importance of meteorological conditions, and HYSPLIT back trajectories. Chapter 3 covers the materials and methods employed in the study, Chapter 4 the results, Chapter 5 the discussion of the results, and Chapter 6 consists of the conclusion and recommendations. Additional information from the study is included in the appendix.

1.2 Rationale and Objectives of the Study

Air pollution can have varied and severe effects on health, ecosystems, and climate. Its impacts are also not limited to the point of release with air quality transcending all scales in the atmosphere from local to global with feedbacks and interactions between all levels (Monks et al., 2009). The World Health Organization estimates that 2.4 million people die each year from causes directly attributable to air pollution (WHO, 2002). It is therefore important to identify and quantify sources of air pollution and their fate and transport globally (Monks et al, 2009). Most studies are conducted in urban areas with few studies taking place at sea or near O&G production facilities. Therefore, there is a paucity of data related to air emissions in marine locations impacted by O&G production (Gibson et al., 2009a, Waugh et al., 2010).

It has been established that further research is needed on the contribution of particulate matter with a mean aerodynamic diameter of 2.5 microns or less ($PM_{2.5}$) and VOCs to the air quality in environments such as the Atlantic Marine Airshed (Gibson et al., 2009a). The relative isolation of Sable Island from local point sources make it a site that is largely marine influenced and it can be considered to be an area transitioning from the polluted continent to a clean marine environment (Duderstadt et al., 1998) making it an ideal location for examining these impacts. Its remote location also makes it an ideal site for looking at the impact of nearby offshore oil and gas activities (Waugh et al., 2010).

Sable Island recently became a National Park (Sable island national park reserve: Park establishment, 2012). This new status only increases the need to improve air quality surveillance and our understanding of pollution sources in order to better protect this fragile ecosystem (Waugh et al., 2010).

The objective of the study is to:

- Apportion the different sources of both gaseous and particulate air pollution affecting the air quality on Sable Island; and
- Investigate the impact of bringing a new O&G platform online through to production.

The results of the study will allow for increased awareness of the main pollution sources and their impacts that can then be used to make informed policy decisions and aid in pollution prevention planning.

The study utilized the different methods outlined below:

- Real time in situ air pollution sampling;
- Statistical analysis; and
- Positive Matrix Factorization (PMF) modelling.

Using the data gathered from these methods, source apportionment; or receptor modelling as it is often called, will be used to accomplish the goal of identifying the various pollution sources impacting Sable Island.

CHAPTER 2 LITERATURE REVIEW

2.1 Sable Island

Sable Island is located in the Atlantic Ocean approximately 300 km southeast of Halifax, Nova Scotia, Canada. A sand bar approximately 42 km long, it has long been known for its shipwrecks (over 350 recorded) and wild horses (Sable island: A story of survival, 2001). The establishment of the Sable Island National Park Reserve made Sable Island the 43rd national park in Canada (Sable island national park reserve: Park establishment, 2012). Figure 1 shows the location of Sable Island in reference to Atlantic Canada with inlays showing the distance from Halifax and the size of the Island.

Figure 1. Map showing the location of Sable Island.

Due to its location and relative isolation from local point sources Sable Island is an example of a site that is largely influenced by marine emissions (sea spray). The island can be considered to be in an area transitioning from the polluted continent to a clean marine environment (Duderstadt et al., 1998). As a result it has been the focus of various air quality related research as far back as the 1960's (Waugh et al., 2010). Local sources for the island do however exist and include offshore O&G production, long-range transport (largely from the Great Lakes and US Eastern Seaboard regions), and other localized emissions. Other local emissions include transportation emissions to and from both the island and offshore facilities by aircraft and ships, emissions from passing ships, and localized emissions on the island itself related to electricity generation and waste incineration (Waugh et al., 2010).

Offshore petroleum activities can result in emissions of NO_x, SO_2, VOCs, airborne particulate matter (PM), reduced sulphur compounds, e.g. H_2S, and greenhouse gases such as carbon dioxide (CO_2) and methane (CH_4) (Waugh et al., 2010). Petroleum activities have been ongoing in the area surrounding Sable Island since 1992. The Cohasset-Panuke project ran from 1992-1999 and was operated by Pan Canadian (now Encana) and Lasmo. The Sable Offshore Energy Project began in 1999 and is operated by Exxon Mobil and partners. It consists of five gas production platforms which can be seen in Figure 2. The Deep Panuke Offshore Gas Development Project is run by Encana Corporation and was brought on-line on July 22nd 2013. It can also be seen in Figure 2 (Offshore projects, 2013).

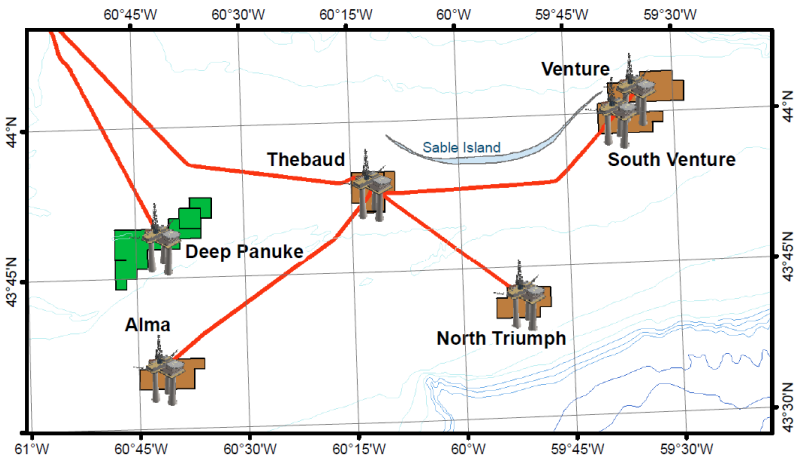

Figure 2. Offshore oil and gas activities near Sable Island (Offshore Projects, 2013).

2.2 Background Literature

A report published by Waugh et al. 2010 summarized the initial set-up and the results from the Sable Island Air Monitoring Station over the first four years of operation. This station was set up as part of the Nova Scotia Ambient Air Quality Monitoring Network. The study consisted of monitoring for NO_x, SO_2, H_2S, and $PM_{2.5}$. Environment Canada used the opportunity provided by the study to also monitor for O_3 as well as greenhouse gases such as carbon monoxide (CO), CO_2, and CH_4. The purpose of the study was to determine the impact of contaminant emissions from petroleum related activities and to report this data to a number of provincial national, and international monitoring programs. The study concluded that it was hard to determine the impact of local sources (offshore oil and gas activities included) due to the lack of information on specific local emission sources. The lack of speciated sample data and limited use of smoke observation data from the Thebaud offshore platform also posed issues, and it was

suggested that additional information from project partners would be needed to determine the impact of local sources on Sable Island's air quality.

A study done by Duderstadt et al., 1998 looked at the instantaneous photochemical production and loss rates of ozone using a numerical photochemical model and three weeks' of summertime surface based chemical and meteorological observations on Sable Island. Meteorological observations included continuous measurements of temperature, relative humidity, UV radiation, wind speed, wind direction, standard meteorological hourly surface observations, and twice daily upper air sonde observations. Chemical measurements included NO, NO_2, total reactive nitrogen, O_3, CO, various hydrocarbons, aerosol measurements, and speciated chlorinated compounds. The study concluded that background photochemistry of the island was impacted by polluted continental plumes with nitrogen oxides, ozone, non-methane hydrocarbons, and solar intensity determined by cloud cover having the greatest impact. The model outputs agreed well with the measured values although issues were posed when intermittent cloud cover, fog, and/or rain were present. This showed the influence of cloud processes on the air parcels reaching Sable.

2.3 Available Data

Monitoring by Nova Scotia Environment on Sable Island has been ongoing since 2003 as part of the Nova Scotia Ambient Air Quality Monitoring Network. They currently measure for hydrocarbons (CH), CO, CO_2, H_2S, NO_x, NO, NO_2, O_3, $PM_{2.5}$, Radon (Rn), SO_2, weather data, and wind speed (Nova Scotia Ambient Air Quality Monitoring Network, 2010). Flask sampling for carbon 13 ($d^{13}C$), and delta-O-18 ($d^{18}O$) in CO, CH_4, CO, CO_2, nitrous oxide (N_2O), sulphur hexafluoride (SF_6), and hydrogen (H_2) was previously performed on the Island but is no longer taking place.

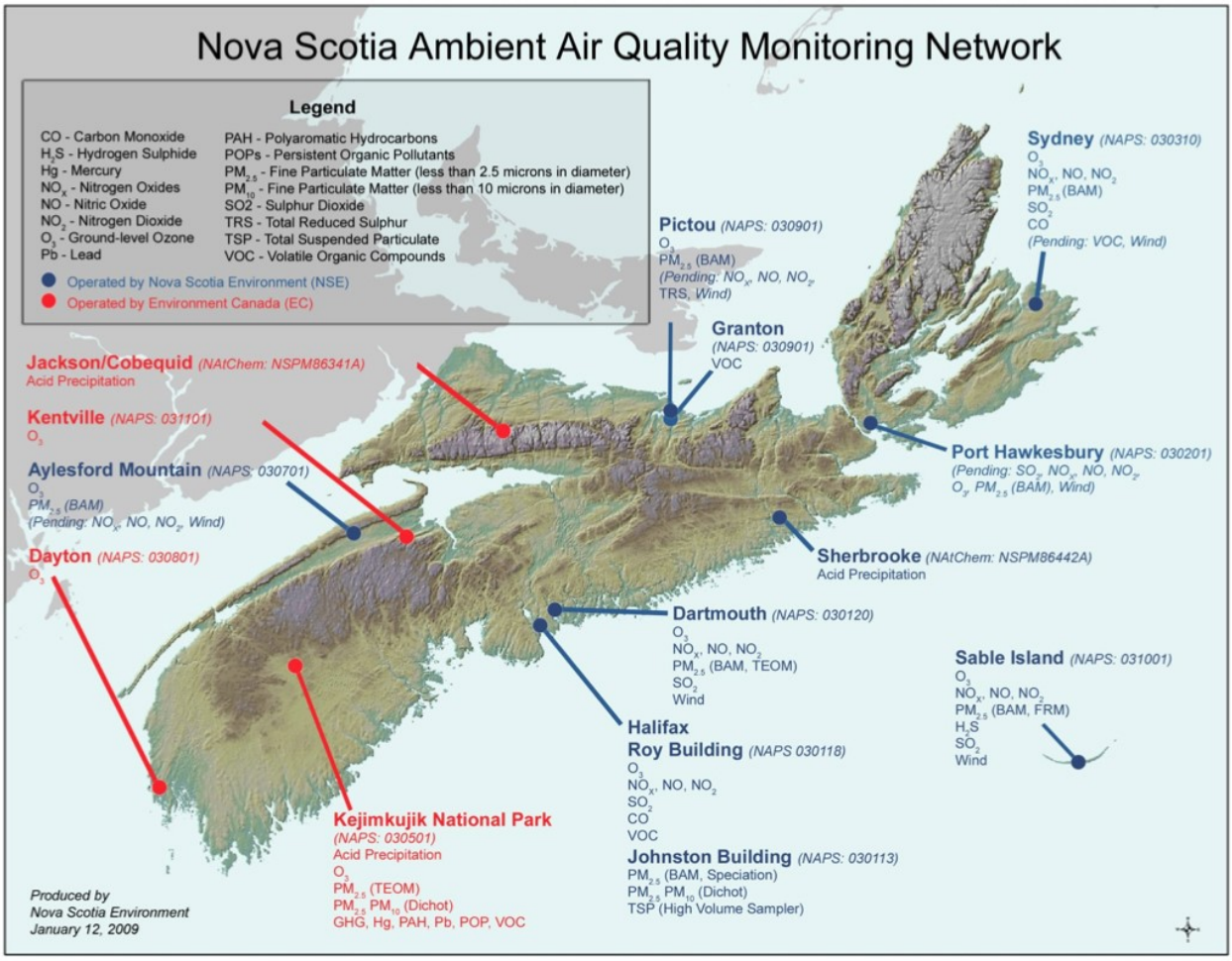

Figure 3. Nova Scotia Ambient Air Quality Monitoring Network (Nova Scotia Ambient Air Quality Monitoring Network, 2010).

2.4 Particulate Matter

Airborne particulates consist of a mixture of both solid and liquid particles and can consist of many different chemical species such as sulphates (SO_4), nitrates (NO_3), chloride (Cl), sodium (Na), BC, organic carbon (OC), elements common to the hydrosphere and lithosphere and trace aliphatic and aromatic organic species, e.g. dodecane and polycyclic hydrocarbons (Gibson et al., 2013). Particulates are classified according to size range (Gibson et al., 2009b). Those with a mean aerodynamic diameter of less than or equal to 10 μm are designated as PM_{10} and those with a mean aerodynamic diameter of less than or equal to 2.5 μm are designated as $PM_{2.5}$ (Harrison et al., 1997; Gibson et al., 2009b; Gibson et al., 2013).

2.4.1 Environmental Effects

Emissions of sulphur and nitrogen gaseous and particulate matter species, e.g. SO_2, NO_2, nitric acid (HNO_3) and sulphuric acid (H_2SO_4) are known to have a direct negative impact on plant species such as lichen and lichen abundance (Gibson et al., 2013a). NO_2 and SO_2 can impact lichen directly while their secondary products (HNO_3 and H_2SO_4) can acidify and damage tree bark (Will-Wolf and Neitlich, 2010). In this way secondary particulate and liquid phase pollutants formed from SO_2 and NO_2 can have the largest impact on sensitive sentinel species such as lichen (Bell and Treshow, 2003; Conti and Cecchetti, 2001).

Aerosol deposition can cause damage such as dissolving limestone and soiling (soot stains) to buildings and other man made materials (Querol et al., 2004). The deposition of acidified aerosols can rapidly accelerate the degradation of building materials and occurs

when deposited particles adsorb or absorb acidic gases from primary pollutants such as SO_2 and NO_2. These acid forming aerosols limit the lifetime of paints and can cause soiling of both painted surfaces and other building materials (Bhattacharjee, et al., 1999). Acid deposition can also effect plant life and aquatic environments (Bell, & Treshow., 2003; Bhattacharjee, et al., 1999; Dillon, et al., 1984). One of the biggest issues is that pollution emitted by a given receptor can be transported long distances and can have negative impacts on sites both near and far (Gibson et al., 2009b). In Europe it is estimated that approximately half of the pollution emitted crosses borders and negatively impacts neighbouring countries (Levy, 1993;Gibson et al., 2009b; Querol et al., 2004). Aerosols can cause changes in the chemistry of aquatic environments such as oceans and lakes with the impacts varying depending on the type of pollution and the ecosystem being affected. Some examples of impacts include changes in naturally occurring organic acidity, depletion of base cation reserves from soils, and changes in nitrogen dynamics (Bell, & Treshow., 2003; Bhattacharjee, et al., 1999). Collectively these air pollution impacts can negatively influence native species such as fish populations. Acid deposition can also impact trees and plant life through acidification of soils and altering of the naturally occurring soil chemistry which in turn negatively impacts the soil nutrition (Bhattacharjee, et al., 1999).

Through the scattering and absorption of sunlight aerosols can directly influence climate both positively and negatively (Solomon, et al., 2007). The magnitude of this forcing depends on the size, abundance, and optical properties of the aerosol particles in question as well as the solar zenith angle of the sun (Solomon, et al., 2007). Scattering of light by particles generally causes UV radiation to be reflected away from the planet and results in

less radiation reaching Earth's surface. This causes a cooling effect. As particle absorbance increases this effect changes. Some aerosols absorb light, which has a net warming effect on climate (Seinfeld & Pandis, 2006; Solomon, et al., 2007). The threshold where particles change from having a warming or a cooling effect depends on particle size, the albedo of the underlying surface, mixing rates of absorbing and reflective particles in the outmost layer of the particle, and many other factors (Seinfeld & Pandis, 2006).

Aerosols can also indirectly influence climate by causing the formation of cloud condensation nuclei. Cloud condensation nuclei formed from aerosols aid in the formation of clouds that have larger number concentrations of water droplets than normal clouds. These droplets also have smaller radii, resulting in clouds with a higher albedo. This higher albedo results in the reflection of greater amounts of solar radiation and causes cooling (Senfield & Pandis, 2006).

2.4.2 Health Effects

Air pollution episodes such as the Muesse Valley incident of 1930, Donora Pensylvania in 1948, and London in December of 1952 undoubtedly showed the cause and effect relationship between air pollution events and mortality/human health. Epidemiological studies followed soon after and can be dated from the London episode (Holgate et al., 1999). Contemporary epidemiological studies such as Dockery et al. (1993), Evans et al. (1984), and Shwartz et al. (1990) have established a direct link between mortality rates and air pollution in US cities as far back as the 1980's.

Dockery et al. (1993) investigated the link between air pollution and mortality rates in six US cities. Previous studies had reported that daily mortality rates could be associated with changes in air quality in London (Schwartz et al., 1990) and other US cities such as Philadelphia (Schwartz et al., 1992). The association between particulate air pollution and mortality rates had been previously established for quite some time through studies such as Evans et al. (1984). However, many of these studies were criticized as they did not correct for cigarette smoking. The study in question looked to estimate the effects of air quality on mortality rates within a well-characterized group of individuals while taking into account smoking status, sex, age, and other risk factors. The study population was obtained from the communities of Watertown, Massachusetts; Harriman, Tennessee (including Kingston); St. Louis; Steubenville, Ohio; Portage, Wisconsin (Wyocena and Pardeeville included); and Topeka, Kansas. The population consisted of 8,111 white individuals between the ages of 25 and 74 who had undergone spirometric testing (a form of lung capacity testing) and completed a standardized questionnaire. The status of each subject was determined annually and the National Death Index checked from 1979 through to 1989. Causes of death were determined from death certificates where possible. Air quality monitoring was performed at a centrally located site in each community. 24-hour integrated sampling of ambient concentrations for total suspended particulate matter, sulphur dioxide, ozone, and suspended sulfates were measured. For total suspended particulate matter, both fine and inhalable particles were monitored. Cox proportional hazards regressions models were then used to assess the effects of air pollution. This involved classifying study participants into age and sex groups as well as applying variables for hazards such as smoking. The effect of air pollution on mortality

rates was then looked at in two ways. It was first estimated including hazard variables and compared to mean pollution levels in each city. Next, city specific pollution levels were included as hazard variables in running the Cox regression model.

It was found that smoking, lack of a high school education, and increased body mass index all increased mortality rates, but after adjusting for these variables significant differences between the six cities still existed. Significant associations between mortality and inhalable, fine, or sulfate particles were found, while correlations with total suspended particles, sulphur and nitrogen dioxide levels, and the acidity of the aerosol were comparatively weak. Only small differences in ozone levels between the six cities existed, making it impossible to determine the impact on mortality rates. It was found that the effect of air pollution on mortality rates was somewhat stronger within subgroups that had occupational exposure to dust, gases or fumes, but positive associations were noted for all subgroups.

The results of the study performed by Dockery et al., (1993) played a key role in establishing the current U.S. ambient air quality objective for fine particles. Because of this, an independent study was performed to validate the results. The study was done in 2 parts. Krewski et al., (2005b) looked to validate the original study by replicating the original results and performing a detailed statistical audit. No discrepancies were identified in the original questionnaires and death certificates with the exception of minor differences in those related to occupational exposure to dust. A computer programming problem was identified that had resulted in the loss of approximately 1% of the reported person-years of follow up. The original six cities study was updated to include this and the results of the study were recreated. The original results were re-produced almost

exactly, including the 26% increase in mortality in Stubenville Ohio (the most polluted city). Krewski et al., (2005b) determined that the discrepancies found in the original study by Dockery et al., 1993 were not of epidemiologic importance and the risk estimates and conclusions drawn were still valid.

In the second part of the study, Krewski et al., (2005a) looked to test the results of the original study by Dockery et al., (1993) by conducting a wide range of sensitivity analyses. Alternative risk models and their impact on estimates of risk were performed taking into account new covariates not included in the original study. This allowed for the identification of covariates that could potentially confound associations between air pollution and mortality. It was found that few subjects changed their original city of residence, therefore limiting the ability to identify critical exposure time windows. It was also found that the risk of mortality was increased when living in a city with higher levels of air pollution, but that occupational exposure likely played a larger role in this risk. As a result, risk factors generally decreased with higher levels of education (it can be assumed that individuals with higher education tend to perform jobs with lower exposure levels). In the end it was concluded that the study by Krewski et al., (2005a) supported the results of the original study and showed the robustness of the conclusions when examined using alternative methods.

Since these studies, interest in particulate matter has only continued to grow as the potential health effects associated with exposure have become increasingly apparent. Acute effects for fine particulate matter (PM) associated with air pollution have been established in studies such as Dominici et al. (2006) and chronic effects in studies such as Pope et al. (2002). Acute effects include but are not limited to cardiovascular and

respiratory distress (Dominici et al., 2006) as well as impaired vascular function and increased diastolic blood pressure (Brook et al., 2009). Chronic effects can include lung cancer and cardiopulmonary mortality (Pope et al., 2002). Of particular concern is the impact of $PM_{2.5}$. Due to their small size they can be transported long distances and can also penetrate deep into the lungs (Harrison et al., 1997). A linear association between airborne concentrations and cardio pulmonary mortality and morbidity has been established in the past by multiple studies (Dockery et al., 2007; Stieb et al., 2002; Donaldson et al., 2001). The findings of the study are especially significant given that there does not appear to be a safe lower limit for negative impacts (Stieb et al., 2008). With this in mind it must be remembered that the impacts on human health can vary depending on both the size fraction, particle counts, and the chemical make-up of the particulates (Mills et al., 2008).

2.4.3 Sources

PM can come from anthropogenic, biogenic, geogenic, primary and secondary, local, or long range sources (Gibson et al., 2009b). Some primary sources include sea spray, fossil fuel combustion, windblown dust, and dust from road transport (Pilling et al., 2005). It is estimated that 32% of the mass flux in terms of sea salt production comes from the Northern Hemisphere (O'Dowd et al., 2007). Secondary particulate components such as SO_4 and NO_3 are formed from the oxidation and chemical transformation of primary SO_2 and NO_x gaseous emissions (Pilling et al., 2005). Some of the major sources in nearby Nova Scotia are power generation, both domestic and industrial space heating using both fossil fuels and biomass, construction activities, and ship emissions (Gibson et al.,

2013b). Approximately 12,000 wildfires every year in North America impact concentrations of surface level $PM_{2.5}$ at long-distances (Gibson et al., 2013a; Palmer et al., 2013; Franklin et al., 2014).

2.5 Volatile Organic Compounds (VOCs)

VOCs are a group of carbon containing organic chemicals that are known to participate in photochemical reactions that can form secondary gases and $PM_{2.5}$ species such as oxalate and formate (Environment Canada, 2012). Of particular interest is the effect VOCs have on ozone formation and related reactions in the troposphere, but they can also have many negative health impacts (Dohoo et al., 2013). Local and long range sources, both biogenic and anthropogenic, exist and there are currently substantial gaps in our understanding of these sources and their relative contributions.

2.5.1 Environmental Effects

Ozone production involves complex chemical reactions, many of which are cyclic, therefore making it difficult to quantify the direct impact of VOCs on ozone formation. However, the impact of VOCs on ozone formation generally increases with their abundance and reactivity with OH (Jacob, 1999). The production of O_3 follows the reaction below.

$$O_3 + h\nu \rightarrow O_2 + O(^1D)$$

$$O(^1D) + M \rightarrow O + M$$

$$H_2O + O(^1D) \rightarrow 2OH$$

Where M represents any atmospheric species that accepts energy in the form of vibrational energy. After this production of HO_x, the chain is propagated by reaction of OH with hydrocarbons (as represented by RH) in the equation below.

$$RH + OH \xrightarrow{O_2} RO_2 + H_2O$$

This RO_2 radical can then go on to produce NO_2 by reaction with NO. The next step of the chain is that NO_2 photolyzes in the presence of oxygen and produces O_3. (Gibson et al., 2009a)

$$RO_2 + NO \rightarrow RO + NO_2$$

$$NO_2 + hv \xrightarrow{O_2} NO + O_3$$

As can be seen, the end result of this set of reactions is that increasing concentrations of VOCs cause an increase in ozone production rates with the impact of individual VOC species depending on their reactivity with OH (Jacob, D.J., 1999; Gibson et al., 2009a).

It has been found through ambient measurements that ozone formation consistently occurs at an increased rate downwind of anthropogenic NO_x and VOC sources but this relationship becomes more complex when the impact of NO_x/VOC concentration ratios on ozone formation is considered. For example, emissions such as those from a power plant that contain low concentrations of VOCs compared to NO_x will initially suppress the formation of O_3 in favor of HNO_3 production. Meanwhile, vehicle emissions (which have higher concentrations of VOCs compared to NO_x) will favor earlier formation of ozone and therefore result in higher concentrations (Ryerson et al., 2003).

Secondary organic aerosols (SOA) can both scatter and absorb solar radiation (Andreae et al., 1997) as well as aid in the formation of cloud condensation nuclei (Novakov et al.,

1993). The combined effect can either positively or negatively influence climate (Pierce and Adams, 2009).

VOCs can increase the formation of SOA and therefore increase the formation of cloud condensation nuclei (Pierce and Adams, 2009). The photooxidation of isoprene, a VOC produced by many terrestrial and marine plants, has been shown to result in the formation of substantial concentrations of SOA (Claeys et al., 2004; Colomb et al., 2009; Shaw et al., 2010).

2.5.2 Health impacts

As previously established through studies such as Dockery et al. (1993), Evans et al. (1984), Shwartz et al. (1990), Krewski et al., (2005), and Krewski et al., (2005b) air pollution can have a negative impact on human health. VOCs specifically are known to cause negative health impacts, with examples including the link between VOCs and chronic respiratory illnesses (Ware et al., 1993). Chronic domestic exposure to VOCs has been shown to increase the risk of asthma in children (Rumchev et al., 2004), and acute effects also exist. A study by Yang et al., (1997) concluded that residents living in a petrochemical-polluted area in Taiwan experienced acute irritative symptoms such as eye irritation, nausea, throat irritation, and chemical odor perception resulting from exposure to VOCs.

2.5.3 Sources

Sources specific to VOCs can include both anthropogenic and natural sources with biogenic sources comprising the majority of VOC emissions within the North American continent. Biogenic sources include soil microbes, vegetation, biomass burning, and lightning (Guenther et al. 2000). Examples of VOCs emitted by these biogenic sources include isoprene, monoterpenes, hydrocarbons, and VOCs (Guenther et al. 2000).

The oceans are a source of non-methane hydrocarbons (NMHCs) from photochemical processes in the water column. The production of many NMHCs show distinct seasonal cycles in surface waters with summer maxima and winter minima (Shaw et al., 2003). In the northwest Atlantic Ocean, massive springtime phytoplankton blooms, dominated by large diatom species (Johnson et al. 2012), occur as a result of a stabilization of the nutrient-rich water column. Throughout the summer, a phytoplankton assemblage dominated by smaller cells (Johnson et al. 2012) is maintained by regenerated nutrients until a secondary autumn bloom occurs due to nutrients being driven upwards as a result of wind driven mixing (Greenan et al. 2004). During the winter months, the water column is mixed and light levels are low, resulting in phytoplankton abundance minimum (Georges et al., 2014). Although the relative oceanic contribution of NMHC's is considered to be minor compared with other terrestrial sources, it is not well quantified or understood and emissions into the atmosphere are considered to be a major loss of oceanic NMHC production (Reimer et al., 2000). Phytoplankton blooms can be a contributor of atmospheric VOC's (Colomb et al., 2008) that would be of concern on Sable Island, with various phytoplankton species being capable of producing isoprene (Shaw et al., 2003). It was found in a paper by Palmer et al., (2005), that global oceanic

emission of isoprene are estimated at 0.1 TgC/yr making the contribution from phytoplankton blooms a source that must be considered. The only known source of this oceanic isoprene flux is phytoplankton blooms (Shaw et al., 2003). The photochemical production of isoprene in phytoplankton is a function of light intensity and temperature and occurs during the growth stage (Shaw et al., 2003). Strong positive correlations between isoprene and bulk chlorophyll concentration, a proxy for phytoplankton biomass, were found in data from surface waters in the East Atlantic and Southern Ocean (Broadgate et al., 1997; Baker et al., 2000). It should be noted that it is possible to measure chlorophyll concentration based on ocean colour. This can be done either in situ or from space using remote sensing techniques (Craig et al., 2012). Ocean colour is directly related to its constituents and many different approaches have been developed to derive water constituents from measurements of ocean colour (Craig et al., 2012). This study will look to employ this in examining the potential contribution of phytoplankton to NHMC concentrations on Sable Island.

Offshore oil and gas activities can have many different sources that result in the release of VOC's into the atmosphere (Beusse et al., 2013) and will be discussed further in Section 2.6. Other than emissions from oil and gas production, anthropogenic VOC sources include vehicle emissions, solvent based products (particularly cleaning products), paints, and many others. The manufacturing of organic chemicals and rubber have been identified as significant sources of VOC's (Piccot et al., 1992).

2.6 Offshore Oil and Gas Production

The production of offshore oil and gas is rapidly expanding on the Scotian Shelf, and the natural gas fields surrounding Sable Island have been the site of offshore activities for many years now. Their location was shown previously in Figure 2. With these activities however, come airborne emissions of pollutants which can be harmful to human health as well as the environment.

2.6.1 Emissions from Offshore Oil and Gas Activities

With increases in offshore oil and natural gas production over the years, a need exists for a thorough understanding of the impacts associated with these activities. In general, there is a need to improve air emissions inventories for the oil and natural gas production sector as found in the report by Beusse et al., (2013) that was performed for the United States Environmental Protection Agency. The recommendations of this report can easily be applied to Canada. Our understanding of emissions from offshore petroleum activities and their impacts are not well understood. This is a clear gap in knowledge that this thesis aims to address.

Offshore oil and gas production activities can result in the emission of greenhouse gases (GHGs), secondary pollutants that act as O_3 precursors, and climate forcing agents (Zahniser, A., 2007, Beusse et al., 2013). The main GHGs associated with offshore oil and gas emissions are CO_2 and CH_4 (Zahniser, A., 2007). Many pollutants involved in the formation of O_3 are emitted through combustion, vented, and fugitive sources. These include N_2O, VOC's, and NO_x (Zahniser, A., 2007; Beusse et al., 2013). Climate forcing agents include PM, BC, and SO_4. Emissions can also include pollutants with health and

environmental concerns such as CO and air toxics such as benzene, toluene, ethylbenzene, xylenes, and H_2S (Beusse et al., 2013).

2.6.1.1 Combustion Sources

Combustion sources are sources associated with the production of oil and gas that include engines, heaters, incinerators, and turbines. Most of these emissions come from the equipment used to obtain the oil or natural gas but flaring is another combustion source (Beusse et al., 2013).

Flaring is the controlled burning of excess natural gas using a flare stack in order to avoid safety issues associated with its build-up. Flaring is performed on excess gas that cannot be supplied to customers, unburned process gas, vapors that accumulate in the tops of tanks, and gas from process upsets. The main emissions produced when flaring is performed efficiently are CH_4 and CO_2. Ideally flaring should be minimized and as much value realized from hydrocarbon accumulations as possible (Kearns, J. et al., 2000). Emissions from combustion sources include NO_x, CO, air toxics, VOC's, and methane (Beusse et al., 2013).

2.6.1.2 Vented Sources

Vented sources include pneumatic devices, dehydration processes, gas sweetening processes, chemical injection pumps, compressors, tanks, and well testing, completions, and work overs (Beusse et al., 2013). The gases produced by these sources are either vented directly into the atmosphere or burned off using a flare.

Venting is the controlled release of gases in order to avoid safety issues associated with their buildup. Vented gases are lighter than air, and for safety reasons, are released at high pressure. For some gases being produced, inert gases in high concentrations will prevent the gas from burning and require that venting be performed over flaring (Kearns, J. et al., 2000). This can result in the direct release of VOCs, air toxics, and methane into the atmosphere (Beusse et al., 2013).

2.6.1.3 Fugitive Sources

Fugitive sources encompass emissions from unplanned sources. These include leaks from valves, connectors, flanges, compressor seals, and other kinds of equipment. It can also include evaporative sources from tanks and other sources of that nature. In an idealized system, these sources would not exist, however, in real world systems they represent a significant contribution of VOCs, air toxics, and CH_4 to the atmosphere (Beusse et al., 2013).

2.6.2 Offshore Oil and Gas Activities Monitoring

An environmental assessment (EA) is required to be submitted to the Canada-Nova Scotia Offshore Petroleum Board (CNSOPB) as part of an application for authorization of an activity offshore. EAs are used to assess the impact of proposed projects through the prediction of environmental effects. All EAs for petroleum activities are undertaken in accordance with the Canadian Environmental Assessment Act as the CNSOPB is a federal authority under this act ("A Synopsis of Nova Scotia's Offshore Oil and Gas Environmental Effects Monitoring Programs," 2011). Some of the predictions are

verified using environmental effects monitoring programs. Nova Scotia environmental effects monitoring programs related to the offshore oil and gas activities surrounding Sable Island look to monitor produced water, the water column, sediment chemistry, and seabird life to ensure no undue harm is done the environment by such activities. However, air quality monitoring to ensure airborne emissions from the sites do not cause undue harm is not performed ("A Synopsis of Nova Scotia's Offshore Oil and Gas Environmental Effects Monitoring Programs," 2011). As previously discussed, monitoring by Nova Scotia Environment on Sable Island has been ongoing since 2003 as part of the Nova Scotia Ambient Air Quality Monitoring Network. This data gives the best available record of the impact of the rigs on air quality. Monitoring of the air quality on the rigs is performed for occupational health and safety reasons but this data is not made public by the operators (Dr. Mark Gibson, personal communication, January 30th, 2014).

Monitoring of airborne emissions is important not only for the surrounding ecosystem, but also for human health. Airborne emissions can have a direct and immediate negative impact on the health of humans (Dockery et al., 1993; Evans et al., 1984; Shwartz et al., 1990; Ware et al., 1993; Rumchev et al., 2004; Yang et al., 1997). The health impacts of various airborne particulates have been well documented and established in the past. Aerosol emissions can also have either a positive or negative impact on climate forcing and the emissions from phytoplankton in the Scotian shelf contribute primary gaseous emissions that can form secondary SO_4, O_3 and secondary organic matter (SOM) (Davison et al., 1996; O'Dowd et al., 2002; O'Dowd et al., 2004; O'Dowd and de Leeuw, 2007; Monks et al., 2009)

2.6.3 Deep Panuke

The Nova Scotia offshore area extends from the low water mark on the coast of Nova Scotia to the edges of the continental margin. This area is approximately 400 000 km^2. Exploration first began in the 1950s and since that time 395 km of 2D seismic and 6076 km^2 of 3D seismic surveys have been recorded and 168 wells have been drilled. A total of 21 significant discoveries and 5 commercial discoveries have been made in the Sable Island area ("Technical Summaries of Scotian Shelf Significant and Commercial Discoveries", 2000). A significant discovery is defined as "a discovery indicated by the first well on a geological feature that demonstrates by flow testing the existence of hydrocarbons in that feature and, having regard to geological and engineering factors, suggests the existence of an accumulation of hydrocarbons that has potential for sustained production ("Technical Summaries of Scotian Shelf Significant and Commercial Discoveries", 2000)". A commercial discover is defined as "a discovery of petroleum that has been demonstrated to contain petroleum reserves that justify the investment of capital and effort to bring the discovery to production ("Technical Summaries of Scotian Shelf Significant and Commercial Discoveries", 2000)."

Offshore petroleum activities have been ongoing in the Scotian Shelf since 1992. The Cohasset-Panuke project ran from 1992-1999 and was operated by Pan Canadian (now Encana) and Lasmo. The Sable Offshore Energy Project began in 1999 and is operated by Exxon Mobil and partners. It consists of five gas production platforms which were shown previously in Figure 2. The Deep Panuke Offshore Gas Development Project is run by Encana Corporation and was brought on-line on July 22nd 2013. It can also be seen in Figure 2 ("Offshore projects", 2013).

The Deep Panuke Comprehensive Study Report was approved in 2002 based on a three platform natural gas drilling project with 176 km of pipeline for tie-in with the pre-existing Maritimes and Northeast Pipeline facilities ("Deep Panuke Offshore Gas Development Environmental Assessment Report," 2006).

Final approval for Deep Panuke was given in 2007 ("Deep Panuke Project Newsleter," December 2007) and production was expected to begin in the summer of 2013 ("Deep Panuke gas production 'on track' for June," 2013). The commissioning phase began on July 22nd 2013 with the introduction of gas to the production field center and production commenced shortly after ("Weekly operations report EnCana Deep Panuke production status," 2013).

The positive economic impacts of a project like Deep Panuke are immediately obvious and include jobs for Nova Scotian's and jobs for Canadians from other provinces ("Deep Panuke Canada - Nova Scotia Benefits," 2013). However, there are potential environmental and health impacts of a project such as this. As previously discussed, there is a lack of adequate monitoring and information on the impacts of offshore oil and gas activities on air quality and human health, particularly those associated with the start-up and commissioning phases of operation. Although there is substantial occupational health and safety monitoring (particularly for H_2S) of personnel on the rig its self, this data is kept by the operators and not used to determine the impact of the rigs on the surrounding air quality (Dr. Mark Gibson, personal communication, January 30th, 2014).

In regards to air quality, the EA for Deep Panuke identifies "the only predicted significant adverse effect is the effect on air quality in the unlikely event of a well blowout or piping rupture resulting in the release of large amounts of acid gas" ("Deep

Panuke Offshore Gas Development Environmental Assessment Report," 2006). It is stated in the document that atmospheric emissions will comply with the *Air Quality Regulations* (Nova Scotia *Environment Act*) and Ambient Air Quality Objectives (*CEPA*) and that flaring of gas will be performed for acid gas.

Monitoring on Sable Island by NSE and Dalhousie University ("Data Display and Source Apportionment of Volatile Organic Compounds on Sable Island") will be taking place to act as the air quality monitoring for the Deep Panuke facility ("Offshore Environmental Effects Monitoring for Deep Panuke," 2012). Monitoring by Nova Scotia Environment on Sable Island has been ongoing since 2003 as part of the Nova Scotia Ambient Air Quality Monitoring Network and the data for this study comes from their instruments and those specific to the Dalhousie University study. This situation requires that the airborne emissions be examined more closely and the potential impacts determined.

2.7 Source Apportionment (Receptor Modelling)

In order to assess the impact of air pollution, it is important to understand pollution sources and their relative contributions. One way of doing this is through the modelling process known as source apportionment or receptor modelling (Brown et al., 2007; Gibson et al., 2009b; Gibson et al., 2010; Harrison et al., 2011; Gibson et al., 2013). Source apportionment can help establish the major polluters and areas to focus on when creating pollution prevention policies (Gibson et al., 2009b). Four different source apportionment modelling methods will be examined. They include Principal Component Analysis/Absolute Principal Component Scores (PCA/APCS), USEPA Chemical Mass Balance (CMB) v8.1, USEPA Positive Matrix Factorization (PMF) version 3.0, and

Pragmatic Mass Closure (PMC) (Thurston and Spengler, 1985; Watson et al., 1998; Jaeckels et al., 2007).

All applications of source apportionment of VOCs and $PM_{2.5}$ to air quality assessment require ambient sampling of the air that is then analyzed in the laboratory in order to produce speciated sample data. This data can then be used in the source apportionment/receptor models. The choice of model depends greatly on the study in question, its goals and aims, the sources of interest, and the availability of existing source chemical species profiles, e.g. the USEPA VOC and $PM_{2.5}$ speciate data base (Watson et al., 1998; Ward et al., 2006a; Ward et al., 2006b; Ward and Noonan, 2008). Meteorological data, knowledge of strong local sources and their chemistry, and knowledge of topography are also important parameters to consider when interpreting the source apportionment model results. The receptor model source factors and profiles only go so far in understanding pollution sources and events, expert knowledge of source chemical fingerprints or conservative source chemical markers is needed. Being able to interpret them in meaningful ways is only possible when they are combined with other data and knowledge and analyzed critically.

2.7.1 Principal Component Analysis/Absolute Principal Component Scores

The PCA/APCS method is a multivariate receptor model that predicts sources, their chemical composition, and their contributions to a sample by simultaneously analyzing a set of speciated sample results. It does not require inputs of source profiles (Guo et al, 2004). The source profiles are estimated using linear regression and then compared to

known source profiles. Based on similarities between the chemical composition of these source profiles, it is determined which source they represent (Thurston et al., 1985). It was first used by Thurston et al., 1985.

Unlike some other factor analysis methods which look to identify all underlying factors within a data set, PCA/APCS looks for the principle factors which explain a majority of the variance within a data matrix. The theory is quite complex, but uses principal component and regression features. The model requires adequate degrees of freedom in order to produce accurate statistical results. Like all multivariate receptor models, PCA/APCS has difficulty in separating sources that are chemically similar or strongly correlated (Guo et al., 2004).

2.7.2 Positive Matrix Factorization (PMF)

One of the most commonly used source apportionment models is PMF (Harrison et al., 2011). PMF modelling has been used in many studies such as Baumann et al. (2008) performed in Alabama, or Buzcu-Guven et al. (2007) which looked at the apportionment of organic carbon and fine particulate matter across the Midwestern United States. PMF is a form of multivariate least squares statistics used when looking at a given data matrix as related to a specific set of variables to determine spatial relationships or structures within (Hubert et al., 2000). PMF involves a data matrix of observations of a given number of objects over a given number of attributes (Hubert et al., 2000). Entries include some measure of relationship between the attributes. The purpose of PMF is then to simplify the matrix and its relationships to generate a better understanding of the matrix and to draw conclusions about the relationships within (Hubert et al., 2000).

The PMF model requires a matrix of speciated sample data as well as an uncertainty file. The uncertainty file outlines uncertainty values or parameters for calculating uncertainty. Uncertainty values provided should encompass things such as sampling and analytical errors. Uncertainties are estimated based on parameters such as minimum detection limits and error fractions (percent error times 100), or general uncertainty values can be applied to all data. Speciated data consists of samples that have been analyzed for their chemical constituents such as anions, cations, metals, etc. By using multivariate statistics to look for correlations in the data, this data is then broken down into two matrices (factor contributions and factor profiles) (Norris et al., 2008). Factor contributions outline the percent contribution of a source to the overall air quality at a given receptor while source profiles outline the chemical fingerprint of that source. Afterwards, background knowledge of wind direction, emission inventories, and in depth knowledge of source chemical markers is used to determine which sources are represented by these factor chemical profiles (Norris et al., 2008). Figure 4 below shows an example of the source profiles obtained during the Gibson et al., (2013d) study. The source profiles outline the different chemical species and the percent they contribute to each factor. From this it can be determined which source each factor represents. For example, a factor containing nickel (Ni) and vanadium (V) are indicative of ship emissions (Gibson et al., 2013d). Figure 5 shows the percent contributions of each source to the overall air quality during the study performed by Gibson et al., (2013d).

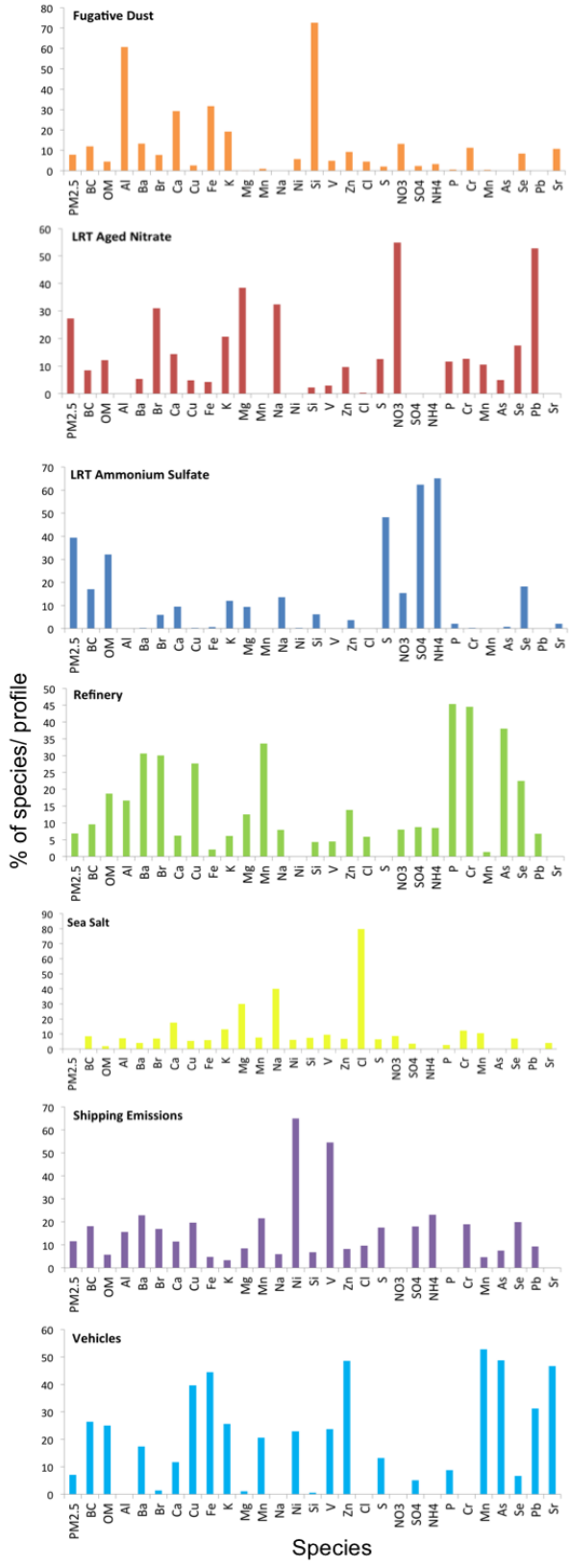

Fig 4. Example of source profile (Gibson et al., 2013d).

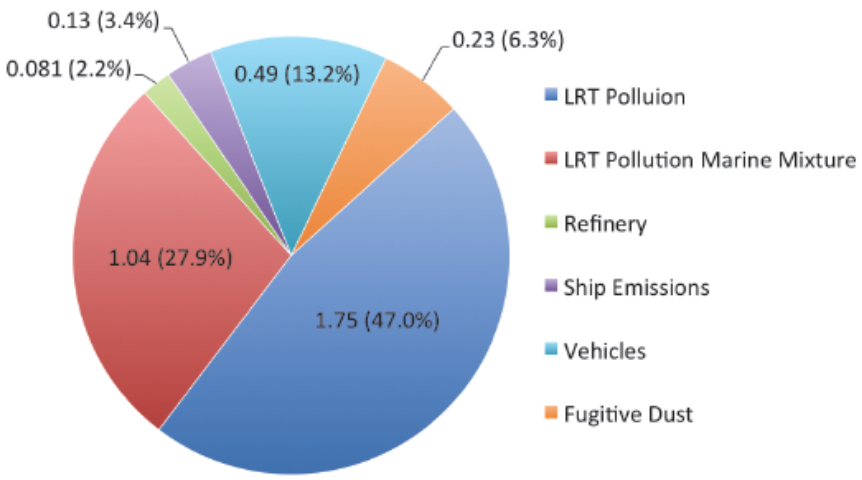

Figure 5. Average mass concentration (µgm−3) of attributed sources and percentage source contributions over the 45 days of sampling (Gibson et al., 2013d).

The end result of applying PMF to air quality research is that source factors and their contributions are generated for the air quality at a given receptor which can then be related to known sources. PMF models do not differentiate between different sources that are chemically similar. For example, the model cannot differentiate between two different coal fired power plants if their fuel types and emissions are similar. The models would include both emissions as one factor as they are not chemically distinct. The contribution of both together could be determined, but not of each individual plant. This would only be possible if one used a different fuel and had a conservative chemical marker related to that fuel and associated emissions and the other power station did not (Paterson et al., 1999). Additionally, only non-negative factors, that is, factors that have positive source contributions, are produced from PMF models (an advantage over other types of models). Error estimates of the data used in the analysis are also included using the uncertainty file (Paterson et al., 1999).

2.7.3 Chemical Mass Balance (CMB)

CMB is a robust method that can be used for the purpose of source apportionment (Gibson et al, 2009b). It requires inputs of speciated sample data and information on the chemical composition of sources in the form of source profiles. Source profile chemistry needs to be well understood as these source profiles describe the chemical composition of specific sources (Ward, 2007). One downside of CMB is that it assumes that source chemical compositions do not change and remain constant. This makes it difficult for the model to properly identify the sources of secondary aerosols formed after emission release (Ward et al, 2006). However, CMB works well when used to apportion primary aerosols (Ward et al, 2006). It may often times be necessary to develop source profiles specific to a study as can be seen in Ward et al., 2006. Oil fired heaters and wood stove source profiles were developed by sampling directly from these sources and analyzing their chemical composition for use in the model.

CMB models take speciated sample data and source profiles and then produce a linear sum of products of source fingerprint abundances and contributions by solving a system of linear equations (Ward et al., 2006b). This is achieved by using an effective-variance least squares method. A number of sources and species are selected (specific to the study) and the model attempts to reconstruct the sample data using these. This process is repeated with many different combinations until an optimal fit is found. The result is that the sources and their contributions to the air pollution sampled are found (Ward et al., 2012).

CMB modelling has been utilized in many studies over the years. Gibson et al., 2010 used CMB to determine the contribution of residential wood smoke to $PM_{2.5}$

concentrations in the Annapolis Valley. Lee et al. (2007) performed a study that used CMB for the apportionment of fine particulate matter (less than 2.5 μm in diameter) in the southeastern United States. Due to the nature of CMB it can be used anywhere that source profiles are well understood. Studies all over the world have used CMB, including studies in India (Guttikunda, 2012).

2.7.4 Pragmatic Mass Closure

Pragmatic mass closure as used in source apportionment modelling for PM uses multivariate statistics to identify pollution sources from ambient sampling alone. It does not require that source profiles be provided to the model, only speciated sample data (Yin et al., 2005). Pragmatic mass closure attempts to account for all of the measured mass of particles through both inferred and measured chemical constituents. Specific measured species are related to other components using coefficients to calculate theoretical values. From this the chemical component masses of the sample can be estimated (Yin et al., 2008). The coefficients used are based on reaction ratios and the interactions between secondary and primary pollutants. These are usually based on experimental values of previous studies and knowledge of tropospheric chemistry (Yin et al., 2005).

Pragmatic mass closure methods can be used to reconstruct chemical component masses with accurate results. Yin et al., 2005 found very strong correlations between the summed reconstructed chemical component masses and the gravimetric masses with R^2 values from 0.82 to 0.96. Yin et al., 2008 also found strong correlations between the summed reconstructed chemical component masses and the gravimetric masses when pragmatic mass closure was applied to data from 3 different sites, with R^2 values that ranged from

0.69 to 0.98. The same coefficients were used for all 3 sites. Although coefficients used in the model would need to be adjusted if applied to a study area with very different airborne particulate climatology, the method approach is applicable anywhere (Yin et al., 2008).

When combined with meteorological data and concurrent sampling at a number of sites pragmatic mass closure can be very useful in showing how prevailing wind directions can greatly affect the chemical composition of PM_{10} (Gibson et al., 2009b). This illustrates the impact of transport, both localized and long range, on PM chemical compositions and the direct link between emissions and composition at nearby sites. The Gibson et al, 2009b study, performed in West-Central Scotland, showed changes in composition with prevailing wind direction. Sites downwind from urban sources showed primary material associated with high density urban emissions while those upwind were impacted primarily by marine and long range transport sources.

2.8 Air Mass Back Trajectories

Air mass back trajectories are a useful tool when looking at air pollution. They can be used to compute both air parcel trajectories and dispersion and deposition simulations. A common air mass back trajectory model used is the HYSPLIT (HYbrid Single-Particle Lagrangian Integrated Trajectory) model initially developed jointly by the National Oceanic and Atmospheric Administration (NOAA) Air Resources Laboratory in Silver Spring, Maryland and Australia's Bureau of Meteorology. The model has since been upgraded with contributions from many different parties. The HYSPLIT model is used to identify either backward or forward trajectories based on meteorological parameter inputs

and assumes either puff or particle dispersion (HYSPLIT - Hybrid Single Particle Lagrangian Integrated Trajectory Model, 2012). The model follows a parcel of air as it moves through space and time, as opposed to Eulerian models which focus on a specific location that the air parcel flows through (Batchelor, 1973). Puff dispersion involves expanding puffs until they exceed the meteorological grid cell size and split into new puffs. Particle dispersion involves a fixed number of particles which are advected around the model domain by a mean wind field and spread by a turbulent component. Default configurations assume 3-dimensional distribution, that is to say both horizontally and vertically (HYSPLIT - Hybrid Single Particle Lagrangian Integrated Trajectory Model, 2012).

The HYSPLIT model has been used in many studies to examine air mass histories, transport, dispersion, and deposition with the goal of mapping pollution sources (Yin et al., 2005; Gibson et al., 2009b; Gibson et al., 2013d). Outputs from the HYSPLIT model can be very useful in interpreting PMF results and identifying sources of pollution events. However, it has been found that errors exist with back trajectory models due to truncation errors, interpolation errors, starting position errors, and amplification of errors. Errors as high as 20% of the distance travelled seem to be typical for trajectories computed from analyzed wind fields (Stohl, 1998). As a result, uncertainties in model outputs need to be considered accordingly when drawing conclusions. However, the uncertainty can be ignored when the VOC and $PM_{2.5}$ species correlate with known upwind source regions, e.g. high concentrations of Na and Cl when air mass trajectories originate from the ocean and high concentrations of $(NH_4)_2SO_4$ when the air mass trajectory originates from the

North Eastern United States (Gibson et al., 2013d). Figure 6 shows an example from Gibson et al., (2013d) of air mass back trajectories grouped by major source region.

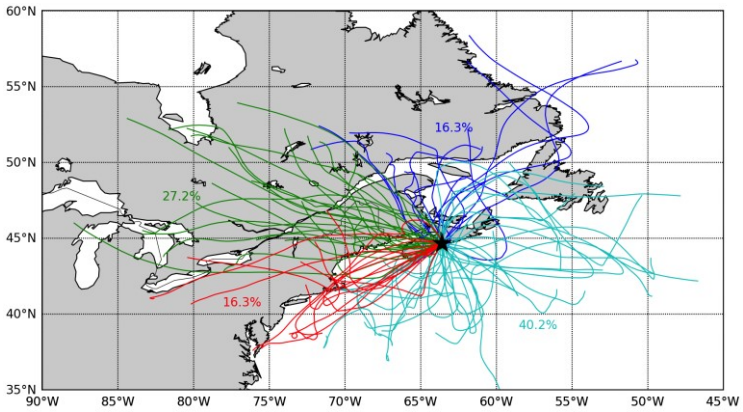

Fig 6. Air mass back trajectories grouped by major source region (Gibson et al., 2013d).

2.9 Meteorological Factors

It is important to measure meteorological conditions in order to be able to properly understand air quality and interpret air quality data. Information on conditions such as temperature, humidity, wind speed and direction, solar radiation, ceiling height, and pressure are all important in understanding how pollution is transported and dispersed as well as the reactions that will occur amongst different pollutants. Meteorological factors can be used to investigate pollutant transport and to establish source-receptor relationships of air pollutants (Stohl, 1998). The link between wind direction and pollution trends can help to link air pollution to a given source. For example, Paterson et al., 1999 linked periods of south and southwesterly flow to long-range transport factors,

and Gibson et al., 2009a found that episodes of high concentrations of anthropogenic photochemical ground level ozone in Atlantic Canada coincided with high temperatures and strong solar radiation coupled with a high-pressure system to the southeast. Harrison et al., 1997 found a marked difference between particulate matter concentrations and composition between the summer and winter months, illustrating the impact seasonal changes in meteorological conditions can have.

CHAPTER 3 MATERIALS AND METHODS

3.1 Sable Island Study

The broader study from which much of the data for this thesis is derived takes place on Sable Island and is funded by the Environmental Studies Research Funds (ESRF) with the funds being administered by Natural Resources Canada (NRCan). The ESRF is under the joint management of a board composed of government, industry, and the public and falls under the Canadian Petroleum Resources Act as well as the NS and NL Accord legislation act. The aim of the ESRF is to sponsor environmental and social studies that pertain to oil and gas development activities in Canada. Levies on oil and gas companies provide funding for these studies (Gibson et al., 2013b).

The study is entitled "Data Display and Source Apportionment of Volatile Organic Compounds on Sable Island" and its aim is to apportion the relative contributions of biogenic and anthropogenic sources of $PM_{2.5}$ and VOCs to the air quality around Sable Island, and to develop an understanding of their combined effects. The study will establish the chemical characteristics of atmospheric particulate matter, size resolved particle number and mass concentrations, and measure VOC species. Source apportionment will then be utilized to determine the different sources and their contributions. All the while, data will be streaming to a live website where it will be displayed in an interactive manner.

3.2 Site Description

All of the equipment for the study was housed in the air chemistry shed located at the Environment/Parks Canada site on Sable Island. The shed is located along the west edge of the site. It can be seen in Figure 7 circled in red and in the center of Figure 8. Modifications were made to the roof and walls of the shed to allow the installation of sampling inlets for the equipment contained inside. Figures 9 and 10 show the sampling inlets installed. Power is supplied from the same diesel generator used to power the rest of the Parks Canada site and a satellite connection allows for data to be transmitted back to the mainland.

Figure 7. Location of the Air Chemistry Shed on Sable Island.

Figure 8. The Air Chemistry Shed on Sable Island.

Figure 9. Sampling inlet for the Thermo Scientific 55i.

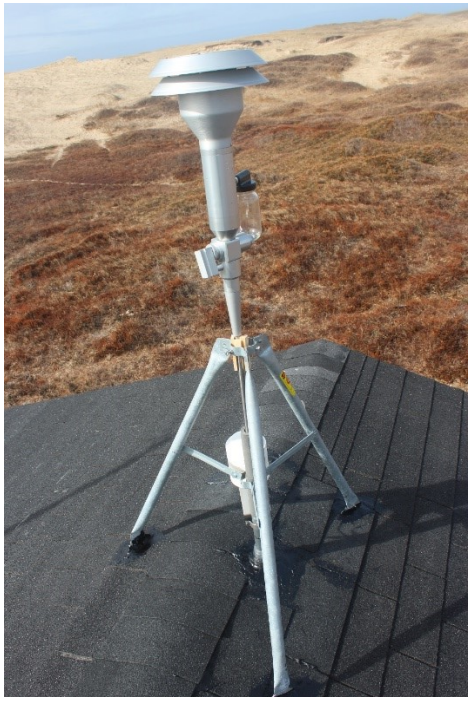

Figure 10. Sampling inlet for the Thermo Scientific 5012.

3.3 Equipment

The various instruments and analysis methods used are outlined below.

3.3.1 55i Methane and Total Non-methane Hydrocarbon (VOC) Analyzer

The Model 55i from Thermo Scientific is a back flush gas chromatography system that provides real time measurements of both methane and non-methane hydrocarbons. It can be seen in Figure 11. The Model 55i operates on the basic principles of gas chromatography and utilizes a proprietary column system. An automated batch analyzer collects samples at preset time intervals. A pump is used to draw in the sample air before it is introduced to an 8 port rotary valve that controls the flow of gases through the analyzer and column. Samples are injected into the column along with an inert carrier gas. Here the different chemical constituents contained within the sample are separated based on retention time. Methane exits the column first where it is then measured using a flame ionization detector (FID). The signal generated by the FID can be related to a concentration through comparison with a calibrant gas of known concentration. Once the methane peak has been detected the rotary valve back flushes the remaining sample through the column and to the FID to analyze for the remaining NMHCs (Model 55i Instruction Manual, 2008). For the purpose of this study only NMHC concentrations were used.

Figure 11. Thermo Scientific 55i set up on Sable Island.

3.3.2 5012 Black Carbon Analyzer

The model 5012 multi angle absorption photometer utilizes aerosol light absorption properties to measure black carbon concentrations. It can be seen in Figure 12. In order to measure black carbon, a sample is first drawn into the instrument inlet using a pump. The aerosol sample is deposited onto a glass fiber filter tape that then advances to a detection chamber. A multi angle absorption photometer is used to analyze changes in the radiation fields in the forward and back hemisphere of the filter. This is than related to a concentration of BC using a data inversion algorithm based on a radiative transfer method. This algorithm takes into account multiple scattering processes inside both the deposited aerosol and between the aerosol layer and filter matrix. Along with the air sample volume and multiple reflection intensities, this data is continuously integrated to determine a real time measurement of BC concentrations (Model 5012 Instruction Manual, 2009).

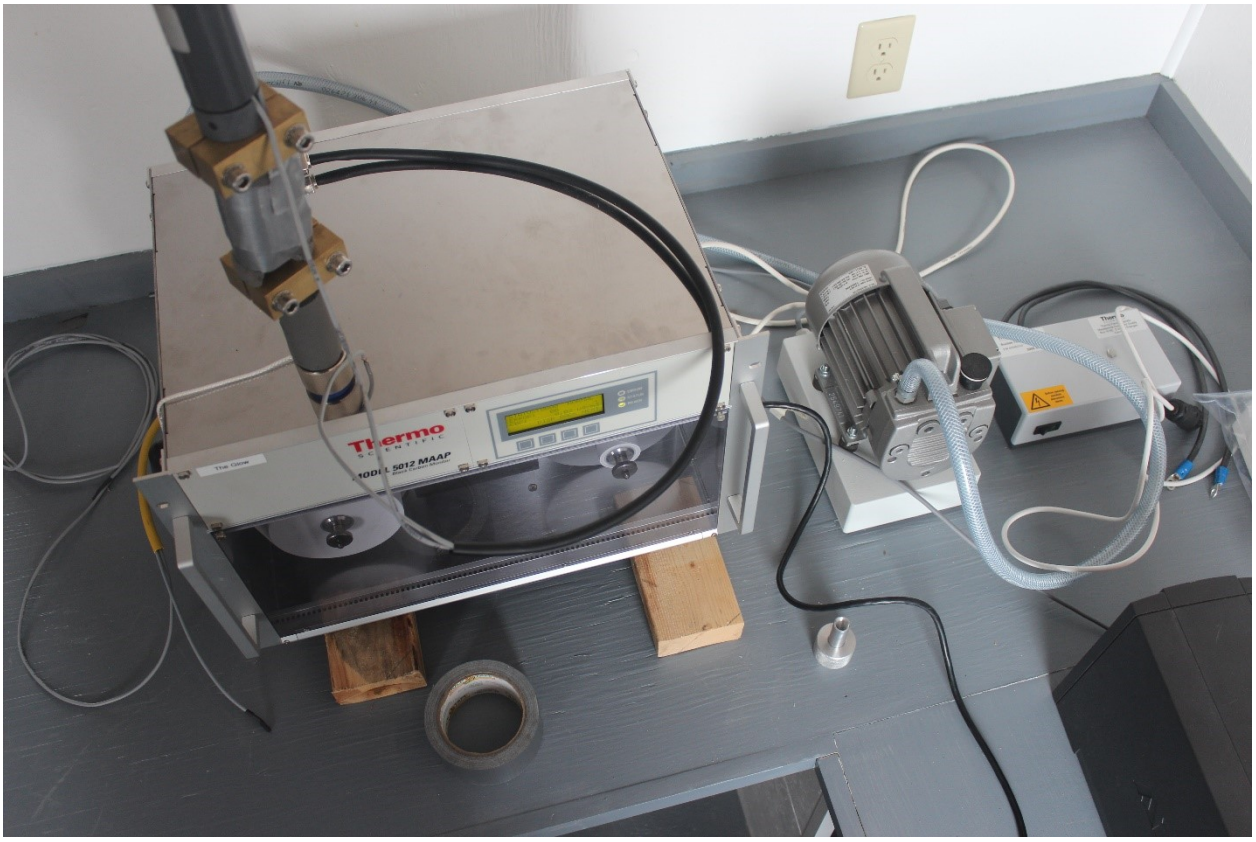

Figure 12. Thermo Scientific 5012 set up on Sable Island.

3.4 Nova Scotia Environment Data

Nova Scotia Environment (NSE) provided measurement data for H_2S, NO_x, NO, NO_2, O_3, $PM_{2.5}$, SO_2, temperature, wind direction, and wind speed. This data comes from various instruments that were already housed in the air chemistry shed as part of the Nova Scotia Ambient Air Quality Monitoring Network which forms part of the Federal government National Air Pollution Surveillance (NAPS) network of over approximately 300 stations (James Kuchta, personal communication, February 4th, 2014). NSE air quality data used in the analyses described herein was taken from a Teledyne T101 H_2S analyzer, Teledyne T100 SO_2 analyzer, TECO 49i O_3 analyzer, METOne 1020 beta attenuation monitor ($PM_{2.5}$), and a Teledyne 200E NO_x analyzer (NO, NO_2, NO_x).

3.5 Equipment Malfunctions

Equipment malfunctions were minimal during the study, but they did occur. This was largely due to the remote nature of the site and the difficulty in performing troubleshooting as a result. The major malfunctions (those that affected daily averages) are summarized in the table below. Reasons for the malfunction are given for equipment run as part of the study, but unfortunately this information was not available for the equipment run by NSE.

Table 1. Equipment Malfunctions over the course of the study.

Date	Error or Malfunction	Comments
June 22nd – July 7th	Thermo Scientific 55i was down	Carrier gas pressure too low, tank needed to be changed.
July 22nd - July 25th	Thermo Scientific 5012 down	Maintenance and Calibration.
October 19th – 22nd	Thermo Scientific 55i down	Carrier gas pressure too low, tank needed to be changed.
June 4th + 5th	NO_x analyzer down	NA
Sept 28th – 30th	H_2S analyzer down	NA
October 5th + 6th, 8th – 17th, 22nd + 23rd, 26th – 29th	H_2S analyzer down	NA
Sept 29th – 3rd, Oct 8th – 13th,	BAM ($PM_{2.5}$) down	NA

3.6 Statistical Analysis

The data collected from the study instrumentation consisted of data averaged over 5 minute intervals while data obtained from NSE consisted of data averaged over 1 hour intervals. All of the data was compiled into a master spreadsheet in excel. The data was filtered and extreme outliers or negative values removed. Extreme outliers were considered to be when concentrations far exceeded guidelines and regulations. Outliers also consisted of single data points, where true pollution events tended to show elevated concentrations for hours or days. It should be noted that data for H_2S, NO, NO_2, and NO_x had to be quality controlled as this had not been performed on the data received from NSE. H_2S values experienced sudden spike after which they remained high for approximately a month, spiking once again before dropping. This first spike was from May 16th to June 12th and the second from June 12th to June 21st. The values were reduced (by 1.3 and 2.8 ppb for each spike) so that the lowest reading for each time period was 0

ppm as it was assumed instrument error had increased the baseline. NO, NO_2, and NO_x values also had calibration issues where they consistently reported negative values. The measurements were adjusted so that values were positive. Data were projected onto common hourly and daily time vectors in order to be able to allow comparison and for use in running PMF. Descriptive statistics, time series analysis, box plots, and other statistical tests were generated using Minitab 16 and SigmaPlot (v12.0). The software used for source apportionment was the USEPA PMF model v3.0.2.2 as discussed in more detail in Section 2.8. A pollution rose or the factors obtained from the PMF model was generated using using IgorPro v6.2.2.2.

3.7 Meteorological Data

Although wind speed, wind direction, and temperature were monitored by NSE this data contained many gaps due to instrument malfunction. As a result, it was not used in any analyses. Instead, hourly and daily meteorological data for the sampling time frame was obtained from Environment Canada. Historical weather data is available for download from the Environment Canada website, with data available from the Sable Island weather station (http://climate.weather.gc.ca/index_e.html). The data was used in generating pollution roses.

3.8 Air Mass Back Trajectories

Air mass back trajectories were generated to aid in the source apportionment process. They were generated using the HYSPLIT model available online from the National Oceanic and Atmospheric Administration (http://ready.arl.noaa.gov/HYSPLIT_traj.php).

Backward trajectories were run for each day of the sampling period. A modelling time of 120 hours (5 days) was used for the back trajectories and the air mass was modeled to arrive at Sable at 23:00 in order to correspond with the end of a daily sampling period. The default arrival height of 500 m was used in running the model to avoid trajectories impacting the surface before reaching the receptor (Sable Island) (Gibson et al., 2009b). Daily back trajectories for the sampling period can be found in the Appendix.

3.9 Receptor Modelling Software

The USEPA PMF model v 3.0.2.2 was used to conduct source apportionment on the data collected. The model was run using daily averages of the data. In order to run, it requires both a species concentration file and species uncertainty file related to the data set.

A concentration file containing daily averages was generated in Excel and quality controlled for input into the model. The model will not run if null values are present so where they did occur a value of -999 was entered to allow the model to run without errors.

The uncertainty file outlines any uncertainties in the data collected. To be safe, an uncertainty of 10% was applied to all the measurements. The value of 10% was used as information on the NSE instruments was not available. If the percent error for measurements from each instrument were known this would have allowed for better estimates of uncertainty. Where there were null values an uncertainty value of half the minimum detection limit was used as recommended by the USEPA (Norris et al., 2008). Minimum detection limits were not available for the NSE data, and so minimum detection limit values available for real time gas monitors used to measure the species in

question were used instead. It was assumed that these values would be comparable if not the same as those for the NSE equipment.

The model was run using the USEPA default of 20 base runs with 4 factors (sources) being chosen. Each run starts at a different point in the time series data in an attempt to account for any elevated concentrations within the data set. It tests to determine if each run has converged and at the end selects the run that best fits the data (Norris et al., 2008). The number of factors selected tells the model how many factor profiles/contributions to look for within the data set. The model was run for a range of factors from 3-10. Based on the results, as well as knowledge of the potential sources on Sable Island identified through the literature review and on Island experience, it was decided that 4 factors gave the best representation. Emissions from offshore O&G activities, LRT, and on-site combustion were the main expected sources on Sable. The base runs are the basis for advanced analysis using bootstrapping or Fpeak (Norris et al., 2008).

The bootstrap and Fpeak models were also applied to the data. Both models help to ensure the base model runs provide stable and robust results. Bootstrapping is performed to estimate the stability and uncertainty of the solution. It randomly selects non-overlapping blocks of samples and creates a new input data file for them. The PMF model is then rerun and each bootstrap factor is mapped to the base run factor for comparison. The Fpeak test looks at whether a pair of factor matrices can be transformed to another pair of matrices with the same "Q" value, or in other words, whether they can be rotated. This is done to ensure that there is little rotational ambiguity in a solution (Norris et al., 2008). The bootstrap model was performed on Run 15 with 100 bootstraps

and a minimum correlation R-value of 0.6. The seed was random and the block size 6. The Fpeak model was run for one Fpeak with a strength of 0.1.

It should be noted that the PMF model was originally developed for source apportionment of $PM_{2.5}$ using speciated sample data obtained from filter based sampling, but can be run with any kind of speciated sample data (Reff et al., 2007). The sample data obtained during the study contains both mass concentrations of $PM_{2.5}$ and BC along with gaseous measurements. As a result, final source contributions to a total air pollutant cannot be accurately determined. However, the model is capable of identifying source factors and their chemical profiles from the data matrix provided and the correlations contained. As a result, factor contribution outputs from the model will not be used. In the future, VOC speciation data as well as more in depth mass concentration measurements would be beneficial to the broader study taking place on Sable in that they would allow for accurate mass contributions to be determined.

CHAPTER 4 RESULTS AND DISCUSSION

After data was collected and compiled into a master spreadsheet descriptive statistics were performed. Time series graphs and box plots were generated and the non-parametric Mann-Whitney statistical comparison test run. The data was then used to run the USEPA PMF model v 3.0.2.2 software. Finally, a pollution rose was generated for the factor profiles obtained through the PMF model. The pollution rose shows the average wind direction and its association with factor contributions from the four factors. Hourly meteorological data from environment Canada was used to obtain daily averages of wind speed and direction for comparison to the PMF factors. The data from the Sable Island instruments was then split into data collected before and after July 22nd to examine the impact of new oil and gas activity which commenced at approximately this time.

4.1 General Air Quality

4.1.1 Time Series Analysis

The following figures show the time series of each pollutant measured. A visual inspection clearly reveals spikes and correlations between pollutants. Data points are shown in red with connecting lines shown in blue.

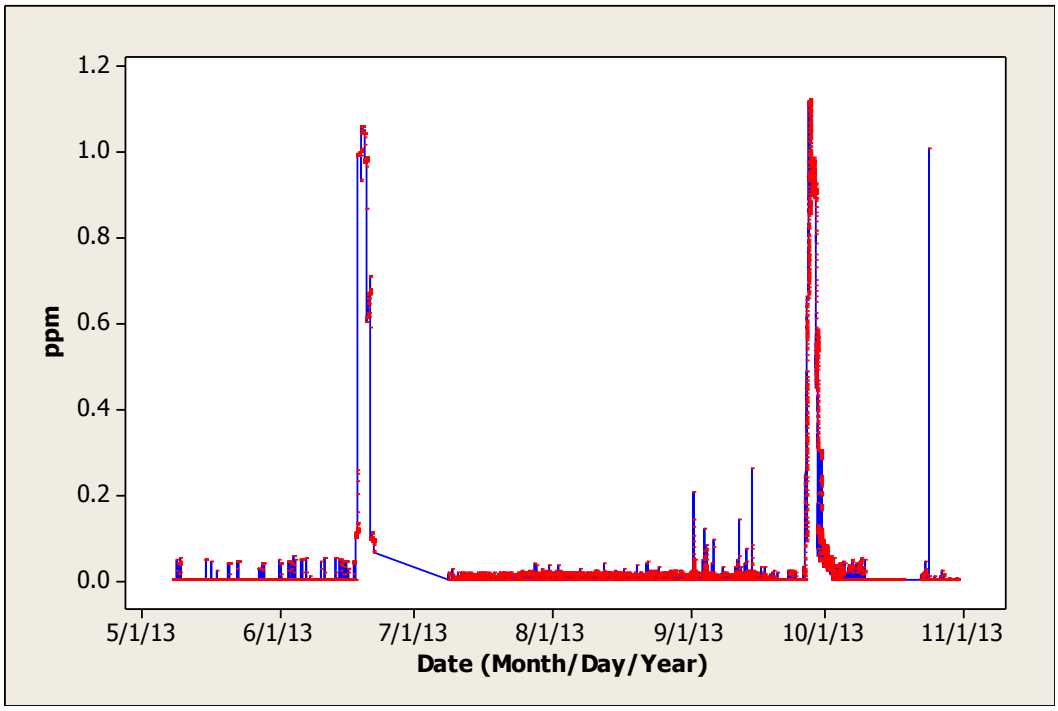

Figure 13. NMHC concentrations over time.

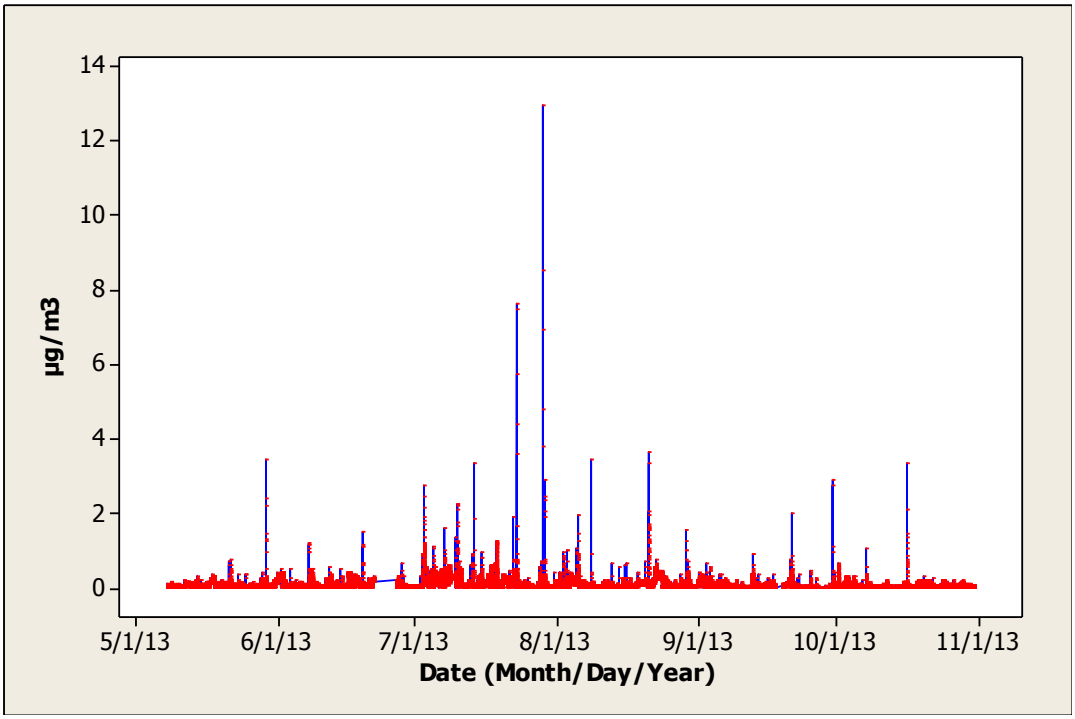

Figure 14. BC concentrations over time.

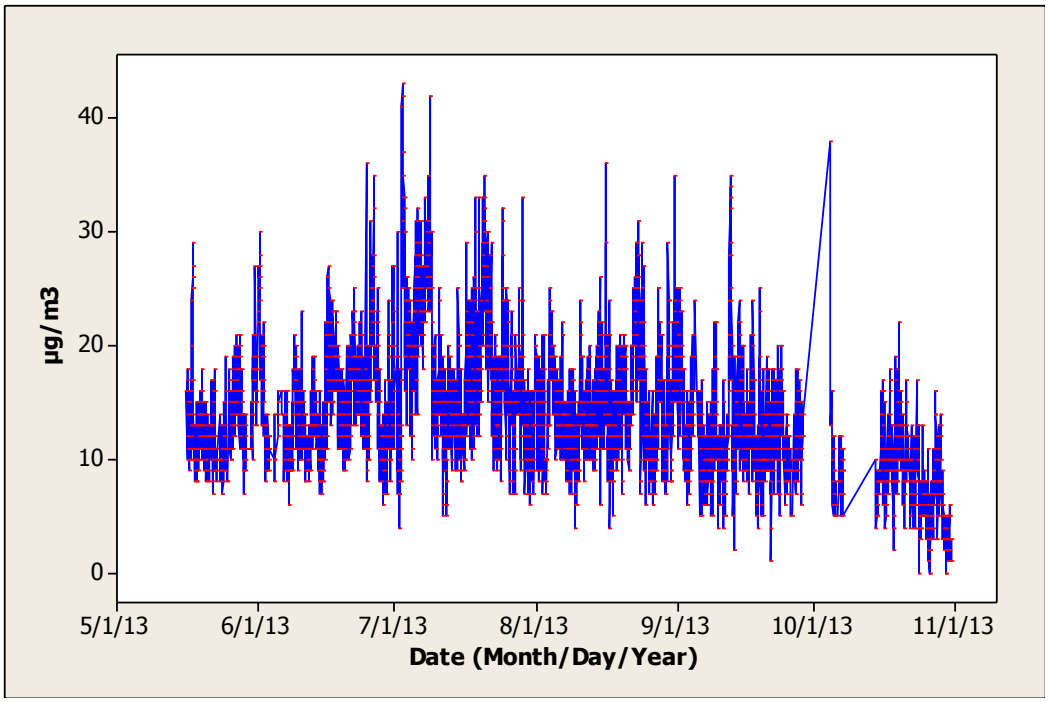

Figure 15. $PM_{2.5}$ concentrations over time.

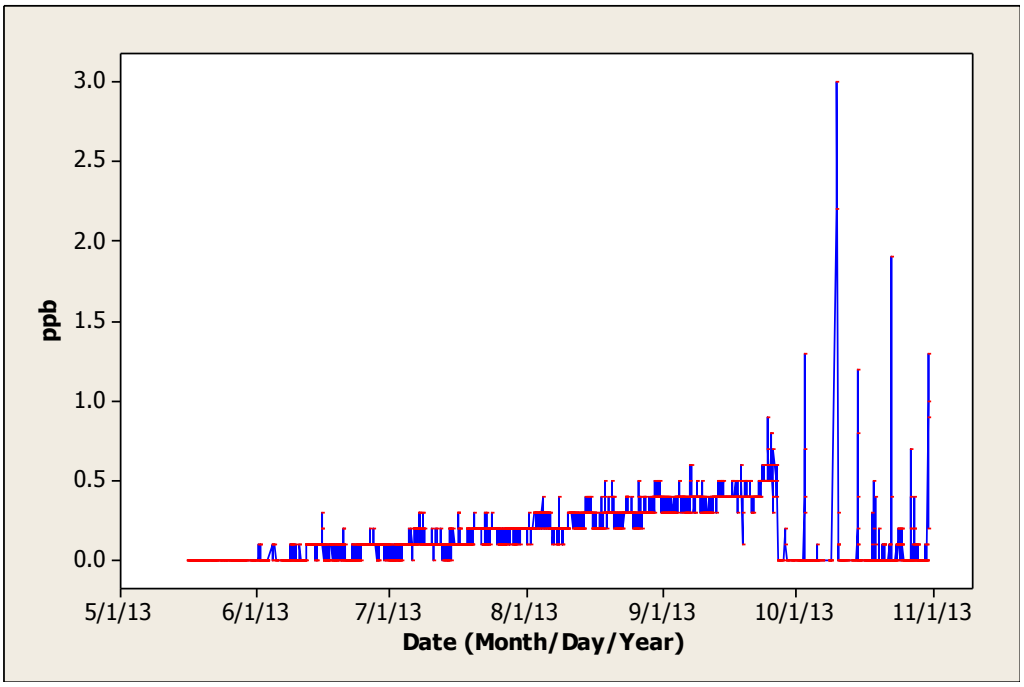

Figure 16. SO_2 concentrations over time.

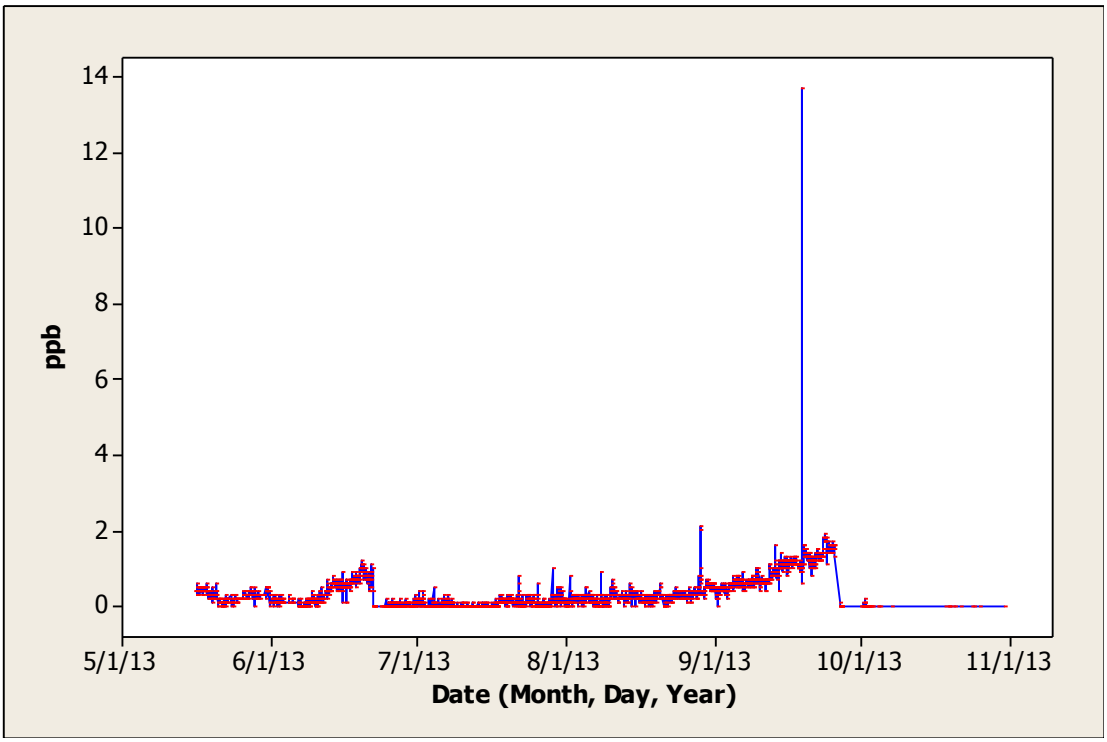

Figure 17. H_2S concentrations over time.

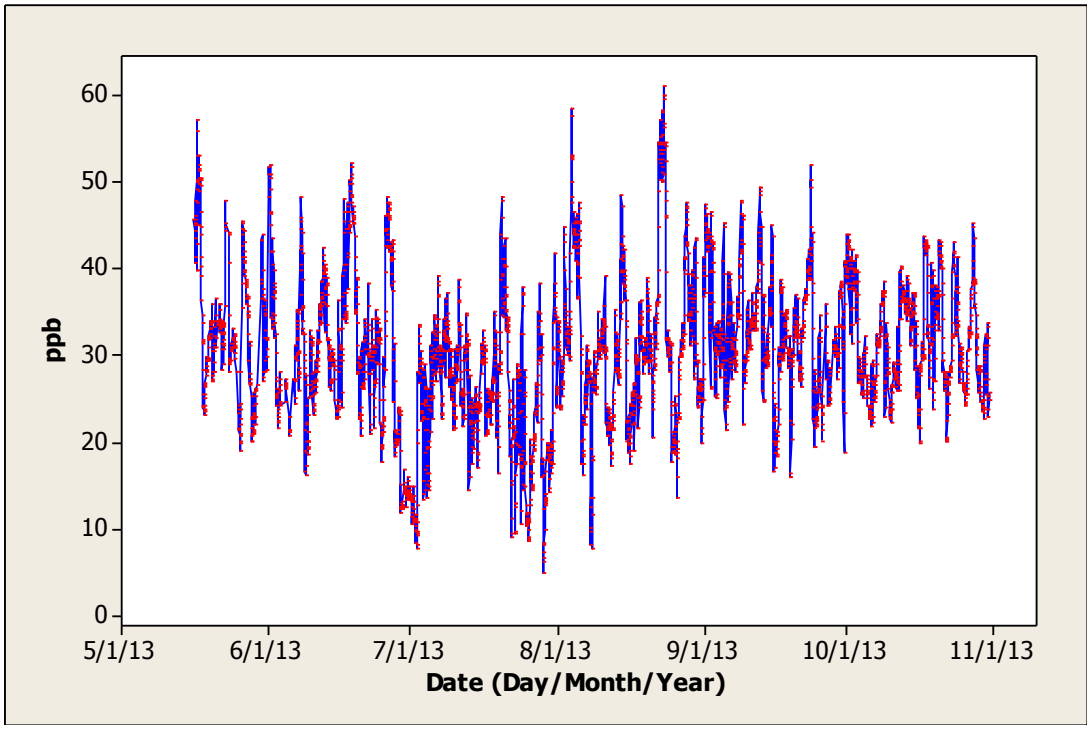

Figure 18. O_3 concentrations over time.

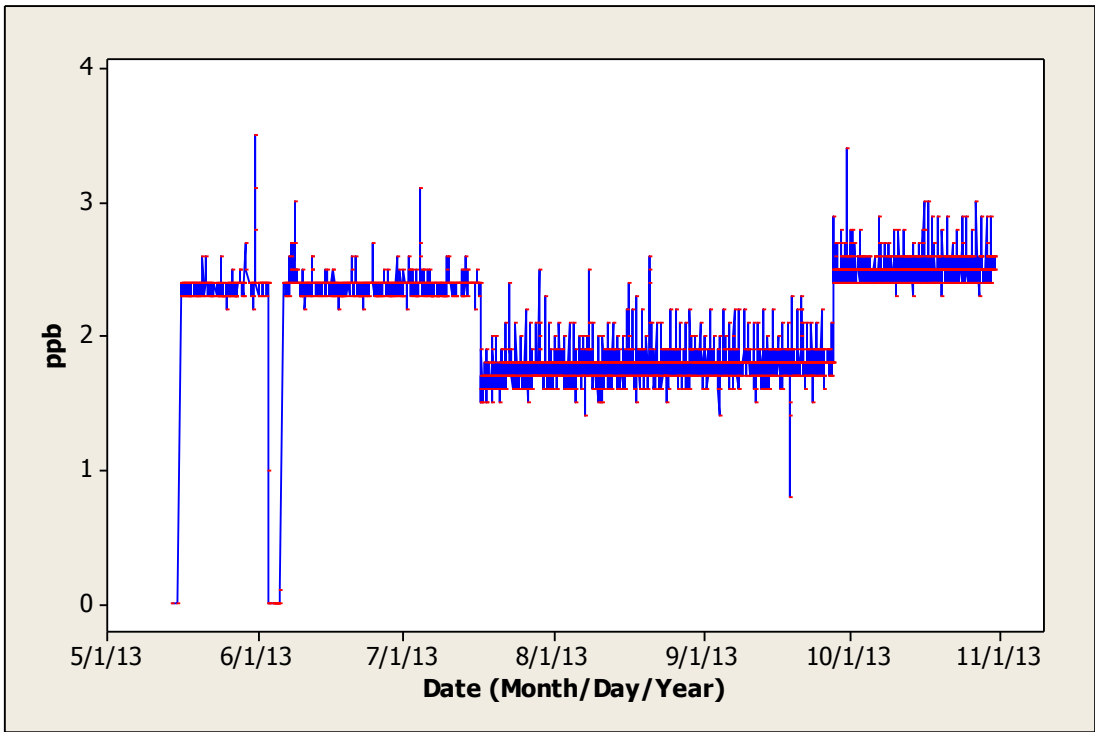

Figure 19. NO concentrations over time.

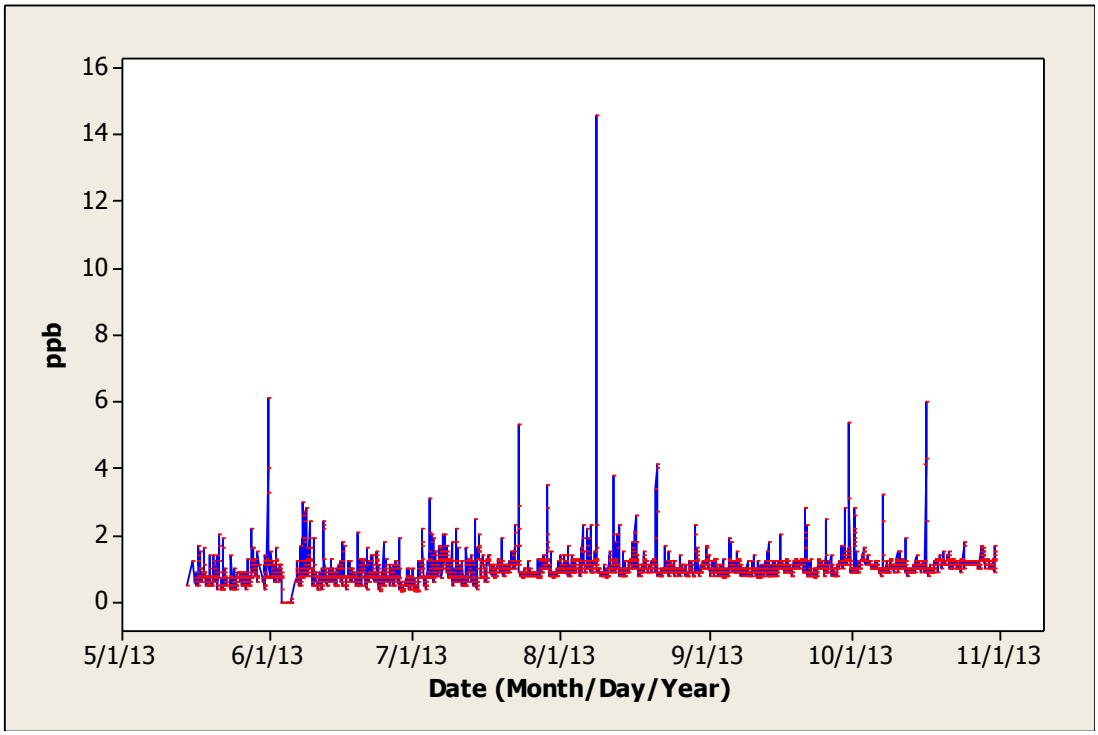

Figure 20. NO_2 concentrations over time.

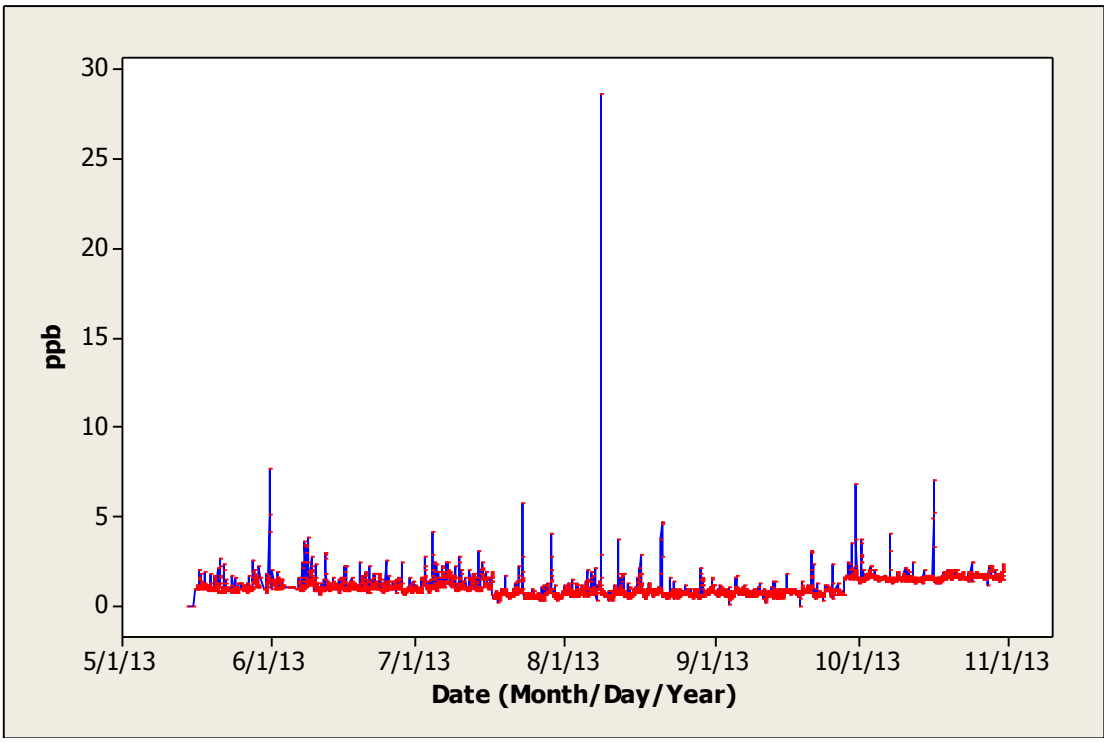

Figure 21. NO_x concentrations over time.

From analyzing the time series plots of the various pollutants certain trends begin to become apparent. For example, it can be seen that NMHC, BC, H_2S, and SO_2 (Figures 13, 14, 16, and 17) concentrations tend to be generally low (at or around zero readings) with proportionally higher spikes occurring at specific times. These spikes are most likely linked to pollution events, meaning that NMHC, BC, H2S, and SO2 concentrations are likely associated with specific sources with intermittent emissions.

On the other hand the time series plots for $PM_{2.5}$, O_3, NO, NO_x, and NO_2 (Figure 15, 18, 19, 20, and 21) tend to show more constant concentrations. The conclusion can be drawn that these pollutants are present in the majority of sources impacting the island and in particular those that are more constant in nature, i.e. background pollutants. For example, it is well known that O_3 in particular can be considered a "background" air contaminant,

while $PM_{2.5}$ can be to a certain extent (through sea salt and LRT) (Gibson et al., 2009a; Gibson et al., 2013d). Specific pollution events are apparent from the time series and they will be discussed further in Section 4.2.2 through the use of HYSPLIT back trajectories and satellite imagery.

4.1.2 Descriptive Statistics

Descriptive statistics for the data is summarized below in Table 2. Skewness is a measure of the asymmetry, while kurtosis is a measure of the peakedness of the probability distribution of a real-valued random variable (Novak, 2004). The closer to zero, the closer the data follows a normal distribution (Novak, 2004).

Table 2. Descriptive statistics for all species.

Variable	Mean	Standard Deviation	Minimum	Q1	Median	Q3	Maximum	IQR	Skewness	Kurtosis
NMHC (ppm)	0.034	0.163	0.00	0.00	0.00	0.00	1.13	0.00	5.29	27.1
BC ($\mu g/m^3$)	0.092	0.170	0.00	0.02	0.05	0.11	13.0	0.09	23.0	1180
$PM_{2.5}$ ($\mu g/m^3$)	14.1	5.71	0.00	10.0	13.0	17.0	43.0	7.00	0.83	1.36
SO_2 (ppb)	0.168	0.173	0.00	0.0	0.10	0.30	3.00	0.30	2.63	28.0
H_2S (ppb)	0.361	0.452	0.00	0.10	0.20	0.50	13.7	0.40	9.49	255
O_3 (ppb)	30.4	8.24	4.90	25.3	30.2	35.0	61.1	9.70	0.18	0.50
NO (ppb)	2.17	0.379	0.00	1.80	2.30	2.40	3.5	0.60	-0.92	2.95
NO_x (ppb)	1.12	0.700	0.00	0.70	1.00	1.50	28.7	0.80	17.0	627
NO_2 (ppb)	0.998	0.434	0.00	0.80	1.00	1.10	14.6	0.30	10.5	269

From looking at the skewness and kurtosis it becomes immediately apparent that the data are not normally distributed, with the exception of ozone and $PM_{2.5}$. This can also be seen from the histograms (Figure 62 – 70) in the Appendix. This was unexpected as environmental data does not usually follow a normal distribution. The normal distributions of O_3 and $PM_{2.5}$ are likely due to their presence as "background" air contaminants present in a number of sources impacting the Island (Gibson et al., 2009a; Gibson et al., 2013d). As a result, the overall data set requires non-parametric statistics to be run. Mean and median concentrations are close to one another, with relatively low standard deviations. However, maximum concentrations tend to be quite a bit higher than mean values, and can be considered as special air pollution episodes or events, e.g. LRT smog or forest fire plumes advecting over Sable Island. Unlike outliers that were removed and consisted of single unrealistically large data points, these pollution events tended to show more realistic concentrations based on maximum permissible guidelines and showed elevated concentrations for hours or even days.

From Table 2 it can be seen that the mean concentration for $PM_{2.5}$ was 14.1 $\mu g/m^3$. This is a rather high value considering Sable Island's remote location in the North West Atlantic. Average concentrations for Halifax, Nova Scotia were found by Jeong et al., 2011 to be around 7.1 $\mu g/m^3$ for the year and approximately 9.0 $\mu g/m^3$ over the summer months. Gibson et.al. (2013d) found the average $PM_{2.5}$ concentration in Halifax during the summer of 2011 to be only 3.9 $\mu g/m^3$. These higher than expected concentrations are likely due to sea salt generated from wave action with potential contributions from the offshore oil and gas activity, on Island trash burning, and diesel power generation.

The mean concentration for NMHCs was 0.034 ppm and for BC was 0.092 μg/m^3. Maximum values are 1.13 ppm and 13.0 μg/m^3 respectively. The mean concentrations for SO_2, H_2S, O_3, NO, NO_x, and NO_2 were 0.17 ppb, 0.36 ppb, 30.4 ppb, 2.17 ppb, 1.12 ppb, and 1.0 ppb respectively. The concentration of O_3 is comparable with the annual average concentration of O_3 in ambient air in Canada which was 33 ppb in 2011 (Environment Canada, 2013).

The Air Quality Regulations from Nova Scotia Environment outline maximum permissible ground level concentrations for H_2S, NO_2, O_3, and SO_2 of 3 pphm, 21 pphm, 8.2 pphm, and 34 pphm respectively over a 1 hour averaging period. This equates to concentrations of 30, 210, 82, and 340 ppb respectively. A summary of the applicable Air Quality Regulations can be seen below in Table 3. All of the average and maximum concentrations for pollutants monitored on Sable Island fall below maximum permissible levels.

Table 3. Maximum Permissible Ground Level Concentrations (Nova Scotia Environment: Air Quality Regulations, 2010).

Contaminant	Averaging Period	Maximum Permissible Ground Level Concentrations (ppb)	Maximum concentrations on Sable Island (ppb)
Hydrogen Sulphide (H_2S)	1-hour	30	13.7
Nitrogen Dioxide (NO_2)	1-hour	210	14.6
Ozone (O_3)	1-hour	82	61.1
Sulphur Dioxide (SO_2)	1-hour	340	3.00

The Canada-Wide Standards for $PM_{2.5}$ outline maximum desirable concentrations of 30 $\mu g/m^3$ over a 24-hour averaging period and concentrations of 65 ppb over an 8-hour averaging period for O_3 (Environment Canada, 2013c). The new 2020 Canadian Air Quality Standards for fine particulate matter and ground level ozone will be adjusted to 27 $\mu g/m^3$ for $PM_{2.5}$ over a 24-hour averaging period and 62 ppb for O_3 over an 8-hour averaging period (Environment Canada, 2013b). Mean concentrations of $PM_{2.5}$ and O_3 on Sable Island were below both of these guidelines, although hourly concentrations for $PM_{2.5}$ did exceed them at times. All recorded O_3 concentrations on Sable Island were below the guidelines.

The World Health Organization outlines maximum desirable concentrations of 25 $\mu g/m^3$ for $PM_{2.5}$ over a 24-hour averaging period, 105 ppb for NO_2 over a 1-hour averaging period, 7.5 ppb for SO_2 over a 24-hour averaging period, and 50 ppb for O_3 over an 8-hour averaging period (WHO Air quality guidelines for particulate matter, ozone, nitrogen dioxide and sulphur dioxide, 2005). Mean concentrations on Sable Island are below these guidelines, although hourly concentrations of $PM_{2.5}$ and O_3 on the Island exceed them at times. The guidelines are summarized below in Table 4.

Table 4. Canada-Wide Standards, 2020 Canadian Air Quality Standards, and World Health Organization maximum desirable air quality metrics.

Pollutant	Canada-Wide Standards	2020 Canadian Air Quality Standards	World Health Organization	Average concentration on Sable	Maximum concentration on Sable Island
$PM_{2.5}$ ($\mu g/m^3$)	30 (24 hours)	27 (24 hours)	25 (24 hours)	14.1	43.0
O_3 (ppb)	65 (8 hours)	65 (8 hours)	50 (8 hours)	30.4	61.1
NO_2 (ppb)	-	-	105 (1 hour)	0.998	14.6
SO_2 (ppb)	-	-	7.5 (24 hours)	0.168	3.00

There was an interesting bimodal distribution for NO concentrations as seen in Figure 68, possibly due to the impact of 2 separate sources (potentially fresh and aged combustion). In future it would be interesting to correlate the wind directions associated with concentrations in these 2 ranges against the location of known NO sources.

4.1.3 Box Plots

Box plots were generated in order to compare the distribution of the data. Due to the vast number of data points the 5^{th}/95^{th} percentiles were shown instead of outliers.

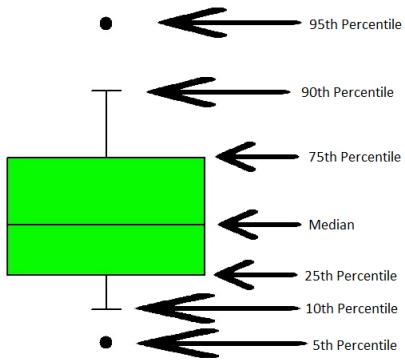

Figure 22. Box plot legend.

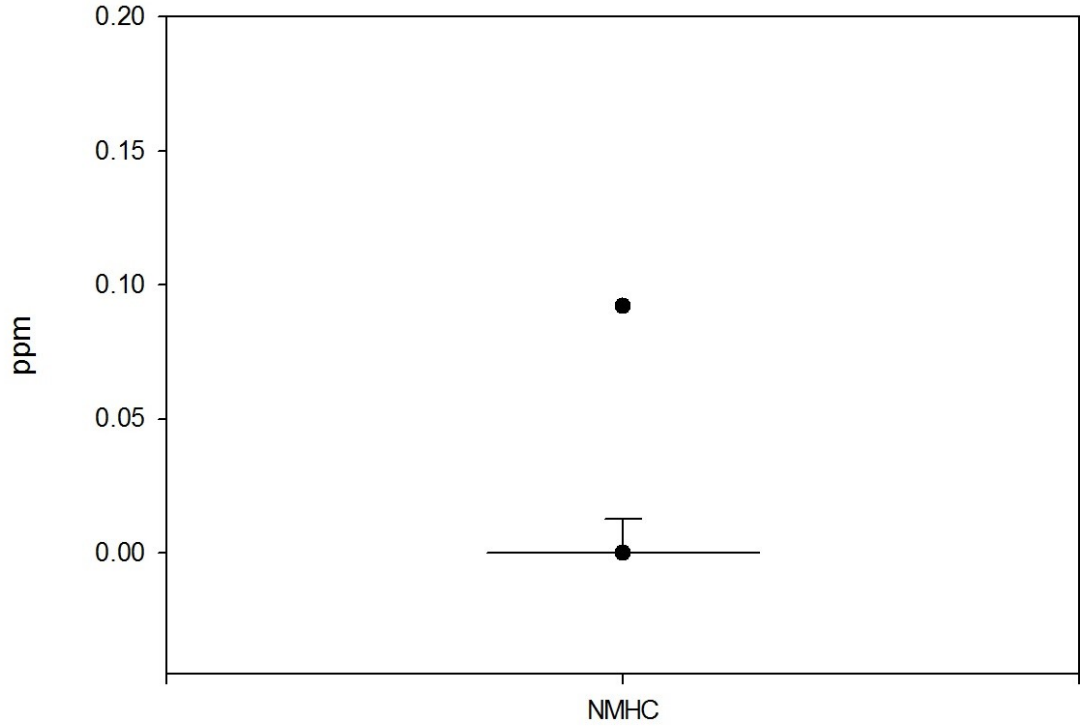

Figure 23. Box plot of NMHCs.

From Figure 23 we can see a median value for NMHCs of 0 ppm. This is due to the fact that the majority of readings taken by the Thermo Scientific 55i were zero readings with intermittent spikes. The 95th percentile is just below 0.1 ppm, indicating the relatively small range of data.

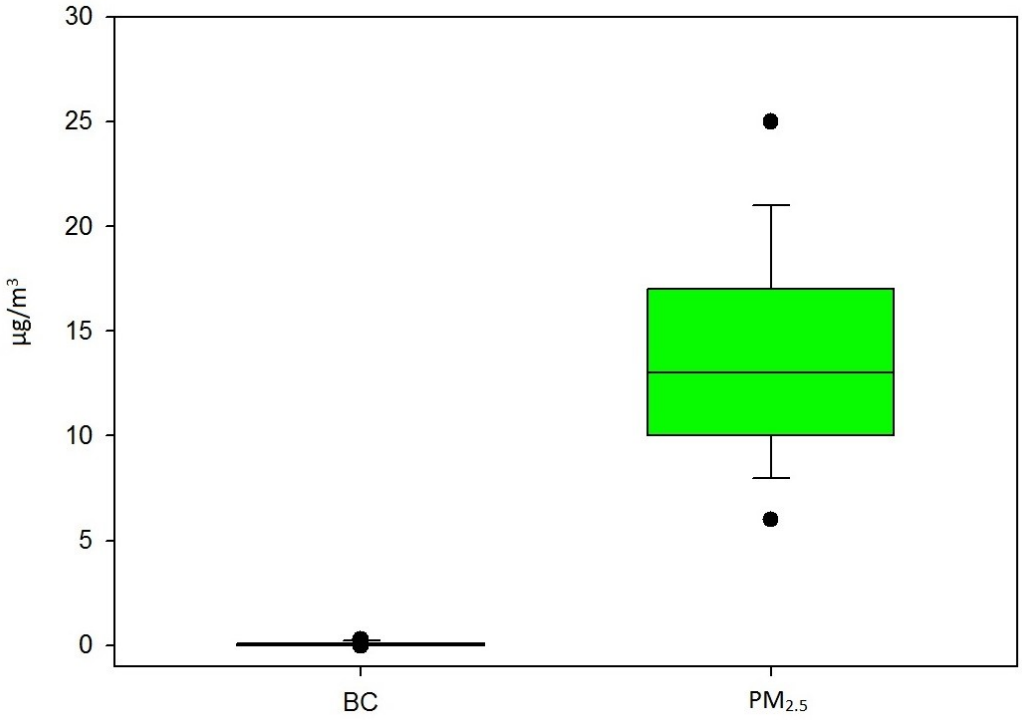

Figure 24. Box plot of Black Carbon and $PM_{2.5}$.

Figure 24 compares BC and $PM_{2.5}$ and shows that median values of $PM_{2.5}$ are considerably higher, which is to be expected as BC is generally a component of $PM_{2.5}$. $PM_{2.5}$ also shows a much greater range of values than BC. This is due to the presence of $PM_{2.5}$ in many sources where BC tends to be associated with a more limited number (Gibson et al., 2013). It should be noted that sea salt is a major contributor to $PM_{2.5}$ (Waugh et al., 2010) and this would likely be part of the reason for higher $PM_{2.5}$ concentrations on a heavily marine influenced location such as Sable Island.

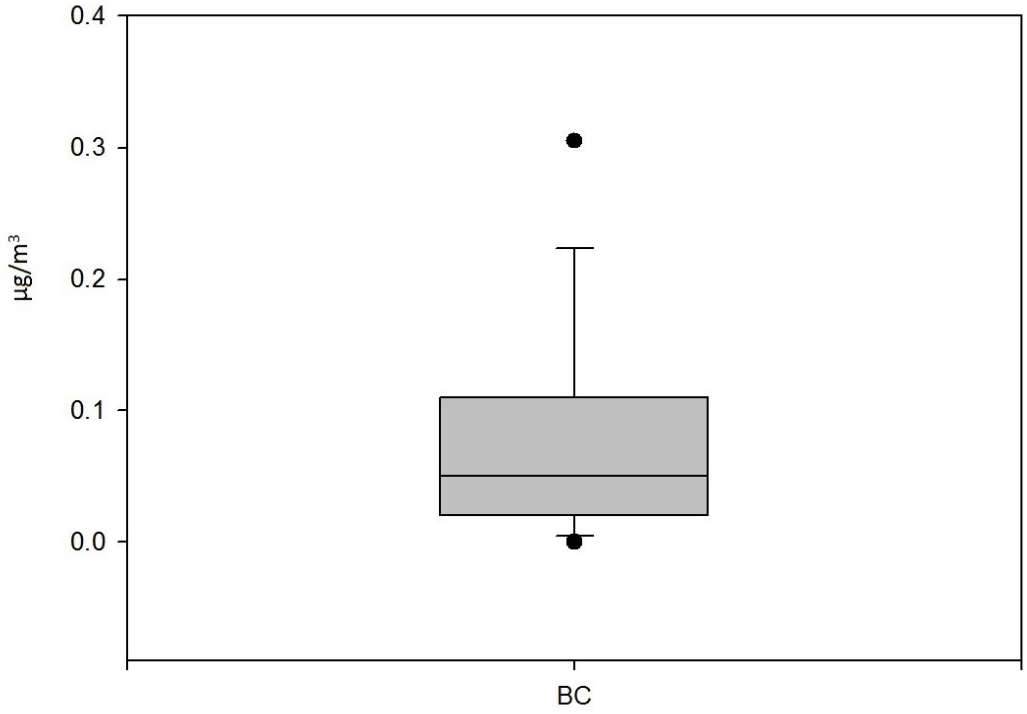

Figure 25. Box plot of Black Carbon.

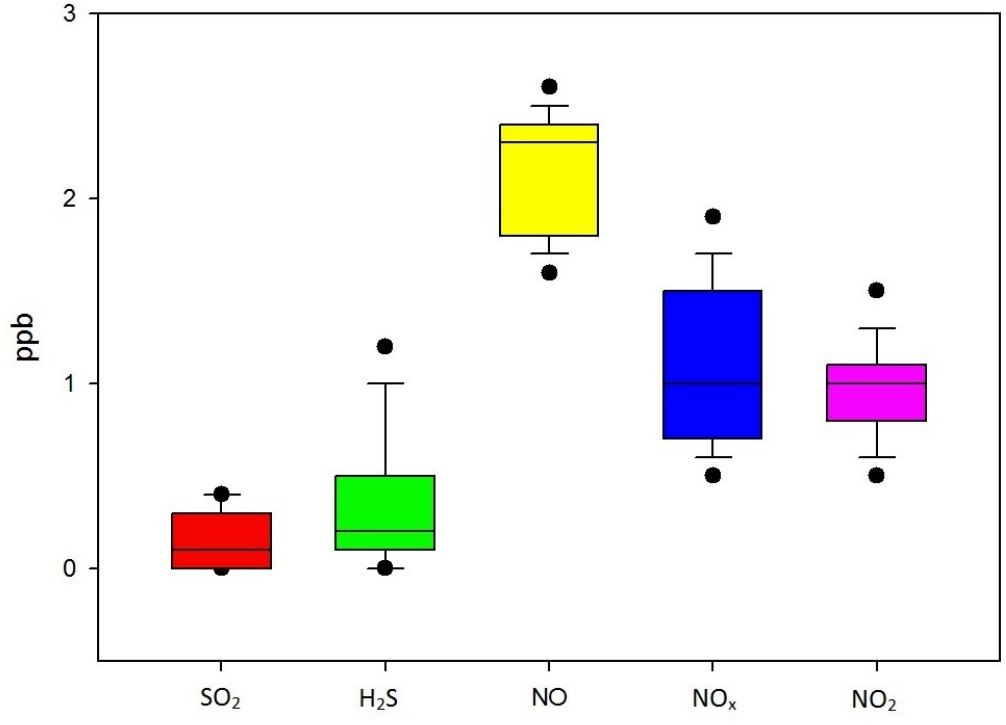

Figure 26. Box plot of SO_2, H_2S, NO, NO_x, and NO_2.

Figure 26 shows box plots for SO_2, H_2S, NO, NO_x, and NO_2. They show similar ranges and median values with NO exhibiting slightly higher values. This is likely due to the large pollution contribution from on-site combustion (including the burning of garbage) of which NO is a large contributor.

4.2 Source Apportionment

4.2.1 PMF Model Run and Results

The outputs from the USEPA PMF model v3.0.2.2 run will be presented in this section. The model was run using 20 base runs and 4 factors. The bootstrap and Fpeak models were also applied to the data. The bootstrap model was performed on Run 15 with 100 bootstraps and a minimum correlation R-value of 0.6. The seed was random and the block size 6. The Fpeak model was run for one Fpeak with a strength of 0.1. As can be seen from the tables below, all runs converged for Q (Robust) and Q (True) and the Fpeak run also converged. In this section predicted and observed concentrations for the base model run, variability in concentration and percentage of species for the bootstrap runs, Fpeak factor profiles and concentrations, and seasonal contributions are shown. Dates shown in figures are in the format dd/mm/yy.

Table 5. PMF base run summary.

Run #	Q(Robust)	Q(True)	Converged	# Steps
1	4129.34	5524.53	Yes	2710
2	4137.42	5445.12	Yes	1593
3	4533.56	6068.03	Yes	2296
4	4533.79	6068.01	Yes	3284
5	4137.18	5445.12	Yes	1935
6	4388.94	6256	Yes	1420
7	4137.82	5444.95	Yes	1772
8	4129.16	5524.38	Yes	2553
9	4110.8	5540.35	Yes	2296
10	4388.98	6256.46	Yes	1645
11	4129.03	5524.31	Yes	2441
12	4128.61	5524.25	Yes	2640
13	4523.98	6134.3	Yes	1086
14	4137.79	5444.94	Yes	1727
15	4109.8	5546.26	Yes	2076
16	4138.46	5445.69	Yes	2290
17	4138.86	5444.88	Yes	2268
18	4128.5	5524.55	Yes	2605
19	4138.17	5444.86	Yes	2026
20	4138.22	5444.93	Yes	1972

It can be seen from Table 5 that for the base model run Q robust and Q true converged for all runs. This demonstrates the stability of the base model run. Q true was found to vary from Q robust by approximately 24 – 30%. This is a less than ideal situation, but is likely due to the impact of large spikes in concentration of species such as NMHC had on the model run.

Table 6. Bootstrap factors mapped to base factors.

	Base Factor 1	Base Factor 2	Base Factor 3	Base Factor 4	Unmapped
Boot Factor 1	70	0	0	2	23
Boot Factor 2	0	38	5	0	52
Boot Factor 3	0	0	88	0	7
Boot Factor 4	0	3	0	86	6

Table 6 shows that out of 380 bootstrap runs, 88 were unmapped. This again demonstrated the impact of spikes in the concentration of certain species on model results.

Table 7. Fpeak Run Summary.

Fpeak #	Strength	Q(Robust)	Q(True)	Converged	# Steps
1	0.1	4111.5	5545.4	Yes	337

Table 7 demonstrates that the Fpeak run converged, showing little rotational ambiguity in the model results.

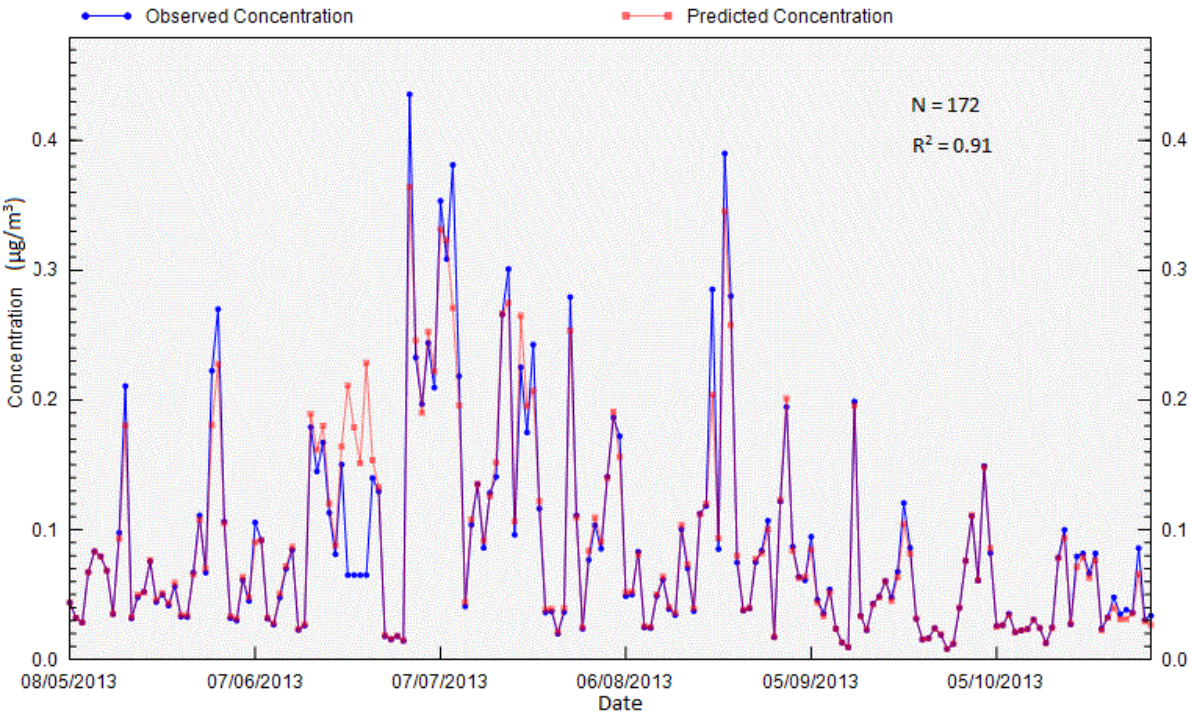

Figure 27. Observed and Model Predicted concentrations of BC.

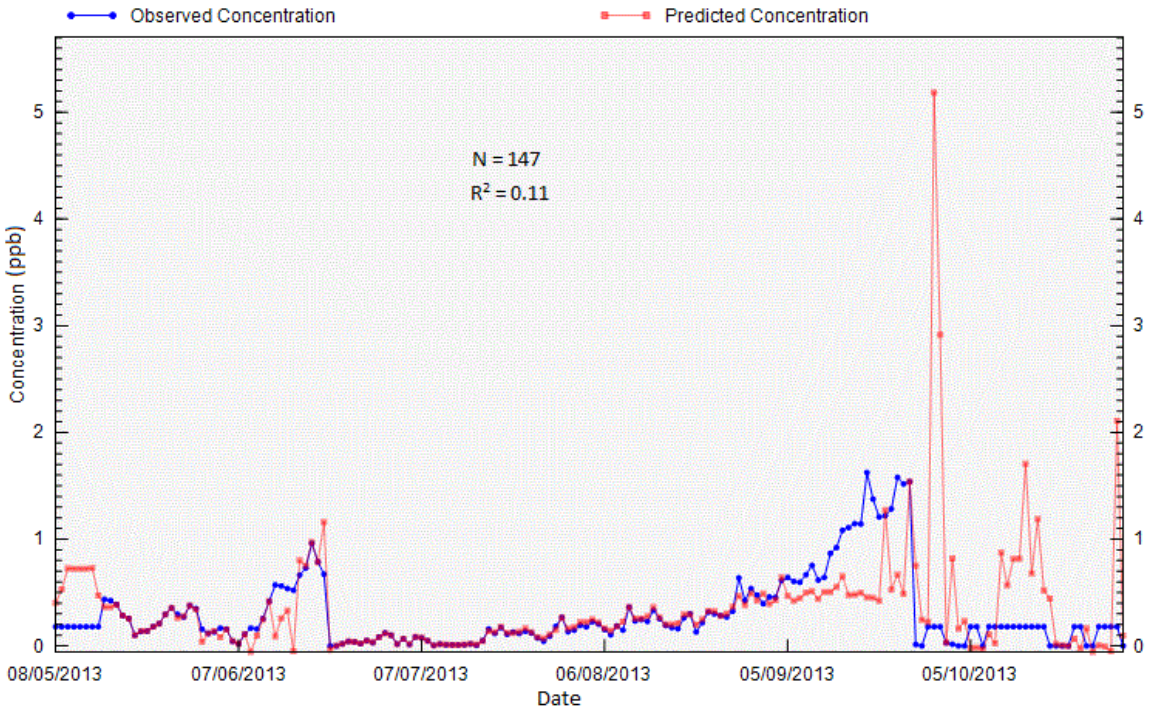

Figure 28. Observed and Model Predicted concentrations of H_2S.

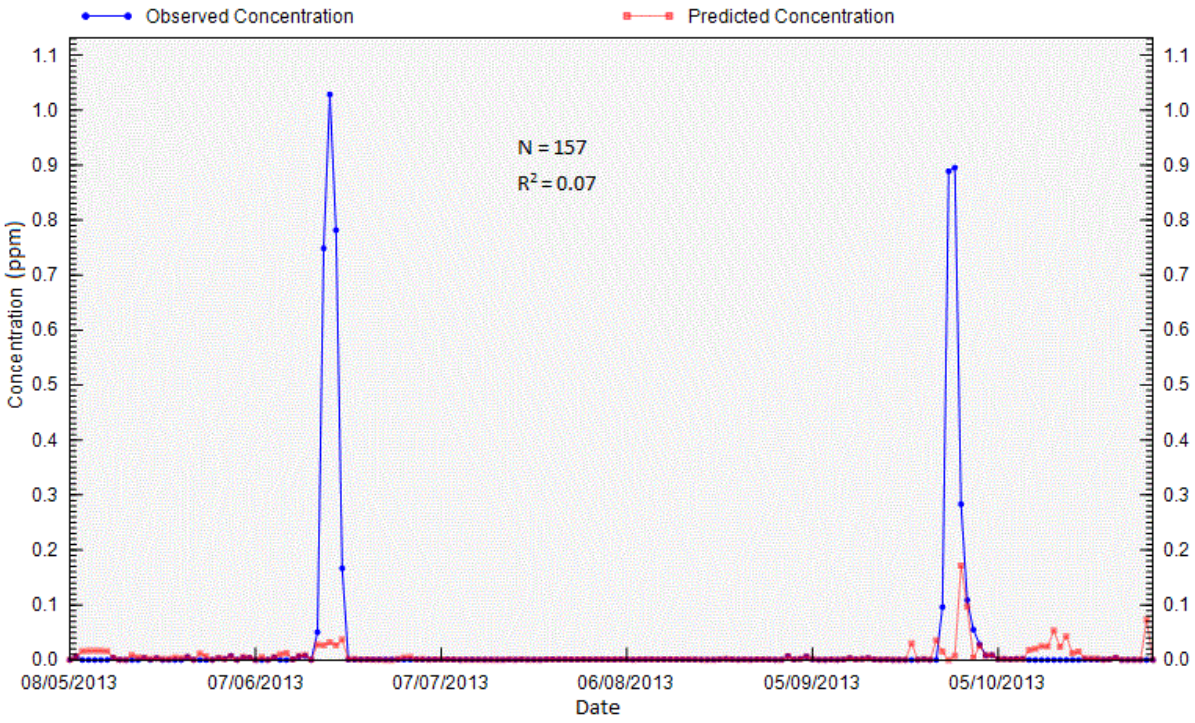

Figure 29. Observed and Model Predicted concentrations of NMHC.

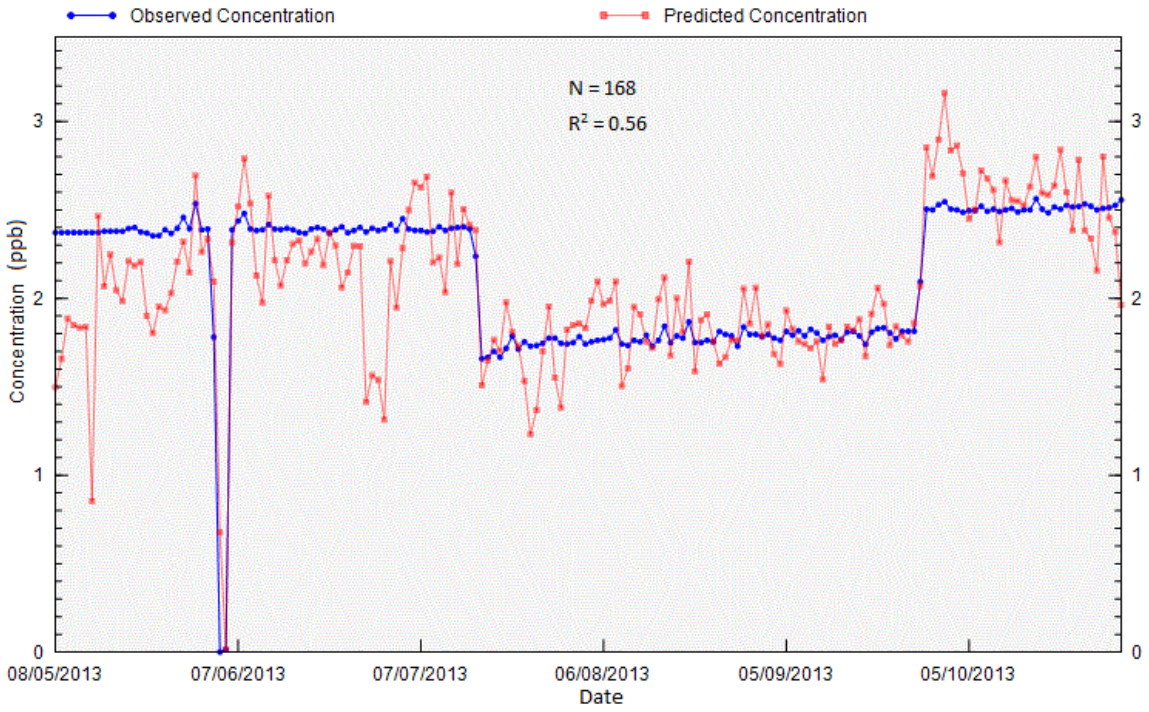

Figure 30. Observed and Model Predicted concentrations of NO.

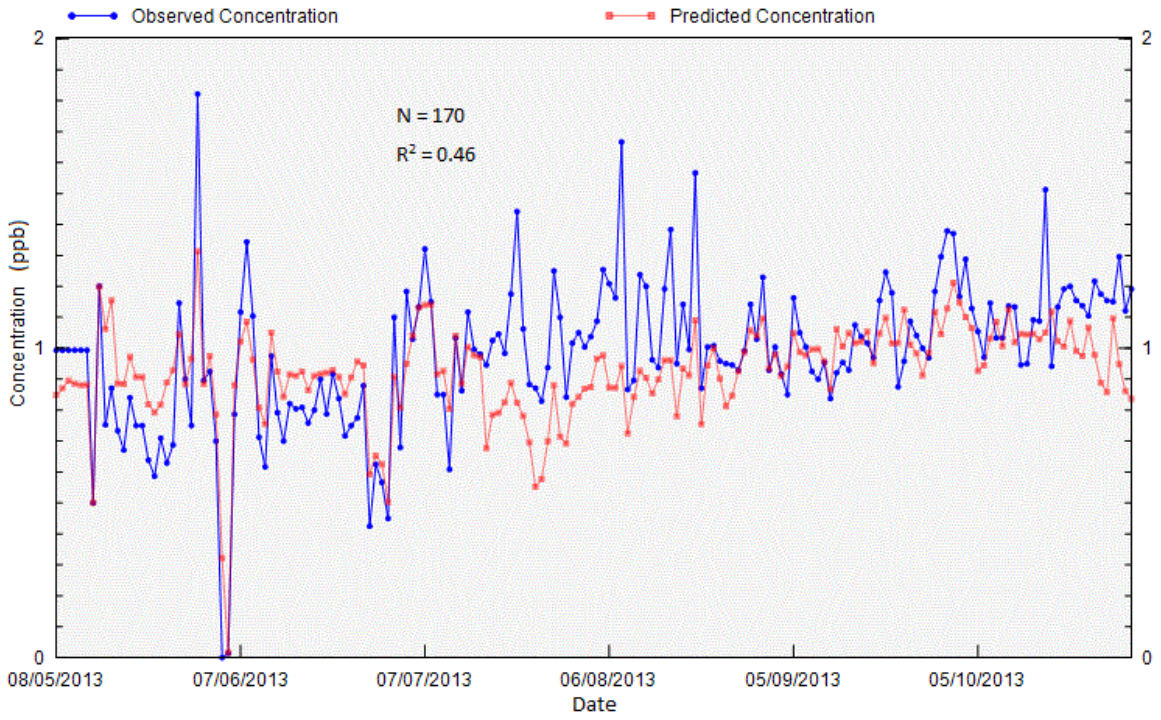

Figure 31 Observed and Model Predicted concentrations of NO_2.

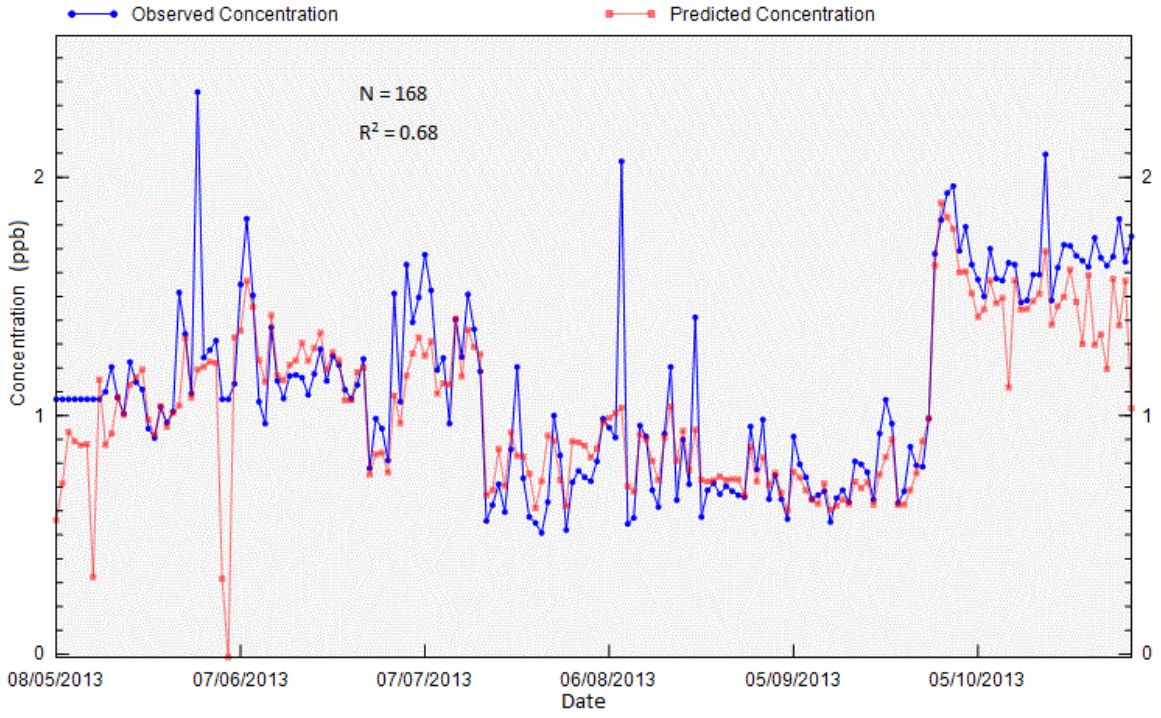

Figure 32. Observed and Model Predicted concentrations of NO_x.

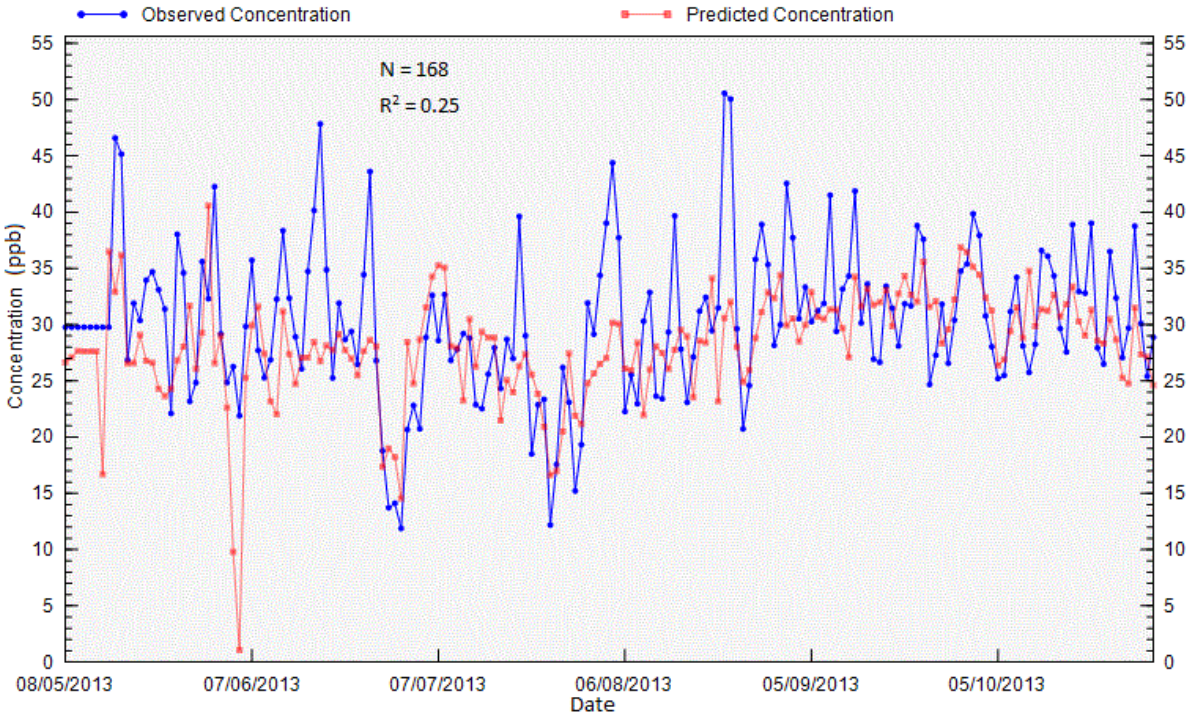

Figure 33. Observed and Model Predicted concentrations of O_3.

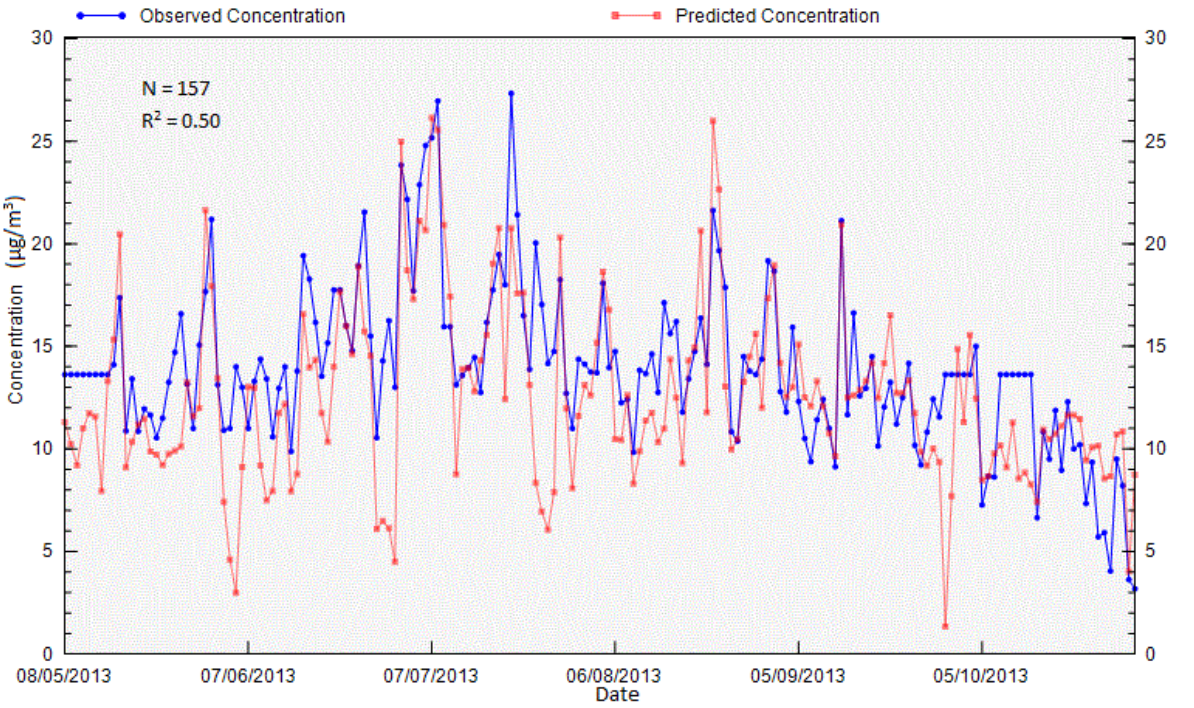

Figure 34. Observed and Model Predicted concentrations of $PM_{2.5}$.

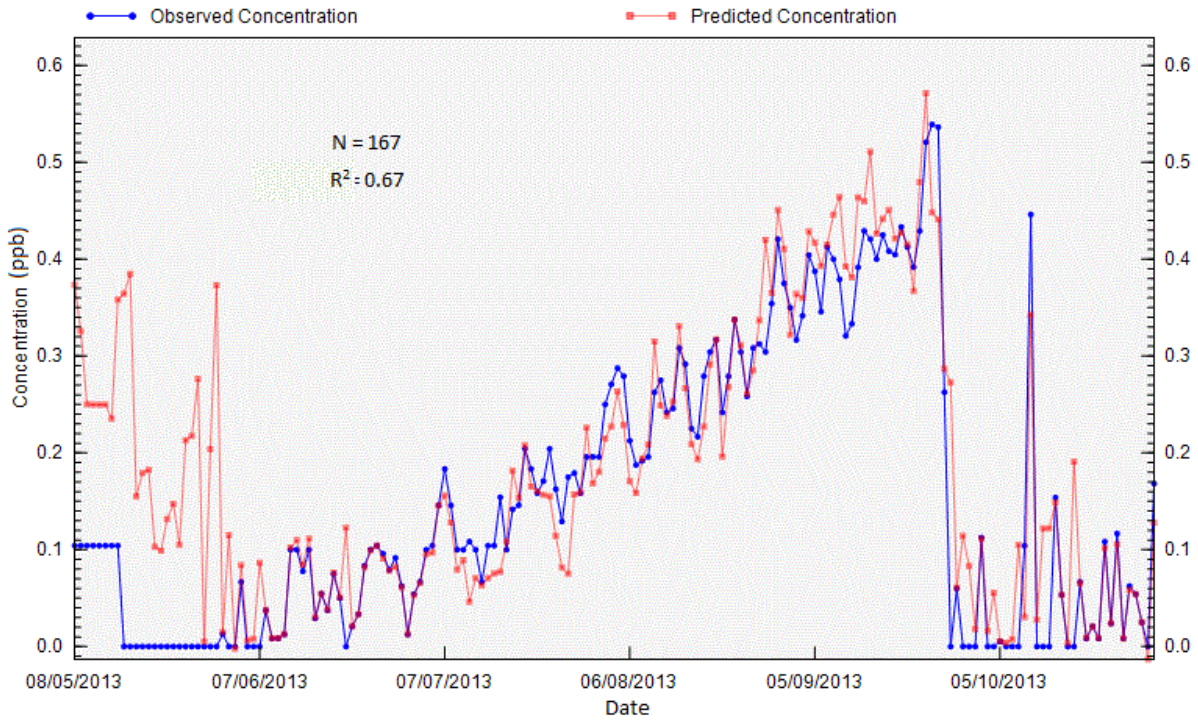

Figure 35. Observed and Model Predicted concentrations of SO_2.

When the plots of observed and model predicted concentrations (Figures 27 – 35) are examined, it can be seen that the highest R^2 values exist for BC, SO_2, NO, NO_x, and NO_2 (>50%) while those for the other species are lower (<50%). The model had the most trouble with species such as NMHC concentrations which generally were measured at low concentrations but periodically exhibited increased concentration spikes. This reinforces what was found when comparing Q true with Q robust.

The model was initially run for between 3 – 10 factors. When 3 factors were run it was found that the factors representing LRT and on-site combustion were blended together, giving a result with the same chemical characteristics of both factors together. That is to say, a factor with high contributions from $PM_{2.5}$, BC, SO_2, NO, NO_x, and NO_2. In reality, and as will be discussed further in the following sections, when split into 2 factors this

scenario describes LRT and on-site combustion more satisfactorily. When more than 4 factors were run it was found all factors with the exception of off-gassing were split into smaller and smaller factors with smaller and smaller contributions and virtually the same chemical fingerprint. Consideration of the model outputs, the number of species monitored, and knowledge of the potential sources impacting Sable Island were considered in the decision to optimally run the model for 4 factors (corresponding to 4 major sources)

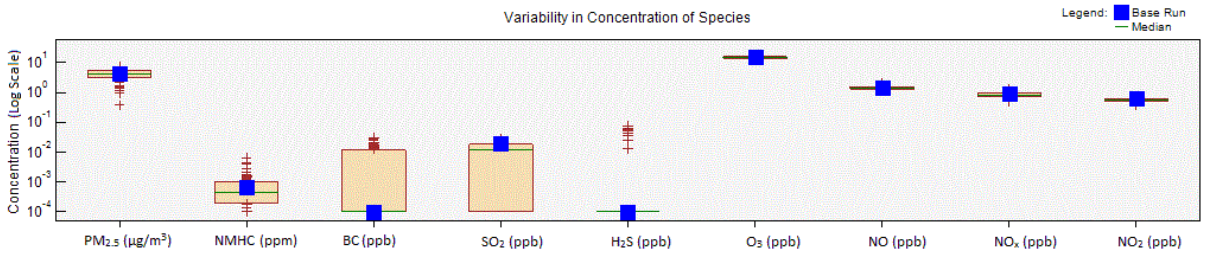

Figure 36. Variability in concentration of species for LRT (Factor 1).

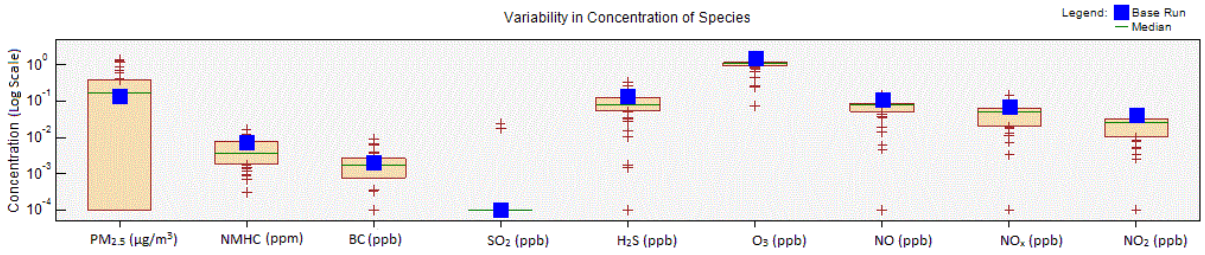

Figure 37. Variability in concentration of species for Off-gassing (Factor 2).

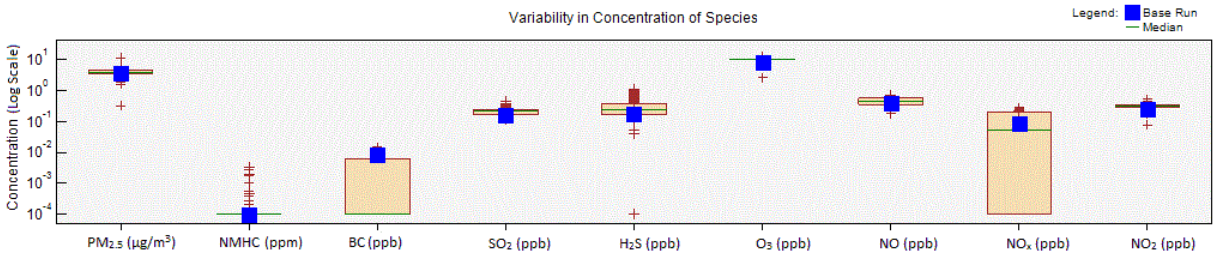

Figure 38. Variability in concentration of species for Flaring (Factor 3).

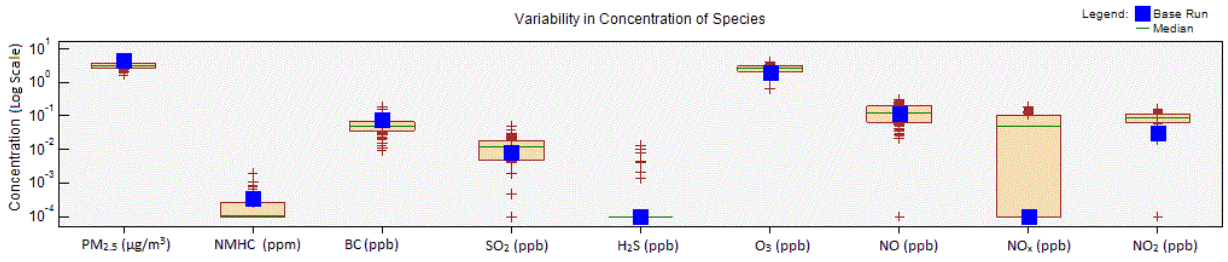

Figure 39. Variability in concentration of species for On-site combustion (Factor 4).

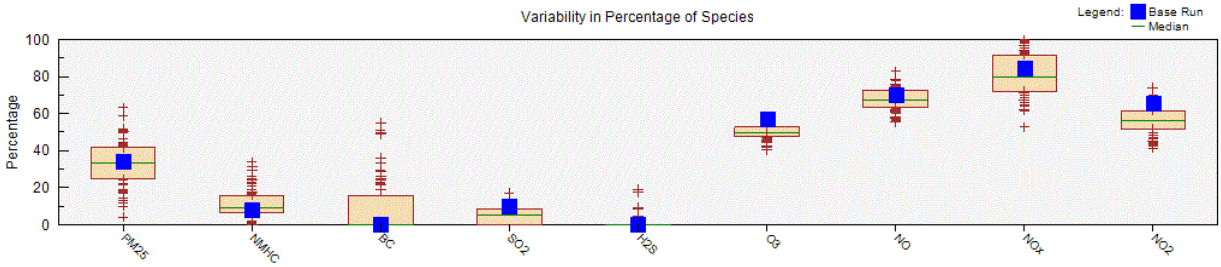

Figure 40. Variability in percentage of species for LRT (Factor 1).

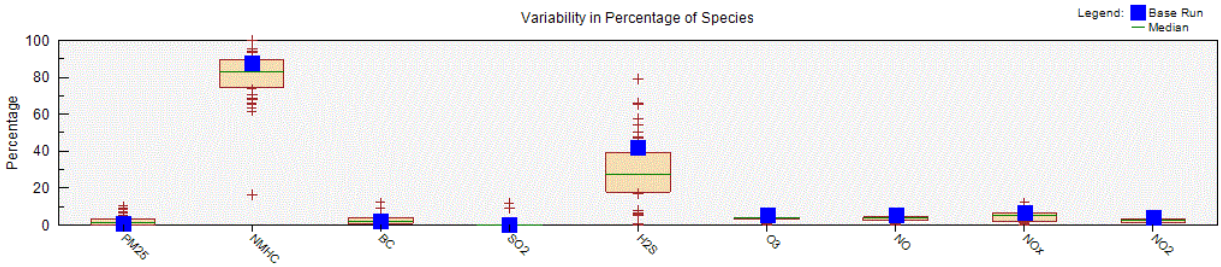

Figure 41. Variability in percentage of species for Off-gassing (Factor 2).

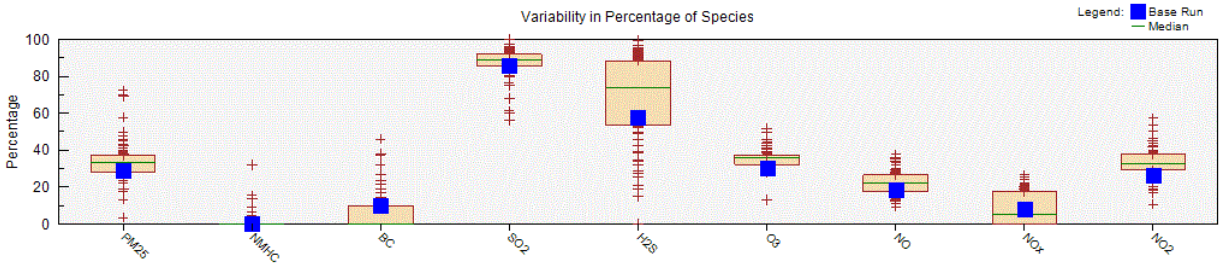

Figure 42. Variability in percentage of species for Flaring (Factor 3).

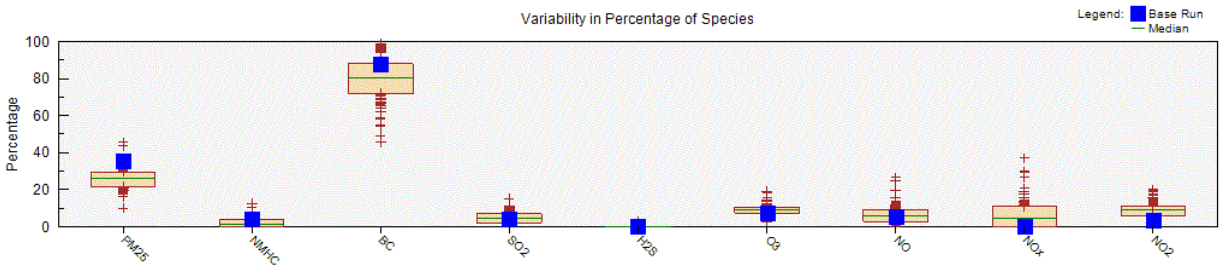

Figure 43. Variability in percentage of species for On-site Combustion (Factor 4).

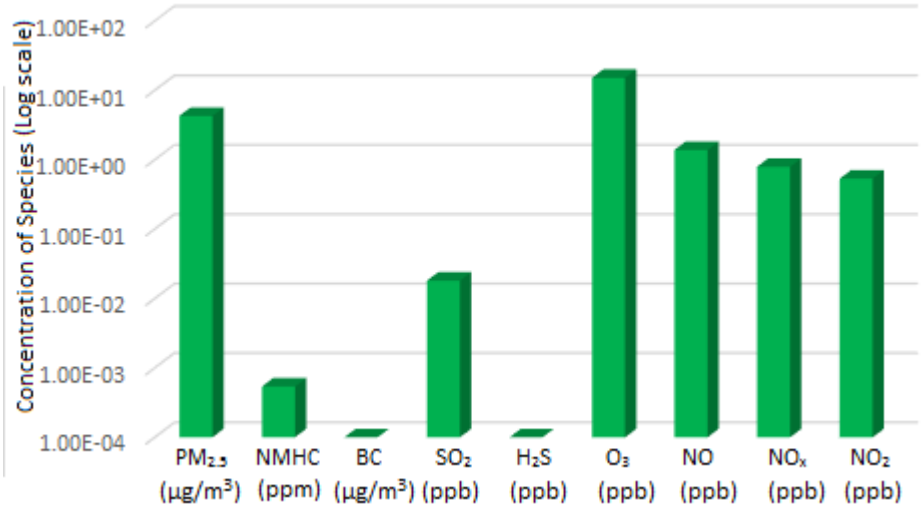

Figure 44. Fpeak Factor Profile for LRT (Factor 1).

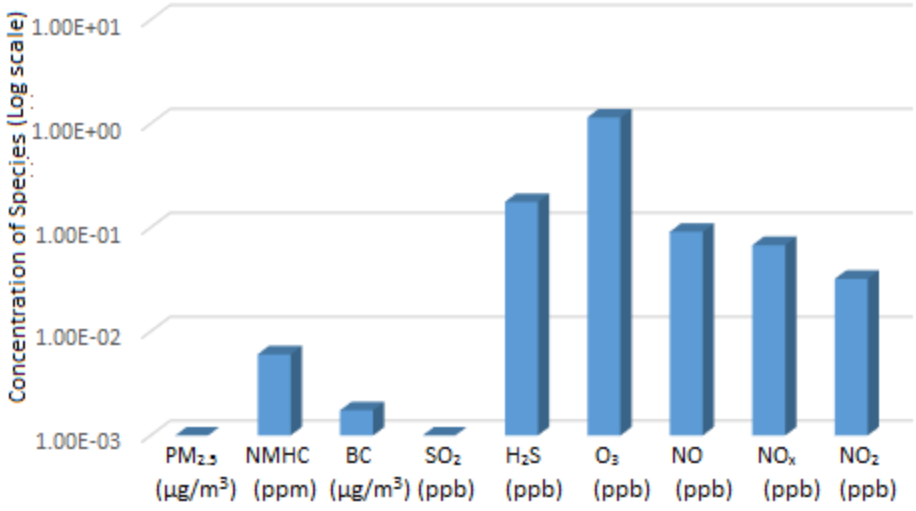

Figure 45. Fpeak Factor Profile for Off-gassing (Factor 2).

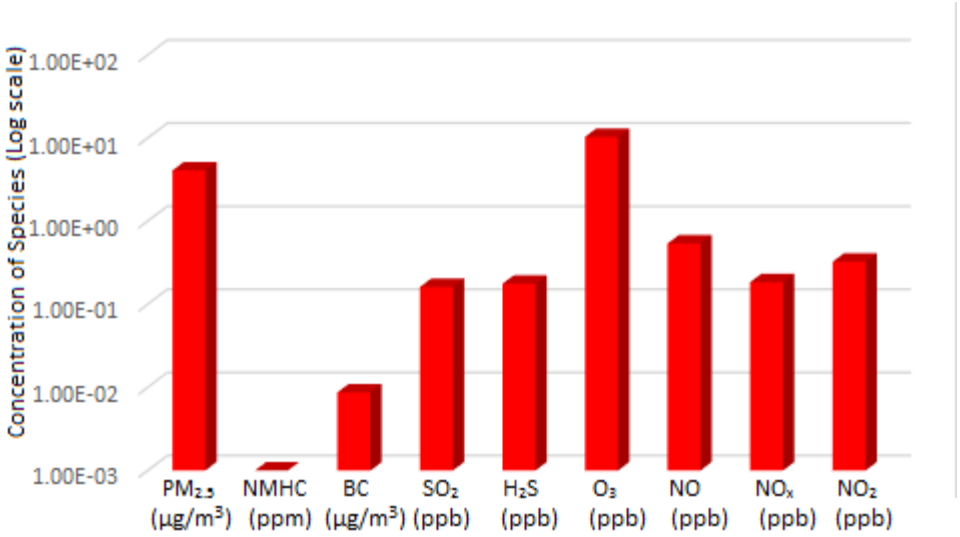

Figure 46. Fpeak Factor Profile for Flaring (Factor 3).

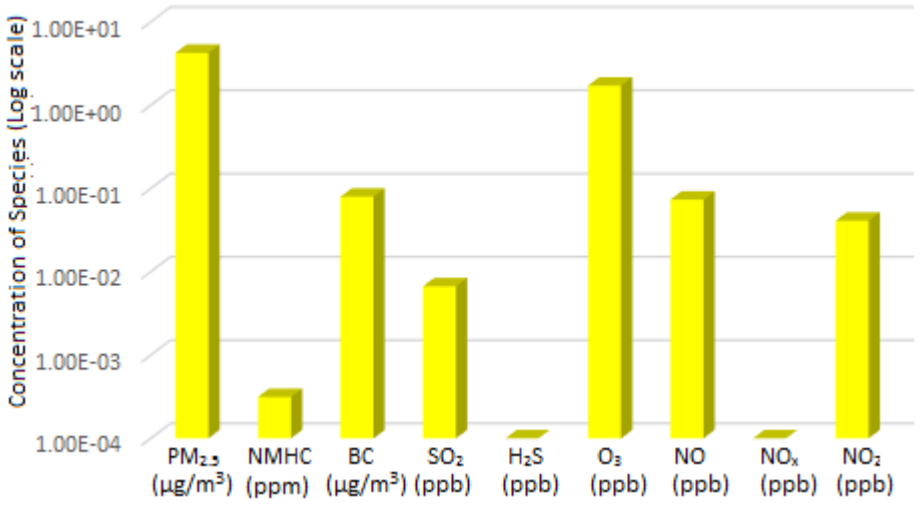

Figure 47. Fpeak Factor Profile for On-site Combustion (Factor 4).

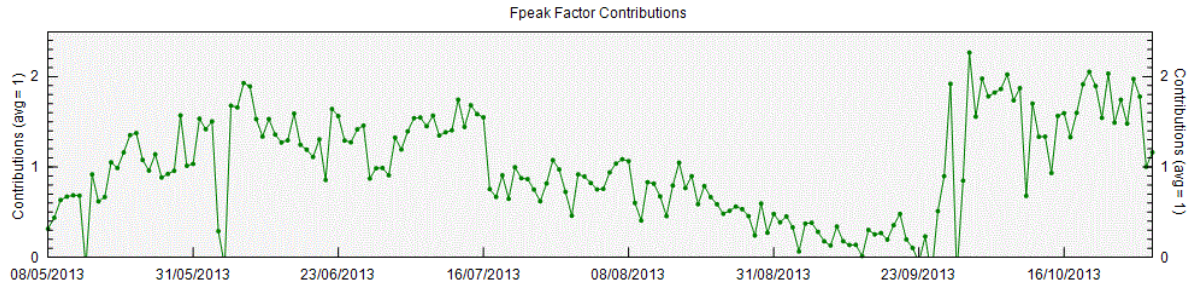

Figure 48. Fpeak Factor Contributions for LRT (Factor 1).

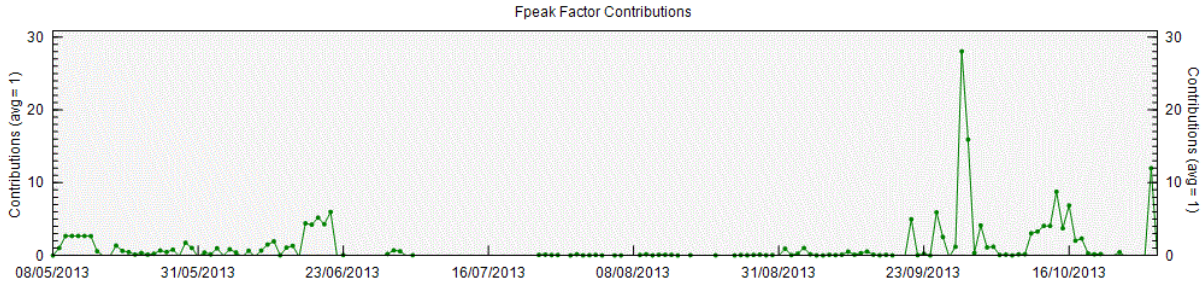

Figure 49. Fpeak Factor Contributions for Off-gassing (Factor 2).

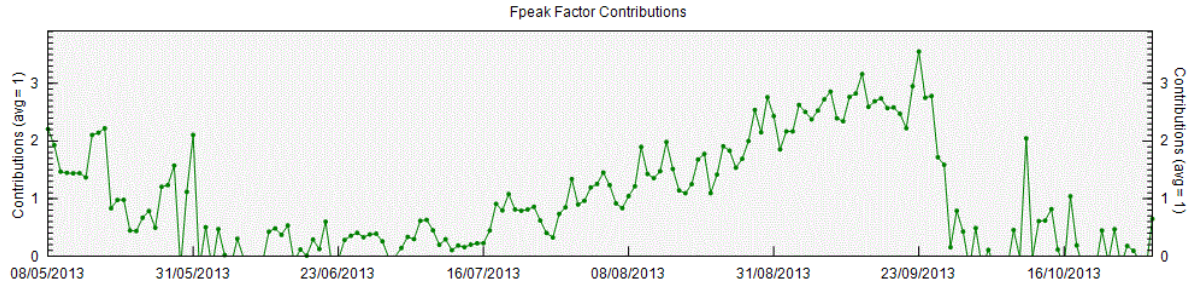

Figure 50. Fpeak Factor Contributions for Flaring (Factor 3).

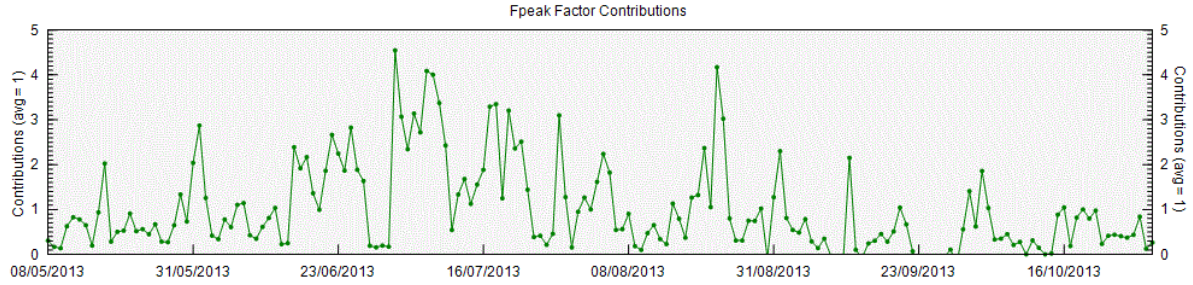

Figure 51. Fpeak Factor Contributions for On-site Combustion (Factor 4).

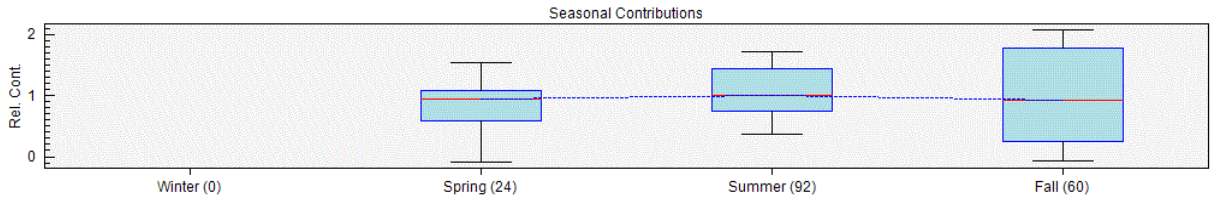

Figure 52. Seasonal contributions for LRT (Factor 1).

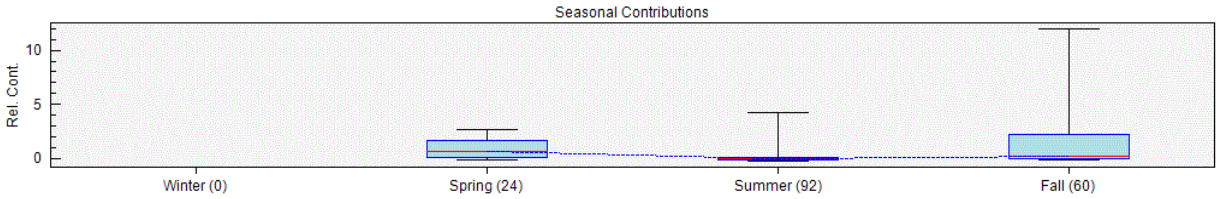

Figure 53. Seasonal contributions for Off-gassing (Factor 2).

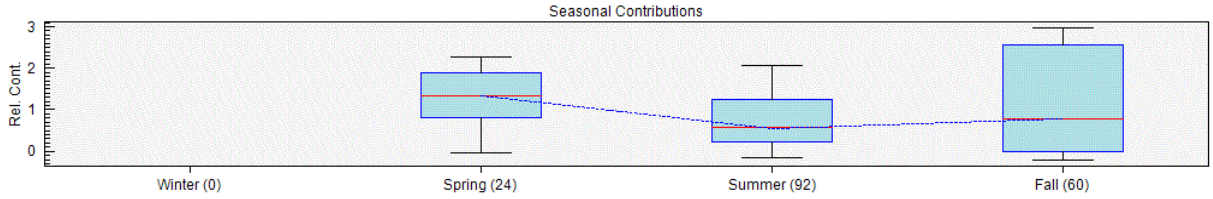

Figure 54. Seasonal contributions for Flaring (Factor 3).

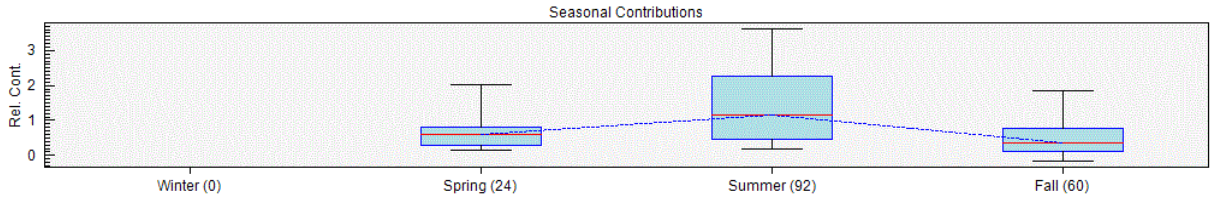

Figure 55. Seasonal contributions for On-site Combustion (Factor 4).

Figure 44 shows the profile for Factor 1. Factor 1 was determined to be contributions from LRT. Factor 1 had high contributions from $PM_{2.5}$, which is typical of LRT (Ward et al., 2006). The high contribution from O_3 indicated a more aged aerosol where ozone formation reactions have had time to take place, and the SO_2 contribution is low (SO_2 being indicative of a local source). Contributions of NO, NO_x, and NO_2 indicate

combustion sources which would fit with LRT transport sources originating from the mainland and consisting of industrial emissions and domestic heating, largely from fossil fuel combustion (Gibson et al., 2009a, Gibson et al., 2013b).

Factor 2 was determined to be off-gassing from offshore O&G activities by the presence of O_3 (a marker for LRT) and the low contributions from $PM_{2.5}$ and BC. As seen in Figure 45, the low contributions from $PM_{2.5}$ and BC are indicative of gaseous emissions with relatively large contributions from NMHCs, NO_x, and H_2S (when compared to other sources) indicating offshore oil and gas activity fugitive emissions as the likely source (Beusse et al., 2013). The strong correlation of O_3 with this factor was likely due to the impact of VOCs on its formation (Jacob, D.J., 1999).

It should be noted that emissions of VOCs from phytoplankton blooms also contribute to a percentage of this factor. Analysis of pollution events showed that during certain periods of time, phytoplankton blooms can contribute significantly to NMHC concentrations. Without a GC-MS to perform VOC speciation it is difficult to apportion exact VOC emissions from offshore oil and gas compared to phytoplankton blooms. Although phytoplankton blooms can be a major contributor of VOCs (Colomb et al., 2008) the high contributions from H_2S and NO_x indicate that Factor 2 is still representative of off-gassing from offshore oil and gas activities (Beusse et al., 2013). A Spearman rank order correlation was run in SigmaPlot and found that NMHC and H_2S concentrations were significantly correlated (correlation coefficient = 0.107, P = 0.0000000446), supporting that Factor 2 is representative of off-gassing. The results of the spearman rank order correlation can be found in Figure 72 in the Appendix. Figure 49 shows that contributions from Factor 2 can be seen to increase after July 22nd, which

would fit well with off-gassing emissions associated with bringing new oil and gas activity online. Furthermore, the study was run mainly over the summer months, therefore likely missing the spring and some of the autumn phytoplankton blooms (Georges et al., 2014; Craig et al., 2011). In future work however, GC-MS speciation of VOC species will be undertaken as part of the Sable Island Study to examine in detail the contribution from marine biogenic emission on Sable Island.

Figure 46 shows the profile for Factor 3. Factor 3 was determined to represent Flaring from offshore oil and gas activity. Profile contributions from $PM_{2.5}$, and BC are indicative of combustion while H_2S, SO_2, and NO_x are characteristic of flaring from offshore oil and gas activity (Beusse et al., 2013). H_2S is a strong indicator in this study of offshore oil and gas activity, only contributing to the factors associated with it. NMHC concentrations are minimal, which is likely due to the fact that they would be burned off during flaring. It can be seen from Figure 50 that factor contributions for Factor 3 increase drastically after July 22nd correlating with increased flaring from new offshore O&G activity. All of these observations together support that Factor 3 represents flaring from offshore O&G activity.

Figure 47 shows the profile for Factor 4. Factor 4 was determined to be on-site combustion. On-site combustion would include local emissions such as transportation emissions to and from both the island and offshore facilities by aircraft and ships, emissions from passing ships, and most importantly, localized emissions on the island itself related to electricity generation (diesel generator) and waste incineration. The latter would likely contribute the largest portion to factor 4. High contributions from $PM_{2.5}$ and BC indicate incomplete combustion from sources such as the diesel generator used for

power generation or localized ship emissions (Gibson et al., 2013). Contributions from SO_2, NO, and NO_2 also indicate the diesel generator and transportation sources (Harrison et al., 1997). Figure 51 shows that the Fpeak factor contributions for on-site combustion decrease during the warmer summer months when less electricity is needed for heating purposes. All of this information provides support for factor 4 being representative of on-site combustion.

4.2.2 Examination of Pollution Events

Pollution events for NMHCs and $PM_{2.5}$ were examined using HYSPLIT back trajectories. Instances where NMHC concentrations exceeded 0.1 ppm and where $PM_{2.5}$ concentrations exceeded 30 $\mu g/m^3$ were considered to be pollution events. For NMHCs the direction of the back trajectory source was examined in order to correlate emissions with the rigs. Additionally, 8-day averages of chlorophyll concentration were examined to ascertain if they could be contributing to NMHC pollution events. These were obtained from the National Aeronautics and Space Administration (NASA) Giovanni website (http://gdata1.sci.gsfc.nasa.gov/daac-bin/G3/gui.cgi?instance_id=ocean_8day). Generated using MODIS Aqua satellite imagery, the 8-day composites of chlorophyll concentrations helped to compensate for cloudy periods that cause patchy coverage and can be found in Figures 73 – 78 in the Appendix. For $PM_{2.5}$ pollution events the area of the North American continent from which the air parcels originated was examined to determine if LRT was the cause. Maps of Canadian fire hotspots obtained from Natural Resources Canada were examined to determine if forest fires may have contributed to these $PM_{2.5}$ pollution events (http://cwfis.cfs.nrcan.gc.ca/maps/fm3?type=fwih&year=2013&mo

nth=10&day=31). Instances of fires on the Eastern Seaboard of the US were also examined. They were obtained from the United States Department of Agriculture (USDA) Active Fire Mapping Program (http://firemapper.sc.egov.usda.gov/index.php). The maps of fire activity and daily HYSPLIT back trajectories for the entire sampling period can be found in Figures 78 – 91 and Figure 61 in the Appendix.

From the time series for NMHCs pollution events were identified as having occurred on June 18th – 20th, September 1st, 4th, 5th, 11th, 13th, and 14th, 27th – 30th, and October 24th 2013. For the pollution events occurring on June 18th – 20th, the air parcels originated to the SW as well as to the N from Nova Scotia and the mainland on June 20th as can be seen in Figure 61. Offshore O&G activities take place to the SW of Sable Island as can be seen in Figure 2. Figure 73 shows an 8-day composite of chlorophyll concentrations for June 18th and it can be seen that concentrations around Sable Island are in the 0.7 – 1 mg/m^3 range with concentrations around Nova Scotia and the Eastern Seaboard of the US as high as 10-30 mg/m^3 in small isolated pockets.

For the pollution events on September 1st, 4th, 5th, and 11th the air parcels originated to the SW. On the 11th the air parcel impacting Sable also passed over Nova Scotia. For the air pollution event on September 13th-14th the air parcels originated from the S as can be seen in Figure 61. Offshore O&G activities take place to the S and SW as shown in Figure 2. Figure 75 shows chlorophyll concentrations for August 21st – September 14th and it can be seen that concentrations S and SW of Sable Island are in the 0.7 – 1 mg/m^3 range with concentrations in small areas around Nova Scotia and the Eastern Seaboard of the US as high as 10 - 30 mg/m^3.

For the pollutions event from September 27th – 30th the air parcel originated from the N, N, W, and SE with the air parcels having passed over or near the coast of Nova Scotia as can be seen in Figure 61. Offshore O&G activity is located to the SE of Sable. Figure 76 shows chlorophyll concentrations for September 22nd – September 30th. It can be seen that concentrations around Sable Island are as high as 2.5 – 10 mg/m^3 and near the coast of Nova Scotia as high as 10 - 30 mg/m^3.

On October 24th the wind direction was from the SSW and the air parcel at one point passed over the SW tip of Nova Scotia as can be seen in Figure 61. Offshore O&G activities are located to the SSW of Sable Island as can be seen in Figure 2. Figure 77 shows chlorophyll concentrations for October 16th – October 24th and it can be seen that elevated concentrations exist around Sable and the throughout the Scotian Shelf with concentrations in many areas reaching the 10 – 30 mg/m^3 range.

All of the back trajectory directions correlate with the direction of offshore O&G activities as can be seen from Figure 2 in the literature review. Figure 74 shows 8-day composites of chlorophyll concentrations for July 28th – August 5th. This was done for comparison as this period of time exhibited low concentrations of NMHCs on Sable Island. The concentrations seem to be higher than in June, but similar to those in August and September, however a notable increase into October appears to take place that may correspond to the beginning of an autumnal bloom. From this examination it appears that phytoplankton blooms may have impacted the events in late August and September and likely impacted the events in October. The results of examining HYSPLIT back trajectories when coupled with this enforce the conclusion that off-gassing and flaring from the rigs is likely the major source of NMHCs on Sable Island with phytoplankton

blooms likely contributing. It should be noted that there is a caveat to using standard ocean colour chlorophyll products in coastal regions. The Nova Scotian current influences the ocean waters surrounding Sable Island, and receives waters from the Gulf of St. Lawrence (Hannah et al., 2001), which may contain coloured dissolved organic matter (CDOM) that can confound the algorithms that are used to estimate chlorophyll from ocean colour (Carder et al., 1989). However, broad seasonal patterns were well reproduced in the NASA GIOVANNI satellite estimates of chlorophyll. For the qualitative purpose of this study, the use of the 8-day composites was acceptable

$PM_{2.5}$ pollution events were identified as having occurred on June 24th, 26th, July 2nd, 8th, 18th – 20th, 28th, August 16th, 31st, September 12th, and October 4th 2013. For June 24th and 26th the air parcel originated over the Eastern Seaboard of the US as can be seen in Figure 61. Figure 85 and 86 show the fire activity detected by the MODIS satellite for June 24th and 26th as obtained from the USDA Active Fire Mapping Program. It can be seen that fire activity was detected in the 6 days prior to the pollution event and likely contributed.

For July 2nd the air parcel originated over Quebec and Nova Scotia before arriving at Sable Island as can be seen in Figure 61. Forest fire activity does not appear to have been particularly active proceeding this event. For July 8th the parcel passed over the eastern US, Ontario, and Nova Scotia as can be seen in Figure 61. A map of Canadian fire hotspots obtained from Natural Resources Canada for July 6th shows a fire index greater than 30 over the area the air parcel impacting Sable Island would have passed over at this time, indicating that forest fires happening in the Quebec and Ontario region likely contributed to this $PM_{2.5}$ pollution event. The map can be seen in Figure 78 in the Appendix. Figure 87 shows fire activity detected by the MODIS satellite for July 8th as

obtained from the USDA Active Fire Mapping Program. It can be seen that forest fires were active in the eastern US, with very recent activity near the great lakes.

For the event from July 18th – 20th the parcel originated on the eastern seaboard of the US and passed over Ontario, Quebec, and Nova Scotia as can be seen in Figure 61. A map of Canadian fire hotspots obtained from Natural Resources Canada for July 16-18th shows a high fire index over the area the air parcel impacting Sable Island would have passed over at this time. Fire index values ranging from 10 to greater than 30 can be seen, indicating that forest fires happening in the Quebec, Ontario, and Nova Scotia region likely contributed to this $PM_{2.5}$ pollution event. The maps can be seen in Figure 79 - 81 in the Appendix. Figure 88 shows fire activity on the eastern seaboard of the US in the 6 days preceding July 20th as well.

The air parcel on July 28th came from Quebec, New Brunswick, and Nova Scotia as can be seen in Figure 61. A map of Canadian fire hotspots obtained from Natural Resources Canada for July 27-28th shows a fire index greater than 30 over an area of Nova Scotia that the air parcel impacting Sable Island would have passed over, indicating that forest fires may have contributed to this $PM_{2.5}$ pollution event. The maps can be seen in Figures 83-84 in the Appendix.

For August 16th the air parcel originated on the eastern seaboard of the US and passed over Ontario and Quebec as can be seen in Figure 61. Figure 89 shows fire activity on the eastern seaboard of the US area that may have contributed. On August 31st, it originated from the eastern seaboard of the US as well as Quebec. Figure 91 shows fire activity on the eastern seaboard of the US preceding this date that may have contributed. On

September 19th, it originated from the eastern seaboard of the US. Figure 92 shows fire activity on the eastern seaboard of the US preceding this date.

Finally, the air parcel impacting Sable Island on October 4th brought pollution from Newfoundland, Quebec, New Brunswick, and Nova Scotia as can be seen in Figure 61. A map of Canadian fire hotspots obtained from Natural Resources Canada for October 4th shows a medium fire index (10-20) over an area in New Brunswick that the air parcel impacting Sable Island would have passed over, indicating that forest fires likely contributed to this $PM_{2.5}$ pollution event. The map can be seen in Figure 84 in the Appendix.

It was hoped that MODIS-Terra satellite imagery obtained from the Active Fire Mapping Program of the USDA (http://firemapper.sc.egov.usda.gov/index.php) could be used to confirm the impact of smoke from forest fires on $PM_{2.5}$ measured on Sable Island on the dates in question. However, cloud cover precluded this on all of the dates in question and allowed limited visibility of the Island.

The results of examining pollution events through HYSPLIT back trajectories reinforce the sources identified through PMF modelling. It was found that the O&G production facilities were most likely the main contributor to pollution events involving NMHCs but that the impact of phytoplankton blooms during certain periods was likely significant. Meanwhile LRT (backed by the associated ozone concentrations) from the eastern United States and Canada that included contributions from forest fire events was most likely the main cause of $PM_{2.5}$ pollution events. The pollution events analyzed can be seen below in Table 8. The examination of both oceanographic and terrestrial sources in concert with

back trajectory models when examining pollution events is a novel approach that yielded positive results.

Table 8. Summary of $PM_{2.5}$ and NMHC pollution events.

Date	Description	Source
June 18th – 20th	NMHC event	Offshore O&G activities
June 24th	$PM_{2.5}$ event	LRT (forest fires likely contributed)
June 26th	$PM_{2.5}$ event	LRT (forest fires likely contributed)
July 2nd	$PM_{2.5}$ event	LRT
July 8th	$PM_{2.5}$ event	LRT (forest fires likely contributed)
July 18th – 20th	$PM_{2.5}$ event	LRT (forest fires likely contributed)
July 28th	$PM_{2.5}$ event	LRT (forest fires likely contributed)
August 16th	$PM_{2.5}$ event	LRT (forest fires likely contributed)
August 31st	$PM_{2.5}$ event	LRT (forest fires likely contributed)
September 1st	NMHC event	Offshore O&G activities
September 4th	NMHC event	Offshore O&G activities
September 5th	NMHC event	Offshore O&G activities
September 11th	NMHC event	Offshore O&G activities
September 12th	$PM_{2.5}$ event	LRT
September 13th	NMHC event	Offshore O&G activities
September 14th	NMHC event	Offshore O&G activities
September 27th – 30th	NMHC event	Likely phytoplankton blooms
October 4th	$PM_{2.5}$ event	LRT (forest fires likely contributed)
October 24th	NMHC event	Likely phytoplankton blooms with contributions from offshore O&G activities

4.2.3 Pollution Rose

A Pollution rose was generated using the statistical analysis program Igor to show the association between factor contributions and the predominant wind direction. Daily factor contributions were plotted against the average wind direction for each corresponding day

for the entire sampling period. The pollution rose can be seen in Figure 56. The factor contributions of LRT, off-gassing, flaring, and on-site combustion were mapped.

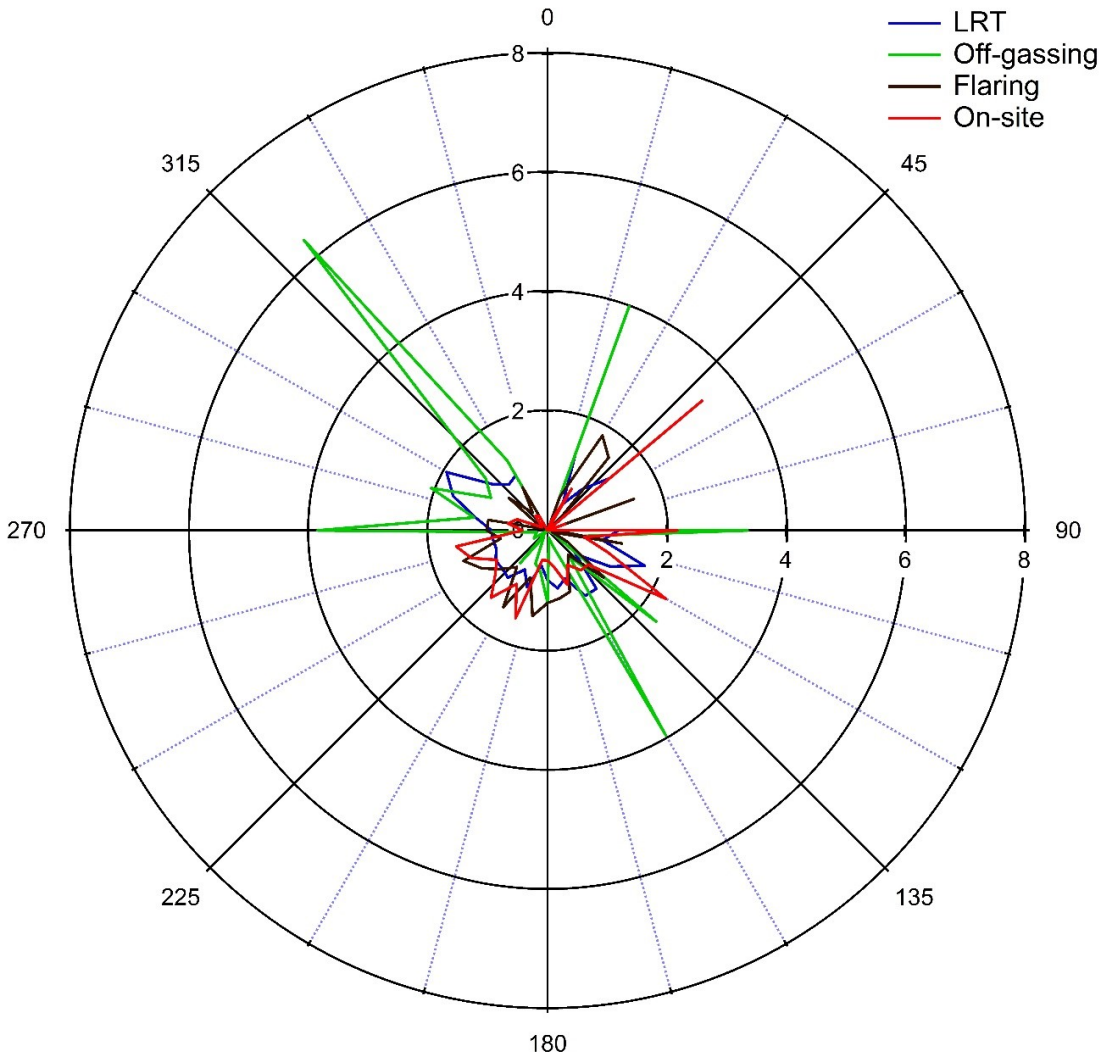

Figure 56. Pollution rose showing association of factor contributions with wind direction.

It can be seen from Figure 56 that wind direction is quite variable and does not come from a predominant direction. This is reinforced by the descriptive statistics of wind speed and direction used in generating the pollution roses. The average wind direction is from 206.5 degrees (SSW) but the data exhibits a large standard deviation (84.05

degrees), sample variance (7064 degrees), and range (360 degrees). A full summary of the descriptive statistics for hourly wind speed and direction can be found in Table 10 in the Appendix. The predominant direction for LRT contributions appears to be to the NW, aligning with the Eastern Seaboard of the United States. For off-gassing, the predominant directions appear to be to the NW, NNE, E, SE, and W. Contributions from NW and NNE are likely a result of contributions from phytoplankton while offshore oil and gas activity is located E, S, and SE of Sable Island as can be seen from Figure 2. HYSPLIT back trajectories reinforce that the rigs are likely the main contributors to NMHC concentrations on Sable Island with phytoplankton blooms perhaps contributing significantly during certain time periods. Contributions from flaring come predominantly from the SE to W directions, again fitting with the location of offshore oil and gas activities. On-site emissions come mainly from the SE to SW. The diesel generator as well as garbage burning takes place in this direction, again correlating well with the predominant wind direction that factor contributions originate from. Contributions coming from other directions attributed to on-site combustion could be due to localized transport in the form of ships, aircraft, and vehicles on the island.

4.3 Impact of New Offshore O&G Production

As outlined previously, the data was split to look for potential differences before and after the start up and commissioning of a new oil and gas platform just off the Coast of Sable Island. The data was split around the date of July 22nd 2013. This was the date when the hook-up and commissioning phase for the new oil and gas activity was initiated (Canada – Nova Scotia Offshore Petroleum Board, 2013). The non-parametric Mann-Whitney statistical test was run in Miniplot. This test was chosen as the data sets contained different numbers of data points. Box plots were generated in SigmaPlot in order to compare the different distributions of the two data sets. A Mann-Whitney statistical test revealed significant differences between the pre and post split data subsets for concentrations of BC, $PM_{2.5}$, SO_2, H_2S, O_3, NO, NO_x, and NO_2. After adjusting for ties all p-values were < 0.05. NMHC was the only pollutant that showed no statistically significant difference with a p-value of 0.2019 after adjusting for ties. Results of the test can be found in Figure 71 in the Appendix. Descriptive statistics and box plots were generated and are presented in Table 9.

Table 9. Descriptive Statistics for all species before and after July 22nd 2013.

Variable	Mean	Standard Deviation	Minimum	Q1	Median	Q3	Maximum
NMHC before (ppm)	0.050	0.203	0.00	0.00	0.00	0.00	1.06
BC before ($\mu g/m^3$)	0.115	0.151	0.00	0.03	0.067	0.155	3.47
$PM_{2.5}$ before ($\mu g/m^3$)	16.0	5.82	4.00	12.0	15.0	19.0	43.0
SO_2 before (ppb)	0.062	0.067	0.00	0.00	0.10	0.10	0.30
H_2S before (ppb)	0.215	0.244	0.00	0.00	0.10	0.30	1.20
O_3 before (ppb)	29.7	8.59	7.80	24.1	29.5	34.1	57.1
NO before (ppb)	2.30	0.339	0.00	2.40	2.40	2.40	3.50
NO_x before (ppb)	1.18	0.472	0.00	0.90	1.10	1.325	7.70
NO_2 before (ppb)	0.863	0.402	0.00	0.60	0.80	1.00	6.10
NMHC after (ppm)	0.025	0.134	0.00	0.00	0.00	0.00	1.13
BC after ($\mu g/m^3$)	0.075	0.181	0.00	0.017	0.04	0.087	13.0
$PM_{2.5}$ after ($\mu g/m^3$)	12.7	5.22	0.00	9.00	12.0	16.0	38.0
SO_2 after (ppb)	0.238	0.186	0.00	0.10	0.30	0.40	3.00
H_2S after (ppb)	0.485	0.542	0.00	0.20	0.30	0.70	13.7
O_3 after (ppb)	30.9	7.99	4.90	26.0	30.7	35.6	61.1
NO after (ppb)	2.02	0.363	0.80	1.70	1.80	2.50	3.40
NO_x after (ppb)	1.08	0.807	0.00	0.60	0.80	1.60	28.7
NO_2 after (ppb)	1.08	0.432	0.70	0.90	1.00	1.20	14.6

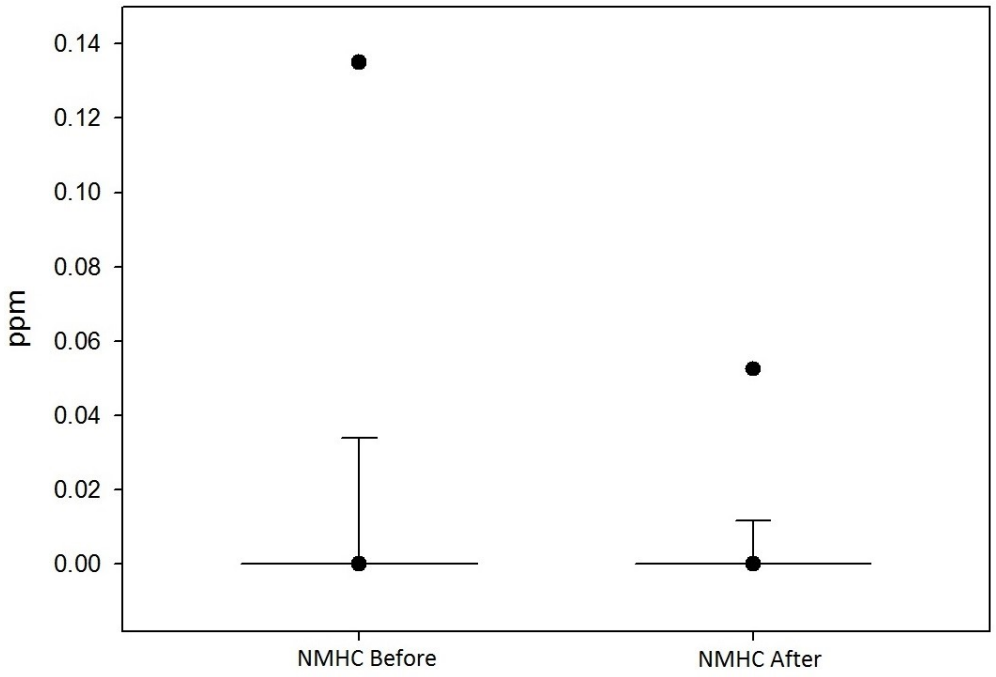

Figure 57. Box plot of NMHC concentrations before and after July 22nd.

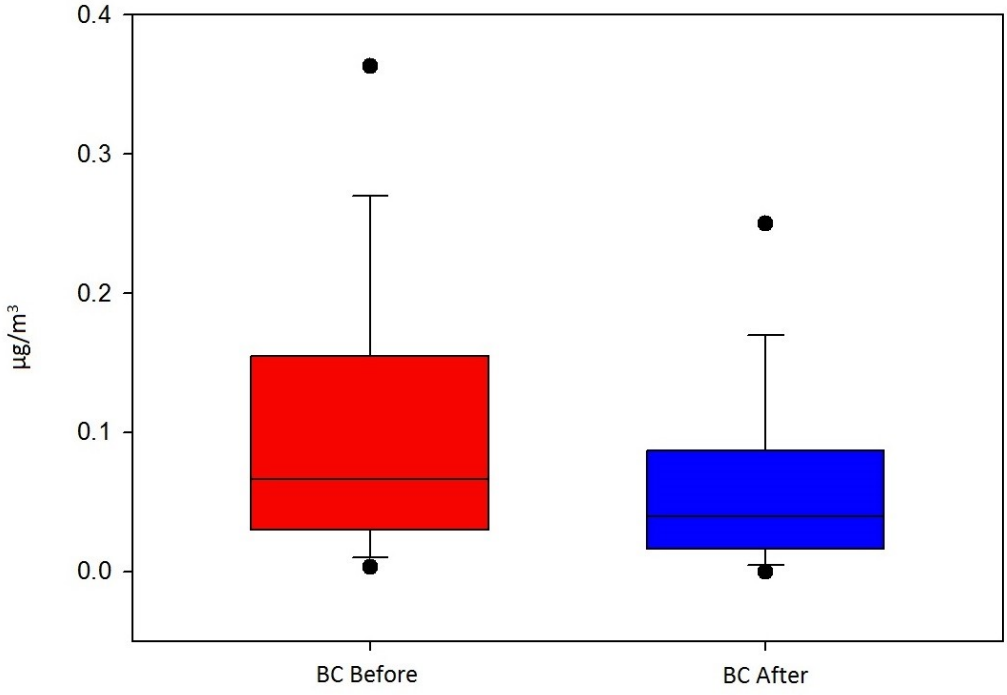

Figure 58. Box plot of BC concentrations before and after July 22nd.

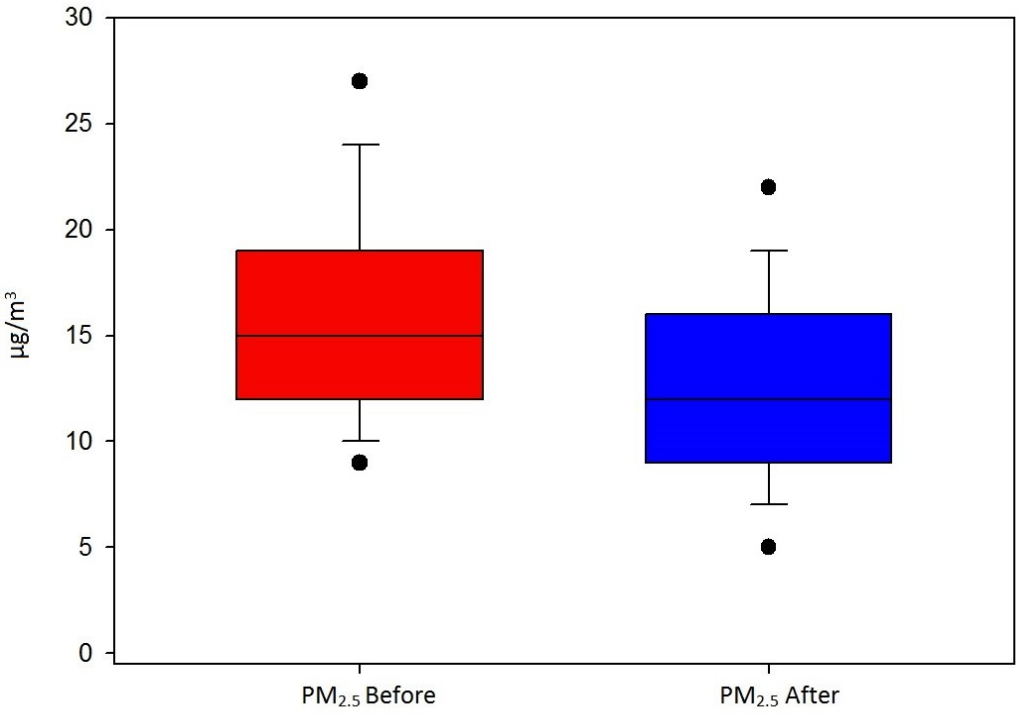

Figure 59. Box plot of $PM_{2.5}$ concentrations before and after July 22nd.

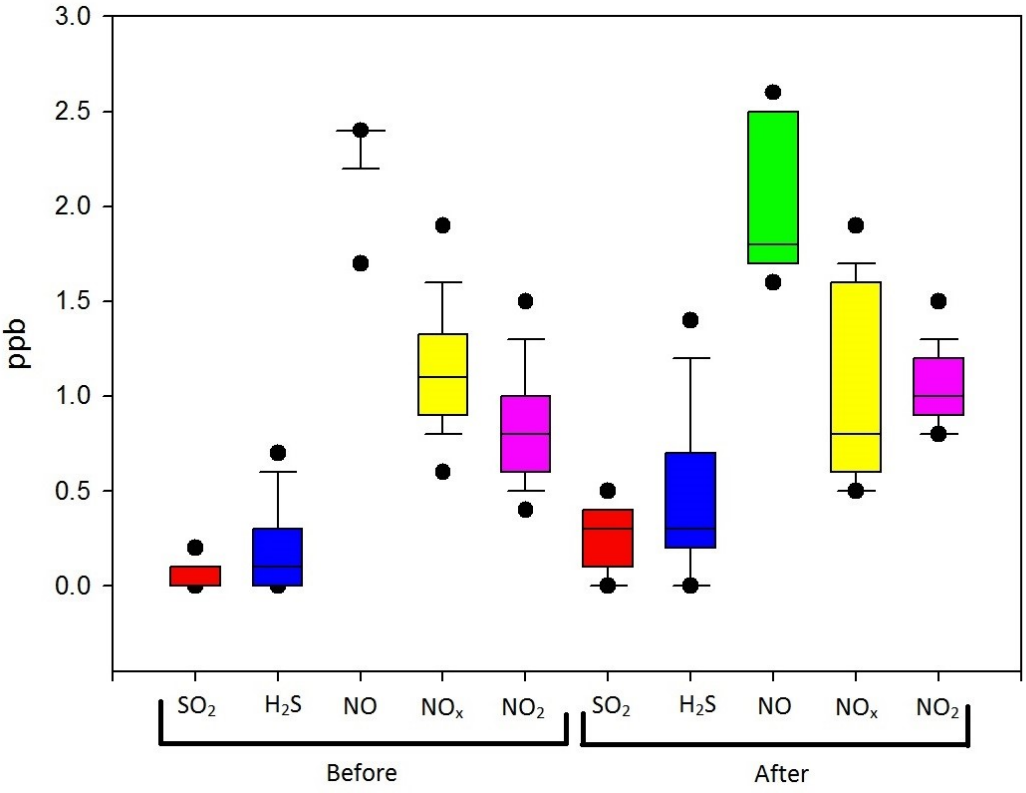

Figure 60. Box plot of SO_2, H_2S, NO, NO_x, and NO_2 concentrations before and after July 22nd.

Results of the Mann-Whitney statistical test for the July 22nd 2013 data split can be found in Figure 71 in the Appendix. The test showed that significant differences exist between concentrations of BC, $PM_{2.5}$, SO_2, H_2S, O_3, NO, NO_x, and NO_2 before and after July 22nd 2013. After adjusting for ties, all p-values were < 0.05. NMHC was the only pollutant that showed no statistically significant difference with a p-value of 0.2019 after adjusting for ties.

From looking at the various box plots before and after July 22nd (Figures 57 – 60) it is reinforced that NMHC concentrations show no significant change before and after July 22nd; the median value remains the same while the 95th and 90th percentile change slightly. All of the other pollutants show a significant change. The median values and upper percentiles for BC, $PM_{2.5}$, NO, and NO_x show decreases after July 22nd, while those for SO_2, H_2S, and NO_2 show increases.

The descriptive statistics in Table 3 show that mean concentrations for SO_2 increased from 0.062 ppb before July 22nd to 0.24 ppb after. Mean concentrations of H_2S increased from 0.21 ppb to 0.48 ppb. This is an increase of 218% for SO_2 and 125% for H_2S. When considered with the factor profiles (Figures 44 – 47) found through the PMF model results it can be seen that SO_2 and H_2S are the main components of flaring, which would likely increase with bringing new O&G activity online. BC, $PM_{2.5}$, NO, and NO_x are more strongly associated with on-site combustion and LRT. Source contributions from these factors likely decreased in the summer months as on-site power needs were less (mainly due to a decreased need for heating). LRT contributions from the mainland were also likely lower for the same reason

CHAPTER 5 CONCLUSIONS AND RECOMMENDATIONS

5.1 Conclusions

The objective of this study was to apportion the major sources of air pollution affecting the air quality on Sable Island with the aim of better understanding the impacts of marine emissions as well as those from nearby offshore O&G activities. In particular, it focused on the impact of bringing a new O&G platform online through to production. This was achieved by performing source apportionment, also known as receptor modelling. Real time sampling data was collected and then used to perform statistical analysis and run the USEPA PMF model. HYSPLIT back trajectories, satellite imagery, weather data, and pollution roses were used in support of the source apportionment modelling process.

The time series plots showed that NMHC, BC, H_2S, and SO_2 concentrations tend to be generally low (compared to the NSE Air Quality Regulations, Canada-Wide Standards, and World Health Organization guidelines) with proportionally higher spikes occurring at specific times. These spikes are most likely linked to pollution events, linking NMHC, BC, H_2S, and SO_2 to sources with intermittent emissions. This was a conclusion reinforced by the PMF model outputs that identified flaring and off gassing from offshore O&G activity (with biogenic contributions from phytoplankton) as their main sources. Time series plots for $PM_{2.5}$, O_3, NO, NO_x, and NO_2 were found to show more constant background concentrations. The conclusion can be drawn that these pollutants are present in the majority of sources impacting the island and in particular those that are more constant in nature, i.e. background air contaminants. Again, this can be reinforced by the PMF model outputs with support from HYSPLIT and satellite data.

Analysis of the descriptive statistics for the data found that the mean concentration for $PM_{2.5}$ was 14.1 $\mu g/m^3$. This is a rather high value considering Sable Island's remote location in the Atlantic. It was determined that offshore O&G activity, dirty power generation using an on-site diesel generator, burning of garbage on-site, and contributions from sea salt are likely the cause of these higher than expected concentrations.

The mean concentration for NMHCs was 0.034 ppm and for BC was 0.091 $\mu g/m^3$. Mean concentrations for SO_2, H_2S, O_3, NO, NO_x, and NO_2 were 0.17 ppb, 0.36 ppb, 30.4 ppb, 2.17 ppb, 1.11 ppb, and 1.0 ppb respectively. The O_3 concentration of 30.4 observed over the course of the study on Sable Island is of a similar magnitude to the Canadian annual average concentration of O_3 of 33 ppb in 2011 (Environment Canada, 2013). This again is a reflection of the source of O_3 being associated with continental outflow of anthropogenic and natural O_3 sources in NA (Gibson et al., 2013d, Gibson et al., 2009a). For H_2S, NO_2, O_3, and SO_2, all of the average and maximum concentrations fall below maximum permissible levels governed by The Air Quality Regulations from Nova Scotia Environment. Mean concentrations of $PM_{2.5}$ and O_3 are below the Canada-Wide Standards (24 hour average for $PM_{2.5}$ and 8 hour average for O_3), although hourly concentrations for $PM_{2.5}$ do exceed them at times. All recorded O_3 concentrations are below the Canada-Wide Standards. Lastly, mean concentrations of all pollutants were below the World Health Organization guidelines (24 hour average for $PM_{2.5}$ and 8 hour average for O_3), although hourly concentrations of $PM_{2.5}$ and O_3 exceeded them at times.

The PMF model run identified 4 factors contributing to the air quality on Sable Island, but source contributions could not be determined due to insufficient speciation data. LRT,

off-gassing, flaring, and on-site combustion were the 4 sources associated with these factors.

Factor 1 was determined to be contributions from LRT. The LRT factor had high contributions from $PM_{2.5}$, O_3, NO, NO_x, and NO_2 with low concentrations of SO_2. The pollution rose and HYSPLIT analysis supported Factor 1 as LRT.

Factor 2 was determined to be off-gassing from O&G production facilities. It had low contributions from $PM_{2.5}$ and BC with higher contributions from NO_x, and H_2S. O_3 was also strongly correlated with this factor. It was found that VOC emissions from phytoplankton blooms could be contributing to this factor during periods of high biomass. However, without a GC-MS to perform VOC speciation it is not possible to apportion exact VOC emissions from offshore O&G compared to phytoplankton blooms. HYSPLIT analysis and pollution rose results supported these conclusions. A Spearman rank order correlation (Figure 72 in the Appendix) was run in SigmaPlot and found that NMHC and H_2S concentrations were strongly correlated, further supporting the rigs as the main contributor to NMHC concentrations. Contributions from Factor 2 can be seen to increase after July 22nd, which would fit well with off-gassing emissions associated with bringing new oil and gas activity online. Furthermore, the study was run mainly over the summer months, therefore likely missing the spring and part of the autumnal phytoplankton blooms. In the future however, GC-MS speciation of VOC species will be conducted on Sable Island resulting in improved source apportionment of phytoplankton emission impacting the air quality on Sable Island.

Factor 3 was determined to represent flaring from offshore oil and gas activity. High contributions from $PM_{2.5}$, BC, H_2S, SO_2, and NO_x were present. H_2S is a strong indicator

in this study of offshore oil and gas activity, only contributing to the factors associated with it. NMHC concentrations are minimal, which is likely due to the fact that they would be burned off during flaring. It can be seen from Figure 50 that factor contributions for Factor 3 increase drastically after July 22nd correlating with increased flaring from new offshore O&G activity. Pollution rose and HYSPLIT analysis also support Factor 3 as representing flaring.

Factor 4 was determined to be on-site combustion including local emissions such as transportation emissions to and from both the island and offshore facilities by aircraft and ships, emissions from passing ships, and most importantly localized emissions on the island itself related to electricity generation and waste incineration. High contributions from $PM_{2.5}$ and BC SO_2, NO, and NO_2 were present in Factor 4. Contributions for on-site combustion decreased during the warmer summer months when less electricity is required. Pollution rose and HYSPLIT analysis also supported Factor 4 as on-site combustion.

Pollution events for NMHCs and $PM_{2.5}$ were examined using HYSPLIT back trajectories and visible satellite images. The results enforced the conclusion that off-gassing and flaring from the rigs is a major source of NMHCs on Sable Island with possible contributions from phytoplankton during certain time periods. Pollution events involving $PM_{2.5}$ were found to be associated with LRT continental outflow from the eastern seaboard of the United States and areas of eastern Canada. From this, it can be concluded that the O&G production facilities were most likely the main contributor to NMHCs and their associated pollution events with contributions from phytoplankton, while LRT from the eastern United States and Canada with contributions from forest fires were most

likely the main cause of $PM_{2.5}$ pollution events. Pollution rose analysis supported the conclusions drawn from the HYSPLIT analysis.

The data before and after July 22nd 2013 was compared in order to determine the impact of new offshore O&G activity that commenced at this time. Significant differences existed between concentrations of BC, $PM_{2.5}$, SO_2, H_2S, O_3, NO, NO_x, and NO_2 before and after July 22nd 2013. NMHC was the only pollutant that showed no statistically significant ($p>0.05$) difference. The median values and upper percentiles for BC, $PM_{2.5}$, NO, and NO_x show decreases after July 22nd, while those for SO_2, H_2S, and NO_2 show increases.

The descriptive statistics before and after July 22nd show that mean concentrations for SO_2 increased from 0.063 ppb to 0.24 ppb. Mean concentrations of H_2S increased from 0.21 ppb to 0.48 ppb. SO_2 and H_2S are the main components of the factor identified as flaring, which would increase with bringing online new O&G activity. BC, $PM_{2.5}$, NO, and NO_x are more strongly associated with the factors representing on-site combustion and LRT. Source contributions from these factors likely decreased in the summer months as on-site power needs were less. LRT contributions from the mainland were also likely lower for the same reason. It was determined from this analysis that bringing new offshore O&G activity online produced a significant change to the air quality of Sable Island, contributing to increased SO_2 and H_2S concentrations. However, these changes were well below The Air Quality Regulations from Nova Scotia Environment.

In conclusion, it was found that the air quality on Sable Island is relatively clean, with all concentrations for the sampling period falling well below those outlined by the Air Quality Regulations from Nova Scotia Environment. Average $PM_{2.5}$ concentrations were

higher than those found previously in Halifax (likely due to sea salt spray), and O_3 concentrations were found to be similar to the Canadian ambient annual average concentrations. The four main factors affecting the air quality on Sable Island are LRT continental outflow, off-gassing from offshore O&G activity (with contributions from phytoplankton blooms), flaring from offshore O&G activity, and on-site combustion sources. New offshore O&G activity brought online July 22nd 2013 was found to cause a significant increase in some air pollutants but concentrations were still well below The Air Quality Regulations from Nova Scotia Environment.

5.2 Recommendations

It is recommended that sampling on Sable Island continue into the future as further characterization of the air quality would be beneficial to understand the impacts further O&G production activity may have on the air quality on Sable Island. In addition, new International Maritime Organization regulations governing the quality of marine fuel will result in significantly reduced emissions from shipping over the next 5-years, in turn changing the air pollution mixture in coastal waters (Sulphur oxides (So_x) Regulation 14, 2014). Air quality monitoring on Sable Island will act as a sentinel to these changes in the source apportionment of air pollution impacting Sable Island. On a global scale, this air quality data on Sable Island will act as an emission inventory that can be fed into climate models, allowing improved predictions of climate change.

Unfortunately, due to practical constraints, this study did not capture seasonal trends or involve sampling during the winter months. A multi-year sampling campaign would further improve our understanding of the seasonal source apportionment of gases and

$PM_{2.5}$ impacting Sable Island. In particular this would allow for sampling equipment to capture the annual spring and autumn phytoplankton blooms that are known to occur on the scotia shelf (Georges et al., 2014; Craig et al., 2012). Coupled with VOC speciation, data obtained using GC-MS, and greater sampling of particulate mass concentration species (using filter based sampling or aerosol monitors), this would allow for more in depth source apportionment modelling of the air quality on Sable Island.

BIBLIOGRAPHY

Andreae, M. O., & Crutzen, P. J. (1997). Atmospheric aerosols: Biogeochemical sources and role in atmospheric chemistry. Science, 276(5315), 1052-1058. doi:10.1126/science.276.5315.1052

Baker, A.R., Turner, S.M., Broadgate, W.J., Thompson, A., McFiggans, G.B., Vesperii, O., Nightengale, P.D., Liss, P.S., & Jickells, T.D., (2000). Distribution and sea– air fluxes of biogenic trace gases in the eastern Atlantic Ocean. Glob. Biogeochem. Cycles, 14 (3), 871– 886.

Batchelor, G.K. (1973). An Introduction to Fluid Dynamics. Cambridge University Press.

Bell, J. N. B., & Treshow, M. (2003). Air pollution and plant life (2nd ed.) John Wiley & Sons. doi:9780471490906.

Beusse, R., & Hauck, E. (2013). EPA needs to improve air emissions data for the oil and natural gas production sector. (Review No. 13-P-0161). U.S. Environmental Protection Agency.

Bhattacharjee, H., Drescher, M., Good, T., Hartley, Z., Leza, J. D., Lin, B., Wu, D. (1999). Particulate matter in New Jersey. (Graduate Class Report). Princeton: Woodrow Wilson School of Public and International Affairs Princeton University.

Broadgate, W.J., Liss, P.S., & Penkett, S.A., (1997). Seasonal emissions of isoprene and other reactive hydrocarbon gases from the ocean. Geophys. Res. Lett., 24 (21), 2675– 2678.

Brook, R. D., Urch, B., Dvonch, T. J., Bard, R. L., Speck, M., Keeler, G., Brook, J. R. (2009). Insights into the mechanisms and mediators of the effects of air pollution exposure on blood pressure and vascular function in healthy humans. Hypertension Journal of the American Heart Association, 54, 659-667. doi:10.1161/HYPERTENSIONAHA.109.130237

Brown, S. G., Frankel, A. & Hafner, H. R. (2007). Source apportionment of VOCs in the Los Angeles area using positive matrix factorization. Atmospheric Environment, 41**,** 227-237.

Carder, K.L., Steward, R.G., Harvey, G.R., & Ortner, P.B. (1989). Marine humic and fulvic acids: Their effects on remote sensing of ocean chlorophyll. Limnology and Oceanography, 34, 68-81.

Claeys, M., Graham, B., Vas, G., Wang, W., Vermeylen, R., Pashynska, V., Maenhaut, W. (2004). Formation of secondary organic aerosols through photooxidation of isoprene. Science, 303, 1173-1176. doi:10.1126/science.1092805

Colomb, A., Yasaa, N., Williams, J., Peeken, A., & Lochte, K. (2008). Screening volatile organic compounds (VOCs) emissions from five marine phytoplankton species by head space gas chromatography/mass spectrometry (HS-GC/MS). Journal of Environmental Monitoring, doi:10.1039/b715312k

Colomb, A., Gros, V., Alvain, S., Sarda-Esteve, R., Bonsang, B., Moulin, C., Klupfel, T. & Williams, J. (2009). Variation of atmospheric volatile organic compounds over the Southern Indian Ocean (30-49ºS). *Environmental Chemistry,* 6**,** 70-82.

Conti, M. E., & Cecchetti, G. (2001). Biological monitoring: Lichens as bioindicators of air pollution assessment - a review. Environmental Pollution, 114(3), 471-492.

Craig, S. E., Jones, C.T., Li, W.K.W., Lazin, G., Horne, E., Caverhill, C., & Cullen, J.J. (2012). Deriving optical metrics of ecological variability from measurements of coastal ocean colour. *Remote Sensing of Environment*, 119, 72-83.

Davison, B., O'Dowd, C., Hewitt, C. N., Smith, M. H., Harrison, R. M., Peel, D. A., Wolf, E., Mulvaney, R., Schwikowski, M. & Baltenspergert, U. (1996). Dimethyl sulfide and its oxidation products in the atmosphere of the Atlantic and Southern Oceans. Atmospheric Environment

Deep Panuke Canada - Nova Scotia benefits. (2013). (Annual Report). Halifax, Nova Scotia: EnCana Corporation.

Deep Panuke gas production 'on track' for June. (2013). Retrieved 06/26, 2013, from http://www.cbc.ca/news/canada/nova-scotia/story/2013/05/23/ns-deep-panuke-june-production.html

Deep Panuke project newsletter. (December 2007). EnCana Corporation.

Deep Panuke Offshore gas development environmental assessment report. (2006). (Environmental Assessment No. DMEN-X00-RP-RE-00-0005 Rev 01U). Halifax, Nova Scotia: EnCana Corporation.

Dillon, P.J., Yan, N.D., Harvey, H.H., Schindler, D.W. (1984). Acidic deposition: Effects on aquatic ecosystems. CRC Critical Reviews in Environmental Control, 13(3), 167-194.

Dockery, D., Pope, C. A., Xu, X., Spengler, J., Ware, J., Fay, M., Speizer, F. (1993). An association between air pollution and mortality in six U.S. cities. New England Journal of Medicine, 329(24), 1753-1759.

Dockery, D. W., & Stone, P. H. (2007). Cardiovascular risks from fine particulate air pollution. New England Journal of Medicine, 356, 511-513.

Dohoo, C., Guernsey, J. R., Gibson, M. D. & Vanleeuwen, J. (2013). Impact of biogas digesters on wood use reliance and cookhouse volatile organic compound exposure. International Society of Exposure Science. Manuscript No. JESEE-13-1601 (accepted with minor corrections).

Dominici, F., Peng, R. D., Bell, M. L., Pham, L., McDermott, A., Zeger, S. L., & Samet, J. M. (2006). Fine particulate air pollution and hospital admission for cardiovascular and respiratory diseases. The Journal of the American Medical Association, 295, 1127-1134.

Donaldson, K., Stone, V., Seaton, A., & MacNee, W. (2001). Ambient particle inhalation and the cardiovascular system: Potential mechanisms. Environmental Health Perspectives, 106, 523-527.

Duderstadt, K. A., Carroll, M. A., Sillman, S., Wang, T., Albercook, G. M., Feng, L., Forbes, G. (1998). Photochemical production and loss rates of ozone at sable island, Nova Scotia during the north atlantic regional experiment (NARE) 1993 summer intensive. Journal of Geophysical Research: Atmospheres, 103(D11), 13531-13555. doi:10.1029/98JD00397

Environment Canada: Ambient levels of ozone. (2013). Retrieved 12/7, 2013, from https://www.ec.gc.ca/indicateurs-indicators/default.asp?lang=en&n=9EBBCA88-1

Environment Canada: Canadian Ambient Air Quality Standards. (2013). Retrieved 1/7, 2014, from http://ec.gc.ca/default.asp?lang=En&n=56D4043B-1&news=A4B2C28A-2DFB-4BF4-8777-ADF29B4360BD

Environment Canada: Canada-Wide Standards (CWS). (2013). Retrieved 1/7, 2014, from http://www.ec.gc.ca/rnspa-naps/default.asp?lang=En&n=07BC2AC0-1

Evans, J. S., Tosteson, T., & Kinney, P. L. (1984). Cross-sectional mortality studies and air pollution risk assessment. Environment International, 10(1), 55-83. doi:10.1016/0160-4120(84)90233-2

Franklin, J.E., Drummond, J.R., Griffin, D., Pierce, J.R., Waugh, D.L., Palmer, P.I., Parrington, M.P., Lee, J.D., Lewis, A.C., Rickard, A.R., Taylor, J.W., Allan, J.D., Coe, H., Chisholm, L., Duck, T.J., Hopper, J.T., Gibson, M.D., Curry, K.R., Sakamoto, K.M., Lesins, G., Walker, K.A., Dan, L., Kliever, J., & Saha, A. (2014) A case study of aerosol depletion in a biomass burning plume over Eastern Canada during the 2011 BORTAS field experiment. Atmospheric Chemistry and Physics Discussions. acp-2014-31

Gibson, M. D., Guernsey, J., Beauchamp, S., Waugh, D., Heal, M., Brook, J. R., Terashima, M. (2009a). Quantifying the spatial and temporal variation of ground-level ozone in the rural Annapolis Valley, Nova Scotia, Canada using nitrite-impregnated passive samplers. Journal of the Air and Waste Management Association, 59, 310-320.

Gibson, M. D., Heal, M. R., Bache, D. H., Hursthouse, A. S., Beverland, I. J., Craig, S. E., Jones, C. (2009b). Using mass reconstruction along a four-site transect as a method to interpret PM10 in west-central Scotland, UK. Journal of the Air and Waste Management Association, 59(12), 1429-1436.

Gibson, M. D., Heal, M. R., Li, Z., Kuchta, J. S., Hayes, A., King, G. H., & Lambert, S. (2013a).
The spatial and seasonal variation of nitrogen dioxide and sulphur dioxide in Cape Breton Highlands National Park, Canada, and the association with lichen abundance. Atmospheric Environment, 64, 303-311. doi:10.1016/j.atmosenv.2012.09.068

Gibson, M. D., & Hopper, J. T. (2013b). Sable island study. Retrieved 10/28, 2013, from http://afrg.peas.dal.ca/sableisland/index.php

Gibson, M. D., Kundu, S., & Satish, M. (2013c). Dispersion model evaluation of PM2.5, NO_x and SO_2 from point and major line sources in Nova Scotia, Canada using AERMOD Gaussian plume air dispersion model. Atmospheric Pollution Research, 4, 157-167. doi:10.5094/APR.2013.016

Gibson, M. D., Pierce, J. R., Waugh, D., Kuchta, J. S., Chisholm, L., Duck, T. J., Palmer, P. I. (2013d). Identifying the sources driving observed PM2.5 variability over Halifax, Nova Scotia, during BORTAS-B. Atmospheric Chemistry and Physics, (13), 4491-4533. doi:10.5194/acpd-13-4491-2013

Gibson, M. D., Ward, T. J., Wheeler, A. J., Guernsey, J. R., Seaboyer, M. P., Bazinet, P., King, G. H., Brewster, N. B., Kuchta, J., Potter, R. & Stieb, D. M. (2010). Woodsmoke source apportionment in the Rural Annapolis Valley, Nova Scotia, Canada. Conference Proceedings of the 103rd Annual Conference of the Air and Waste Management Association, Calgary.

Georges, A.A., El-Swais, H., Craig, S.E., Li, W.K.W & Walsh, D.W. (2014) Metaproteomic analysis of a winter to spring succession in coastal northwest Atlantic Ocean microbial plankton. International Society for Microbial Ecology, 14, 1751-7362.

Greenan, B. J. W., Petrie, B. D., Harrison, W. G., & Oakey, N. S. (2004) Are the spring and fall blooms on the Scotian Shelf related to short-term physical events? Continental Shelf Research. 24, 603-625, 10.1016/j.csr.2003.11.006.

Guenther, A., Geron, C., Pierce, T., Lamb, B., Harley, P., & Fall, R. (2000). Natural emissions of non-methane volatile organic compounds, carbon monoxide, and oxides of nitrogen from North America. Atmospheric Environment, 34 (12-14), 2205-2230. doi:10.1016/S1352-2310(99)00465-3

Guo, H., Wang, T., & Louie, P. K. K. (2004). Source apportionment of ambient non-methane hydrocarbons in Hong Kong: Application of a principal component analysis/absolute principal component scores (PCA/APCS) receptor model. Environmental Pollution, 129, 489-498.

Hannah, C.G., Shore, J.A., Loder, J.W., & Naimie, C.E. (2001). Seasonal Circulation on the Western and Central Scotian Shelf. Journal of Physical Oceanography, 31.

Harrison, R. M., Beddows, D. C. S. & Dall'Osto, M. (2011). PMF Analysis of Wide-Range Particle Size Spectra Collected on a Major Highway. Environmental Science & Technology, 45, 5522-5528

Harrison, R. M., Deacon, A. R., & Jones, M. R. (1997). Sources and processes affecting concentrations of PM_{10} and $PM_{2.5}$ particulate matter in Birmingham (U.K.). Atmospheric Environment, 31(24), 4103-4117. doi:1352-2310/97

Hoffmann, T., Bandur, R., Marggraf, U., & Linscheid, M. (2012). Molecular composition of organic aerosols formed in the α-pinene/O_3 reaction: Implications for new particle formation processes. Journal of Geophysical Research: Atmospheres, 103(D19), 25569-25578. doi:10.1029/98JD01816

Holgate, S.T., Samet, J.M., Koren, H.S., & Maynard, R.L. (1999) Air Pollution and Health (pp 1-2). Academic Press.

Hubert, L., Meulman, J., & Heiser, W. (2000). Two purposes for matrix factorization: A historical appraisal. Society for Industrial and Applied Mathematics, 42(1), 68-82. doi: PII: S0036144598340483

HYSPLIT - hybrid single particle lagrangian integrated trajectory model. (2012). Retrieved 10/28, 2013, from http://www.arl.noaa.gov/HYSPLIT_info.php

Jacob, D. J. (1999). Ozone air pollution. Introduction to atmospheric chemistry (pp. 231-242). Princeton, New Jersey: Princeton University Press.

Jaeckals, J. M., Bae, M.S. & Schauer, J. J. (2007). Positive Matrix Factorization (PMF) Analysis of Molecular Marker Measurements to Quantify the Sources of Organic Aerosols. Environmental Science & Technology, 41**,** 5763-5769.

Jeong, C., McGuire, M., Herod, D., Dann, T., Dabek-Zlotorzynska, E., Wang, D., Evans, G. (2011). Receptor model based identification of PM2.5 sources in Canadian cities Atmospheric Pollution Research, 2, 158-171. doi:10.5094/APR.2011.021

Johnson, C., Harrison, G., Head, E., Spry, J., Pauley, K., Maass, H., Kennedy, M., Porter, C., Yashayaeva, I., and Casault, B. (2012). Optical, chemical and biological conditions in the maritimes resion in 2009 and 2010. Canadian Science Advisory Secretariat (CSAS). Bedford Institute of Oceanography

Kearns, J., Armstrong, K., Shirvill, L., Garland, E., Simon, C., & Monopolis, J. (2000). Flaring & venting in the oil and gas exploration & production industry. (No. 2.79/288). International Association of Oil and Gas Producers.

Khoo, H. H., & Tan, R. B. H. (2006). Environmental impact evaluation of conventional fossil fuel production (oil and natural gas) and enhanced resource recovery with potential CO_2 sequestration. Energy and Fuels, 20, 1914-1924. doi:10.1021/ef060075+

Kim, Y. M., Harrad, S., & Harrison, R. M. (2001). Concentrations and sources of VOCs in urban domestic and public microenvironments. Environmental Science and Technology, 35(6), 997-1004. doi:10.1021/es000192y

Krewski, D., Burnett, R., Goldberg, M., Hoover, K., Siemiatycki, J., Abrahamowicz, M., Villeneuve, P. & White, W. 2005a. Reanalysis of the Harvard Six Cities Study, Part II: Sensitivity Analysis. *Inhalation toxicology,* 17**,** 343-353.

Krewski, D., Burnett, R., Goldberg, M., Hoover, K., Siemiatycki, J., Abrahamowicz, M., & White, W 2005b. Reanalysis of the Harvard Six Cities Study, Part I: Validation and Replication. *Inhalation toxicology,* 17**,** 335-342.

Levy, M. A. (1993). In Haas P. M., Keohane R. O. and Levy M. A. (Eds.), European acid rain: The power of tote-board diplomacy (Institution for the Earth ed.). Massachusetts: The MIT Press.

Mills, N. L., Robinson, S. D., Fokkens, P. H. B., Leseman, D. L. A. C., Miller, M. R., Anderson, D., Cassee, F. R. (2008). Exposure to concentrated ambient particles does not affect vascular function in patients with coronary heart disease. Environmental Health Perspectives, 116, 709-715.

Model 5012 instruction manual. (2009). Franklin, MA: Thermo Scientific.

Model 55i instruction manual. (2008). Franklin, MA: Thermo Scientific.

Monks, P. S., Granier, C., Fuzzi, S., Stohl, A., Williams, M. L., Akimoto, H., Amann, M., Baklanov, A., Baltensperger, U., Bey, I., Blake, N., Blake, R. S., Carslaw, K., Cooper, O. R., Dentener, F., Fowler, D., Fragkou, E., Frost, G. J., Generoso, S., Ginoux, P., Grewe, V., Guenther, A., Hansson, H. C., Henne, S., Hjorth, J., Hofzumahaus, A., Huntrieser, H., Isaksen, I. S. A., Jenkin, M. E., Kaiser, J., Kanakidou, M., Klimont, Z., Kulmala, M., Laj, P., Lawrence, M. G., Lee, J. D., Liousse, C., Maione, M., Mcfiggans, G., Metzger, A., Mieville, A., Moussiopoulos, N., Orlando, J. J., O'dowd, C. D., Palmer, P. I., Parrish, D. D., Petzold, A., Platt, U., Poschl, U., Prevot, A. S. H., Reeves, C. E., Reimann, S., Rudich, Y., Sellegri, K., Steinbrecher, R., Simpson, D., Ten Brink, H., Theloke, J., Van Der Werf, G. R., Vautard, R., Vestreng, V., Vlachokostas, C. & Von Glasow, R. 2009. Atmospheric composition change – global and regional air quality. Atmospheric Environment*,* 43**,** 5268-5350.

The new dustrak II and DRX aerosol monitors (2011). TSI Incorporated.

Niinemets, U., Loreto, F., & Reichstein, M. (2004). Physiological and physicochemical controls on foliar volatile organic compound emissions. Trends in Plant Science, 9(4), 180-186. doi:10.1016./j.tplants..2004.02.006

Norris, G., Vedantham, R., Wade, K., Brown, S., Prouty, J., & Foley, C. (2008). EPA positive Matrix Factorization (PMF) 3.0 fundamentals & user guide. U.S. Environmental Protection Agency.

Nova Scotia ambient air quality monitoring network. (2010). Retrieved 10/28, 2013, from https://www.novascotia.ca/nse/air/docs/AirMonitoringNetworkMap.pdf

Nova Scotia Environment: Air quality regulations, Environment Act U.S.C. 12 (2010).

Novak, C. (2004). The oxford dictionary of statistical terms Dodge Y (ed). Pharmaceutical Statististics. doi: 10.1002/pst.128.

Novakov, T., & Penner, J. E. (1993). Large contribution of organic aerosols to cloud-condensation-nuclei concentrations. Nature, 365, 823-826. doi:10.1038/365823a0

O'Dowd, C. D., Aalto, P., Hmeri, K., Kulmala, M., & Hoffmann, T. (2012). Aerosol formation: Atmospheric particles from organic vapours. Nature, 416(6880), 497-498. doi:10.1038/416497a

O'Dowd, C. D., Aalto, P., Hmeri, K., Kulmala, M. & Hoffmann, T. (2002). Aerosol formation: Atmospheric particles from organic vapours. Nature*,* 416**,** 497-498.

O'Dowd, C.D., & Leeuw, G. (2007). Marine aerosol production: a review of the current knowledge. Philosophical Transactions of the Royal Society A, 365, 1753 – 1774. doi: 10.1098/rsta.2007.2043

O'Dowd, C. D., Facchini, M. C., Cavalli, F., Ceburnis, D., Mircea, M., Decesari, S., Fuzzi, S., Yoon, Y. J. & Putaud, J.P. (2004). Biogenically driven organic contribution to marine aerosol. Nature, 431**,** 676-680.

Offshore environmental effects monitoring for deep panuke. (2012). (Program Annual Report No. DMMG-X00-RP-EH-90-0001.03U). Halifax, NS: EnCana Corporation.

Offshore projects. Retrieved 06/03, 2013, from http://www.cnsopb.ns.ca/offshore-activity/offshore-projects

Palmer, P. I., & Shaw, S. L. (2005). Quantifying global marine isoprene fluxes using MODIS chlorophyll observations. Geophysical Research Letters, 32(L09805) doi:10.1029/2005GL022592

Palmer, P. I., Parrington, M., Lee, J. D., Lewis, A. C., Rickard, A. R., Bernath, P. F., Duck, T. J., Waugh, D. L., Tarasick, D. W., Andrews, S., Aruffo, E., Bailey, L. J., Barrett, E., Bauguitte, S. J. B., Curry, K. R., Carlo, P. D., Chisholm, L., Dan, L., Drummond, J. R., Forster, G., Franklin, J. E., Gibson, M. D., Griffin, D., Helmig, D., Hopkins, J. R., Hopper, J. T., Jenkin, M. E., Kindred, D., Kliever, J., Breton, M. L., Matthiesen, S., Maurice, M., Moller, S., Moore, D. P., Oram, D. E., O'Shea, S. J., Owen, R. C., Pagniello, C. M. L. S., Pawson, S., Percival, C. J., Pierce, J. R., Punjabi, S., Purvis, R. M., Remedios, J. J., Rotermund, K. M., Sakamoto, K. M., Strawbridge, K. B., Strong, K., Taylor, J., Trigwell, R., Tereszchuk, K. A., Walker, K. A., Weaver, D., Whaley, C. & Young, J. C. (2013). Quantifying the impact of BOReal forest fires on Tropospheric oxidants over the Atlantic using Aircraft and Satellites (BORTAS) experiment: design, execution and science overview. Atmos. Chem. Phys., 13**,** 6239-6261.

Paterson, K. G., Sagady, J. L., Hooper, D. L., Bertman, S. B., Carroll, M. A., & Shepson, P. B. (1999). Analysis of air quality data using positive matrix factorization**.** Environmental Science and Technology, 33(4), 635-641.

Pen, T., Hingston, M., Waugh, D., Keast, S., Mcpherson, J., Worthy, D., & Forbes, G. (2009). Sable Island air monitoring program report: 2003-2006 (Technical Report). Meteorological Service of Canada Atlantic Region Science.

Pierce, J. R. & Adams, P. J. (2009). Uncertainty in global CCN concentrations from uncertain aerosol nucleation and primary emission rates. Atmospheric Chemistry and Physics, 9**,** 1339-1356.

Piccot, S. D., Watson, J. J., & Jones, J. W. (1992). A global inventory of volatile organic compound emissions from anthropogenic sources. Journal of Geophysical Research, 97(D9), 9897-9912. doi:0148-0227/92/92JD-006825

Pilling, M., ApSimon, H., Carruthers, D., Carslaw, D., Colvile, R., Derwent, R., Stevenson, K. (2005). Particulate matter in the United Kingdom: Summary. London, U.K.: Air Quality Expert Group.

Pope, C. A., Burnett, R. T., Thun, M. J., Calle, E. E., Krewski, D., Ito, K., & Thurston, G. D. (2002). Lung cancer, cardiopulmonary mortality, and long-term exposure to fine particulate air pollution. The Journal of the American Medical Association, 287, 1132-1141.

Qeurol, X., Alastuey, A., Ruiz, C. R., Artinano, B., Hansson, H. C., Harrison, R. M., Buringh, E., Ten Brink, H. M., Lutz, M., Bruckmann, P., Straehl, P. & Schneider, J. 2004. Speciation and origin of PM_{10} and $PM_{2.5}$ in selected European cities. Atmospheric Environment, 38, 6547-6555.

Reimer, D.D., Milne, P.J., Zika, R.G., & Pos, W.H. (2000). Photoproduction of nonmethane hydrocarbons (NMHC) in seawater. Marine Chemistry. 71, 177– 198.

Rumchev, K., Spickett, J., Bulsara, M., Phillips, M., & Stick, S. (2004). Association of domestic exposure to volatile organic compounds with asthma in young children. Thorax, 59, 746-751. doi:10.1136/thx.2003.013680

Ryerson, T. B., Trainer, M., Angevine, W. M., Brock, C. A., Dissly, R. W., Fehsenfeld, F. C., Sueper, D. T. (2003). Effect of petrochemical industrial emissions of reactive alkenes and NO_x on tropospheric ozone formation in Houston, TX. Journal of Geophysical Research: Atmospheres, 108(D8), 27. doi:10.1029/2002JD003070

Sable Island national park reserve: Park establishment. (2012). Retrieved 06/03, 2013, from http://www.pc.gc.ca/eng/pn-np/ns/sable/plan/plan01.aspx

Sable Island: A story of survival. (2001). Retrieved 06/03, 2013, from http://museum.gov.ns.ca/mnh/nature/sableisland/english_en/index_en.htm

Schawrtz, J., & Marcus, A. (1990). Mortality and air pollution in London: A time series analysis. American Journal of Epidemiology, 131, 185-194.

Seinfeld, J. H., & Pandis, S. N. (2006). Atmospheric chemistry and physics - from air pollution to climate change (2nd ed.) John Wiley & Sons. Retrieved from: http://www.knovel.com/web/portal/browse/display?_EXT_KNOVEL_DISPLAY_bookid=2126&VerticalID=0

Shaw, S.L., Chisholm, S.W., Prinn, R.G. (2003). Isoprene production by Prochlorococcus, a marine cyanobacterium, and other phytoplankton. Marine Chemistry, 80, 227– 245.

Shaw, S. L., Gantt, B. & Meskhidze, N. (2010). Production and Emissions of Marine Isoprene and Monoterpenes: A Review. Advances in Meteorology, 2010.

Shwartz, J., & Dockery, D. W. (1992). Increased mortality in Philadelphia associated with daily air pollution concentrations. The American Review of Respiratory Diseases, 145, 600-604.

Solomon, S.D., Qin, M., Manning, Z., Chen, M., Marquis, K.B., Averyt, M., Tignor, & Miller, H.L. (2007). Contribution of Working Group I to the Fourth Assessment Report of the Intergovernmental Panel on Climate Change. Cambridge University Press.

Stieb, D. M., Burnett, R. T., Smith-Doiron, M., Brion, O., Shin, H. H., & Economou, V. (2008). No-threshold air quality health index based on short-term associations observed in daily time-series analyses. Journal of the Air and Waste Management Association, 58, 435-450. doi:10.3155/1047-3289.58.3.435

Stieb, D. M., Judek, S., & Burnett, R. T. (2002). Meta-analysis of time-series studies of air pollution and mortality: Effects of gases and particles and the influence of cause of death, age, and season. Journal of the Air and Waste Management Association, 52, 470-484.

Stohl, A. (1998). Computation, accuracy and applications of trajectories - A review and bibliography. Atmospheric Environment, 32(6), 947-966. doi:10.1016/S1352-2310(97)00457-3

Sulphur oxides (So_x) Regulation 14. (2014). International Maritime Organization. Retrieved from: http://www.imo.org/OurWork/Environment/PollutionPrevention/AirPollution/Pages/Sulphur-oxides-(SOx)-%E2%80%93-Regulation-14.aspx.

A synopsis of Nova Scotia's offshore oil and gas environmental effects monitoring programs. (2011). (Summary). Canada - Nova Scotia Offshore Petroleum Board.

Technical Summaries of Scotian Shelf Significant and Commercial Discoveries. (2000). (Technical Summary). Canada - Nova Scotia Offshore Petroleum Board.

Thurston, G. D. & Spengler, J. D. (1985). A Quantitative Assessment of Source Contributions to Inhalable Particulate Matter Pollution in Metropolitan Boston. Atmospheric Environment (1967), 19**,** 9-25.

Volatile organic compounds (VOCs). (2012). Retrieved 06/04, 2013, from: http://www.ec.gc.ca/air/default.asp?lang=En&n=15B9B65A-1

Ward, T., Trost, B., Conner, J., Flanagan, J., & Jayanty, R. K. M. (2012). Source apportionment of PM2.5 in a subarctic airshed - Fairbanks, Alaska. Aerosol and Air Quality Research, 12, 536-543.

Ward, T. J. (2007). The Missoula, Montana PM2.5 source apportionment research Study. The University of Montana – Missoula Center for Environmental Health Sciences.

Ward, T. J., Hamilton JR, R. F., Dixon, R. W., Paulsen, M. & Simpson, C. D. (2006a). Characterization and evaluation of smoke tracers in PM: Results from the 2003 Montana wildfire season. Atmospheric Environment, 40, 7005-7017.

Ward, T. J., Rinehart, L. R., & Lange, T. (2006b). Aerosol Science and Technology, The 2003/2004 Libby, Montana PM2.5 source apportionment research Study, 40, 166-177.

Ward, T. J. & Noonan, C. (2008). Results of a residential indoor PM2.5 sampling program before and after a woodstove changeout. Indoor Air, 18, 408-415.

Ware, J. H., Spengler, J. D., Neas, L. M., Samet, J. M., Wagner, G. R., Coultas, D., Schwab, M. (1993). Respiratory and irritant health effects of ambient volatile organic compounds. American Journal of Epidemiology, 137(12), 1287-1301.

Watson, J. G., Robinson, N. F., Fujita, E. M., Chow, J. C., Pace, T. G., Lewis, C. & Coulter, T. (1998). CMB8 Applications andValidation Protocol for PM2.5 and VOCs. Report No. 1808.2D1 Reno, Nevada: Desert Research Institute.

Waugh, D., Inkpen, D. T., Hingston, M., Keast, S., McPherson, J., Worthy, D., & Forbes, G. (2010). Sable island air monitoring program report: 2003-2006. (No. 181). Dartmouth: Environmental Studies Research Funds.

Weekly operations report EnCana Deep Panuke production status. (2013). Canada - Nova Scotia Offshore Petroleum Board.

WHO Air quality guidelines for particulate matter, ozone, nitrogen dioxide and sulphur dioxide. (2005). (Summary of risk assessment). World Health Organization.

WHO, 2002. World Health Report: Reducing Risks, Promoting Healthy Life. World Health Organization, Geneva, Switzerland.

Will-Wolf, S., & Neitlich, P. (2010). Development of lichen response indexes using a regional gradient modelling approach for large-scale monitoring of forests (General Technical Report No. PNW-GTR- 807).United States Department of Agriculture.

Yang, C., Wang, J., Chan, C., Chen, P., Huang, J., & Chengs, M. (1997). Respiratory and irritant health effects of a population living in a petrochemical-polluted area in Taiwan. Environmental Research, 74, 145-149. doi:0013-9351/97

Yin, J., Allen, A. G., Harrison, R. M., Jennings, S. G., Wright, E., Fitzpatrick, M., McCusker, D. (2005). Major component composition of urban PM10 and PM2.5 in Ireland. Atmospheric Research, 78, 149-165.

Yin, J., & Harrison, R. M. (2008). Pragmatic mass closure study for PM1.0, PM2.5 and PM10 at roadside, urban background and rural sites. Atmospheric Environment, 42, 980-988.

Zahniser, A. (2007). Characterization of greenhouse gas emissions involved in oil and gas exploration and production operations. California Air Resources Board.

APPENDIX

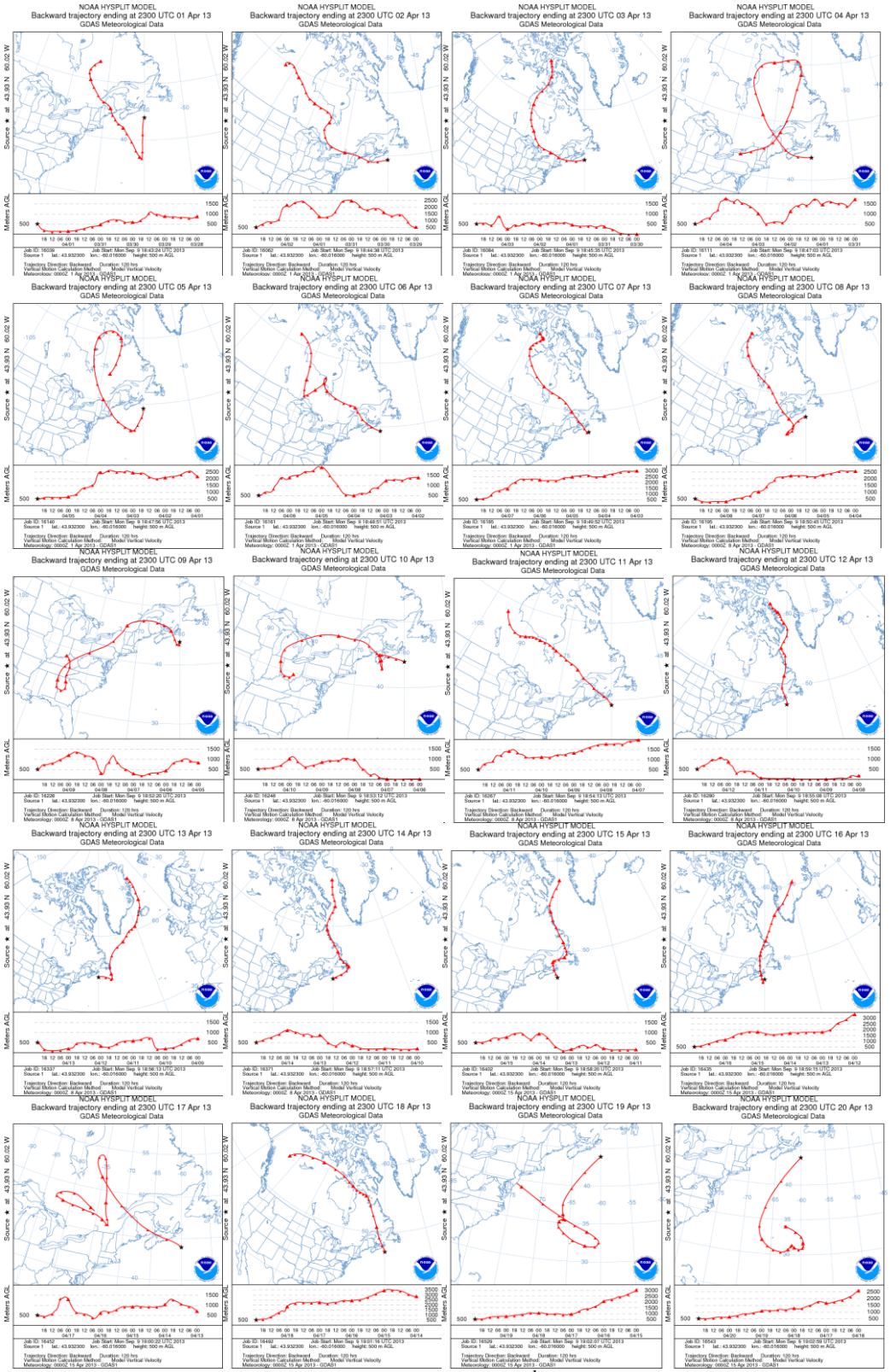

April 1st – 20th, 2013

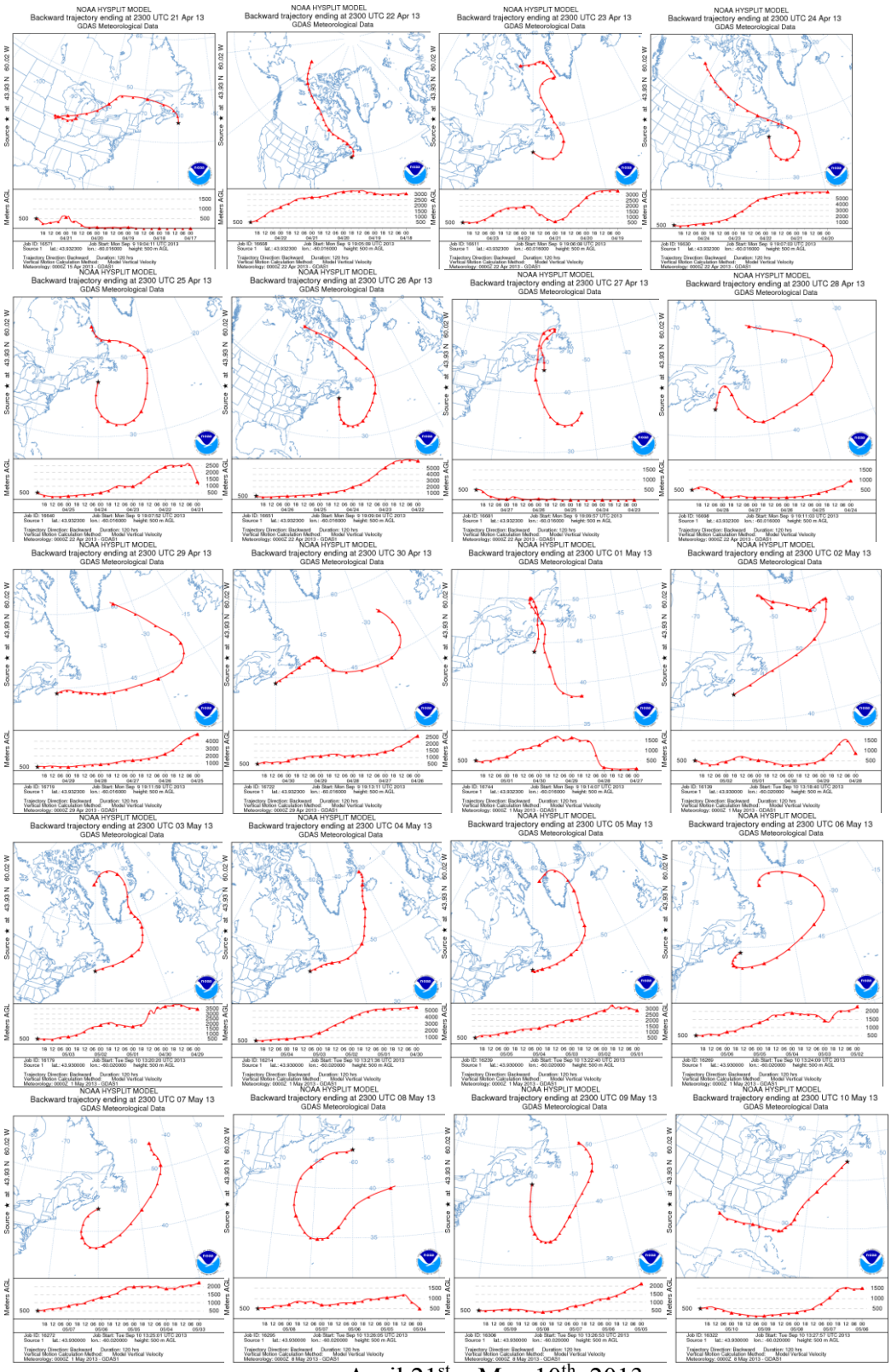

April 21st – May 10th, 2013

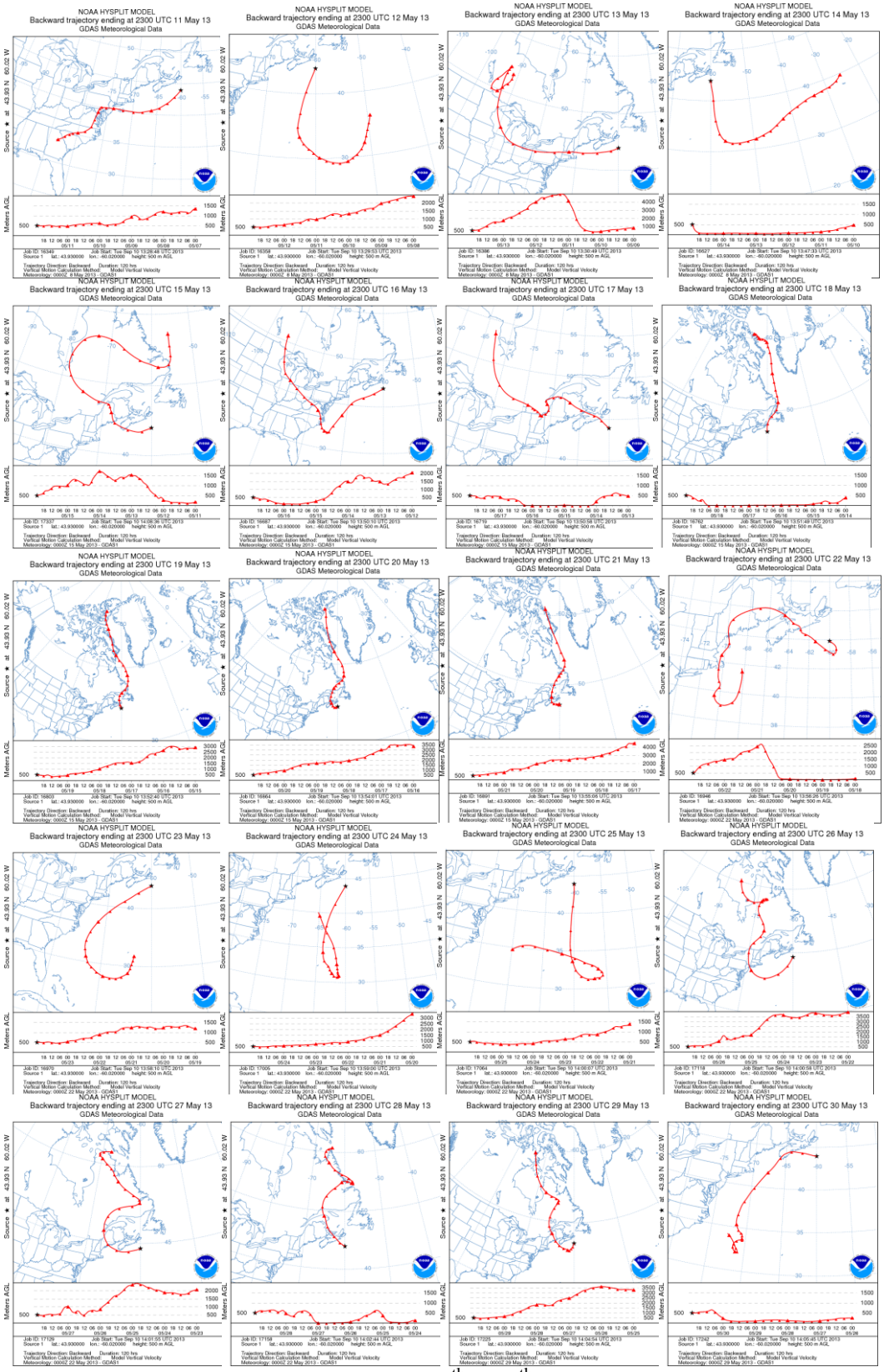

May 11th – 30th, 2013

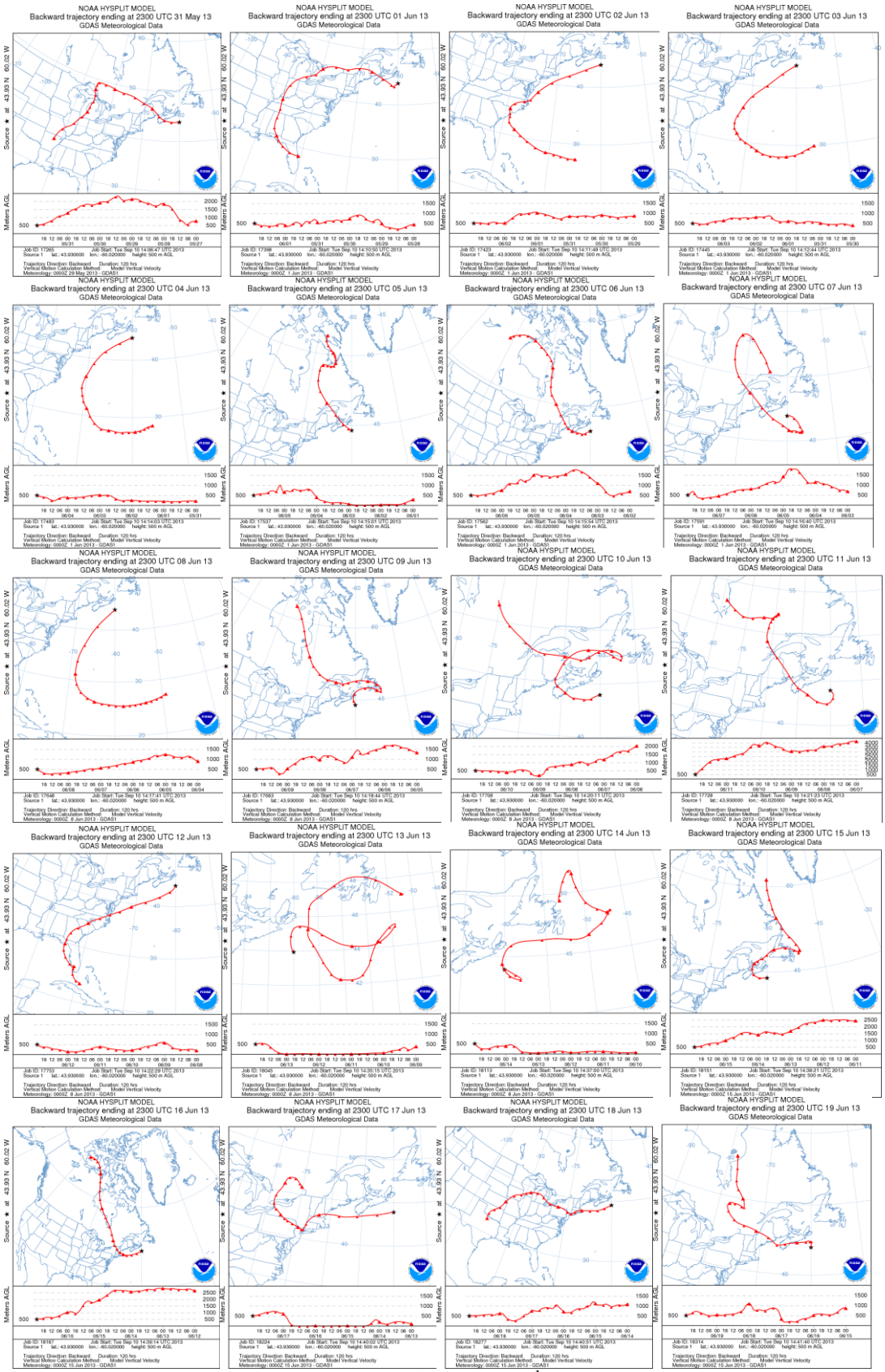

May 31st – June 19th, 2013

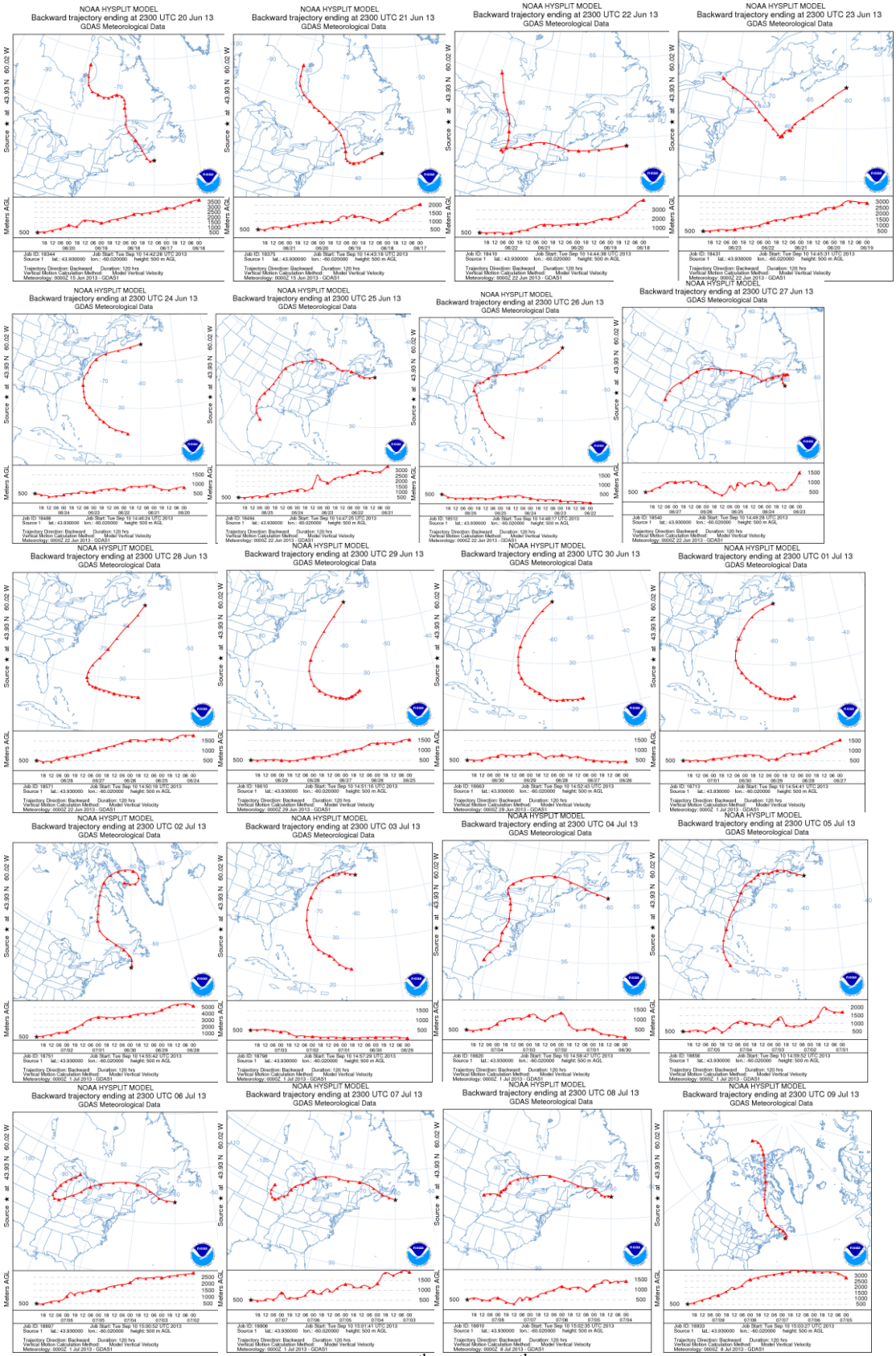

June 20th – July 9th, 2013

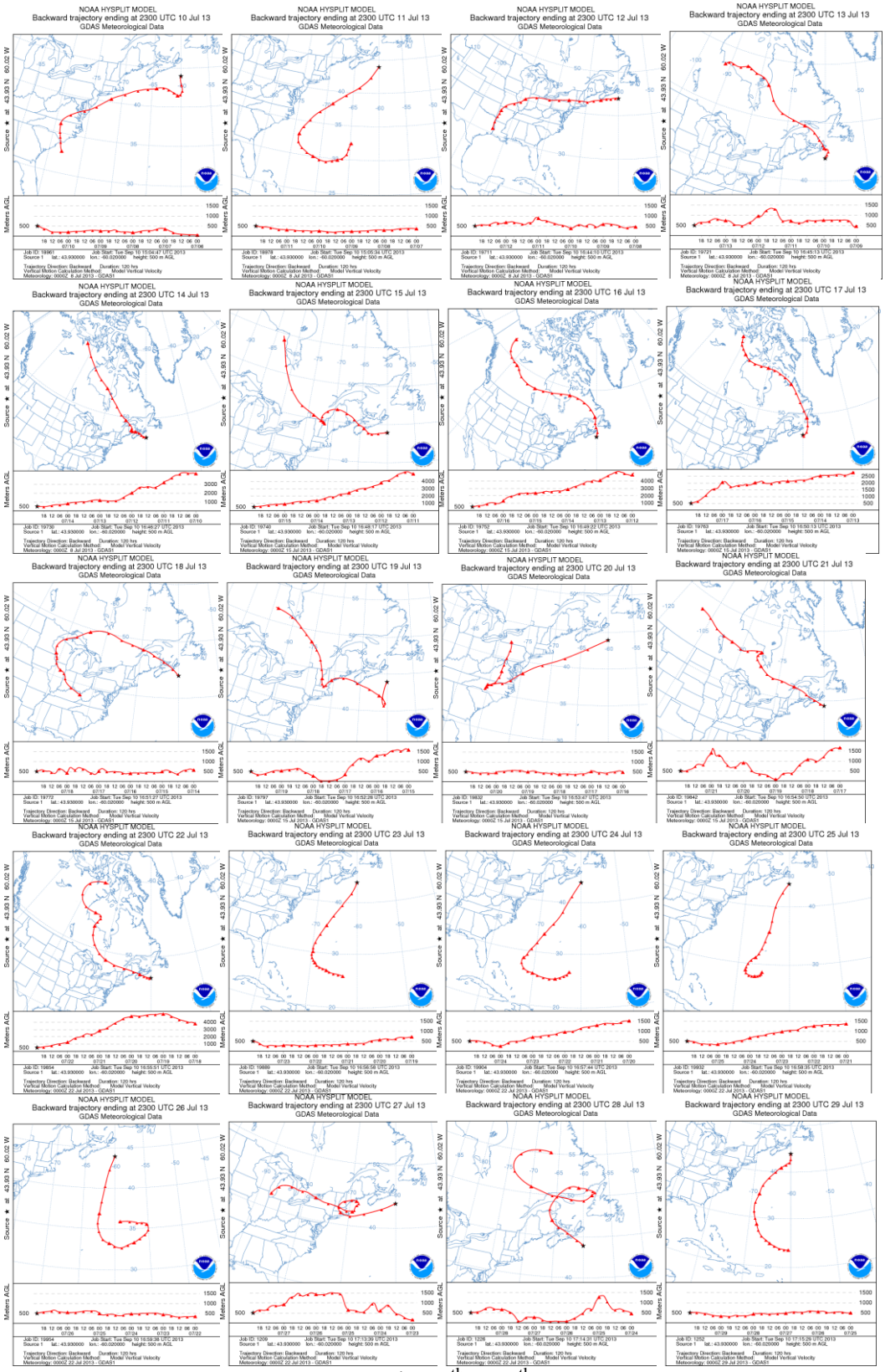

July 10th – 29th, 2013

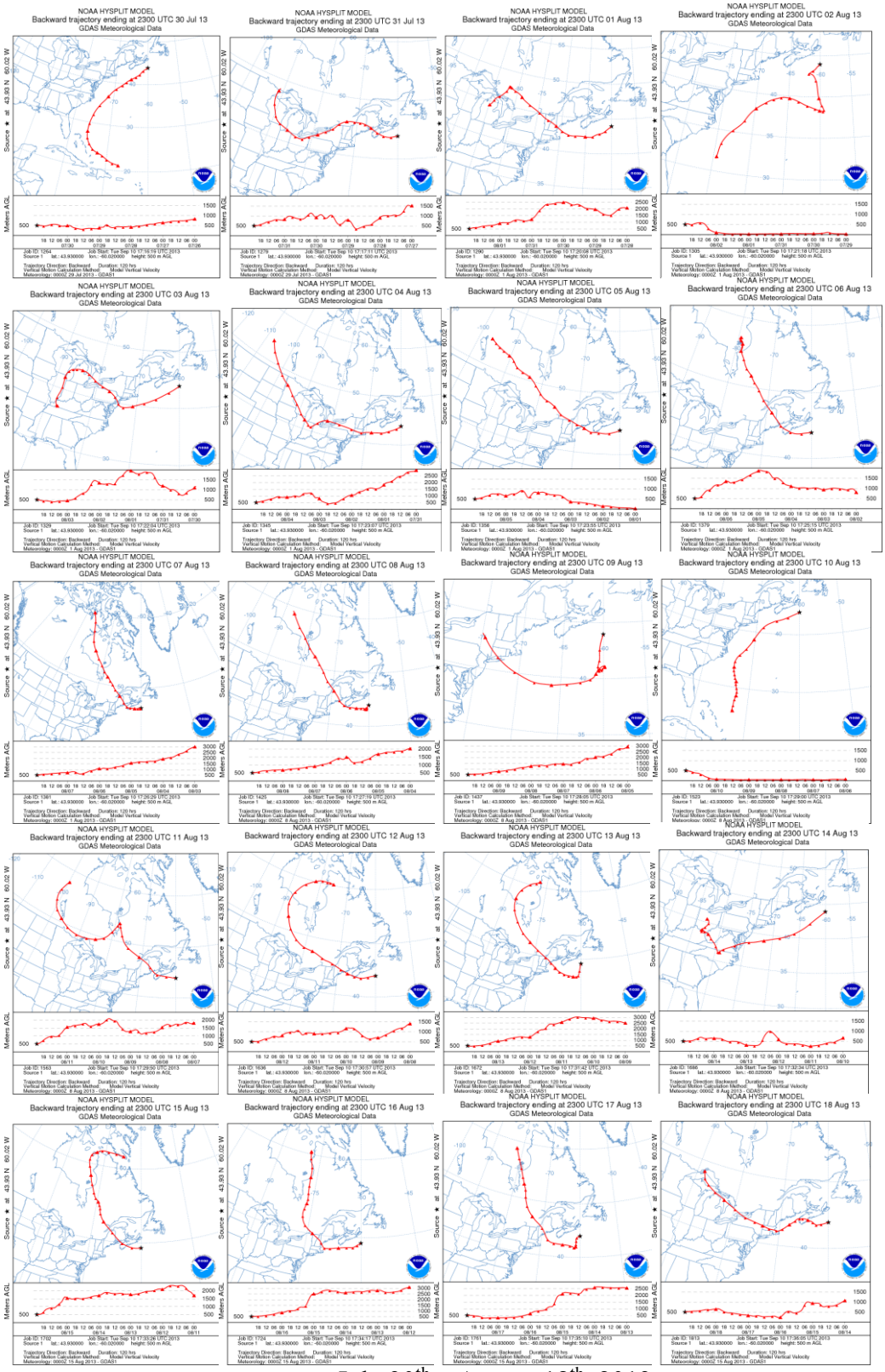

July 30th – August 18th, 2013

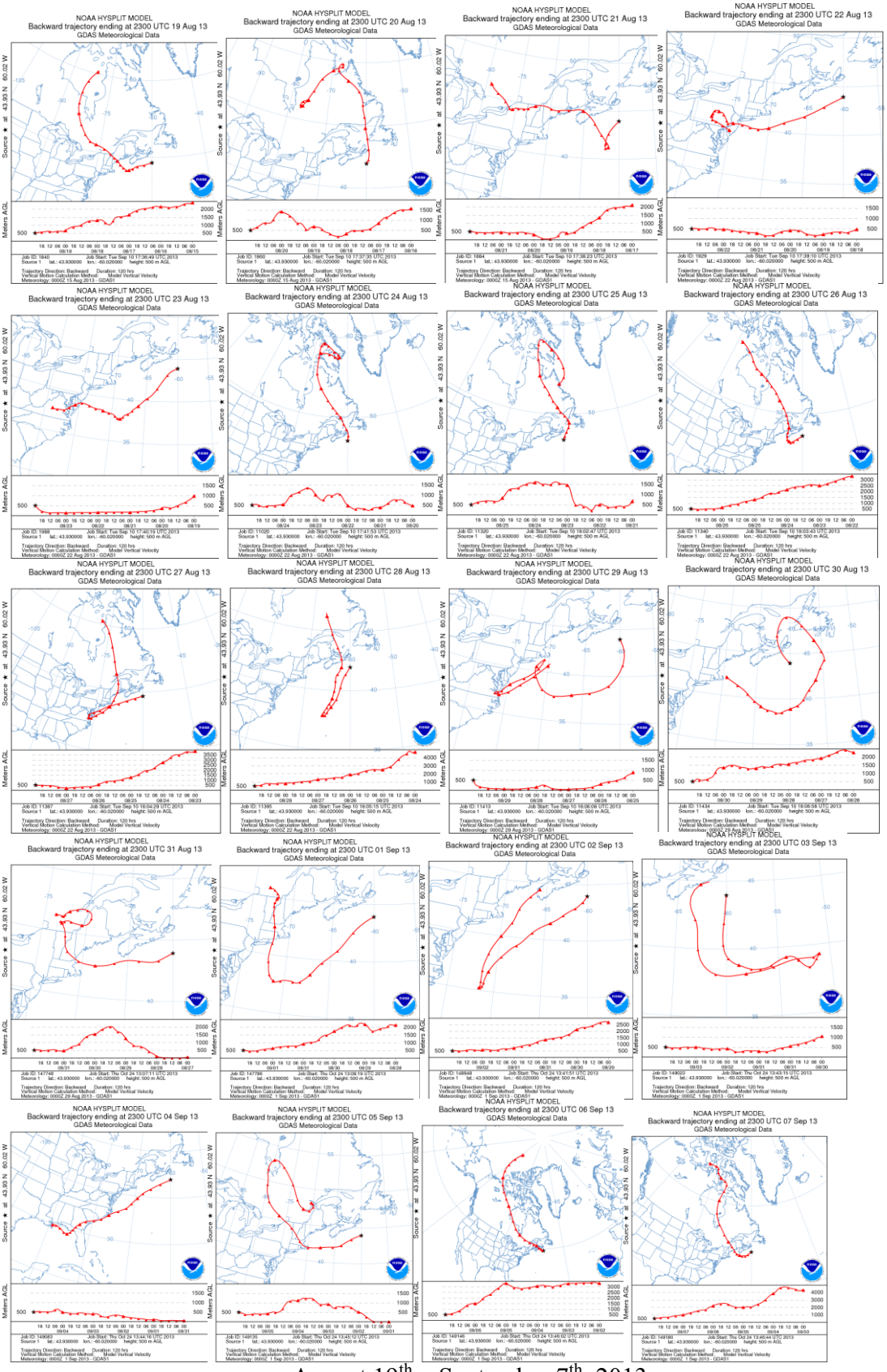

August 19th – September 7th, 2013

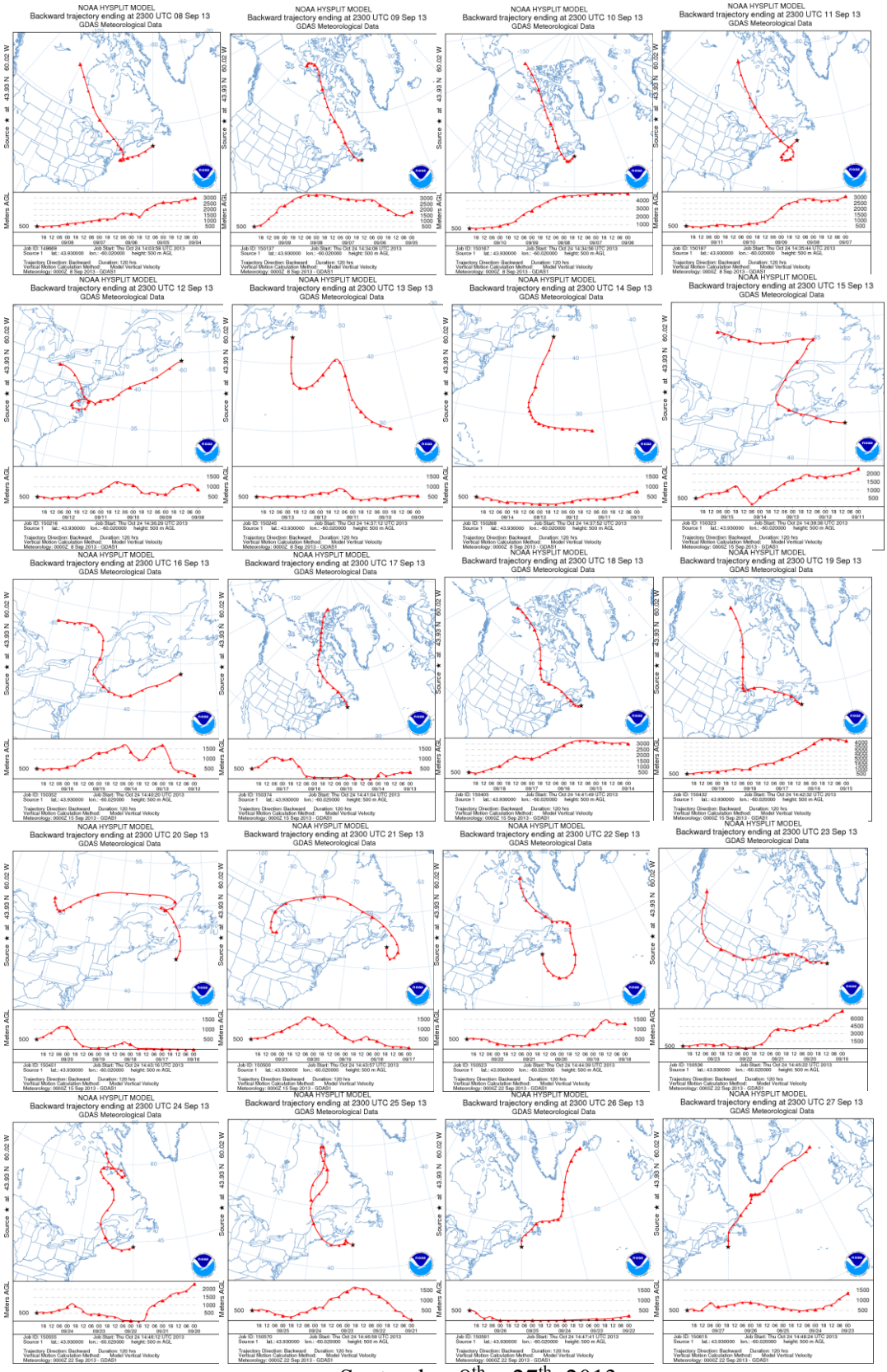

September 8th – 27th, 2013

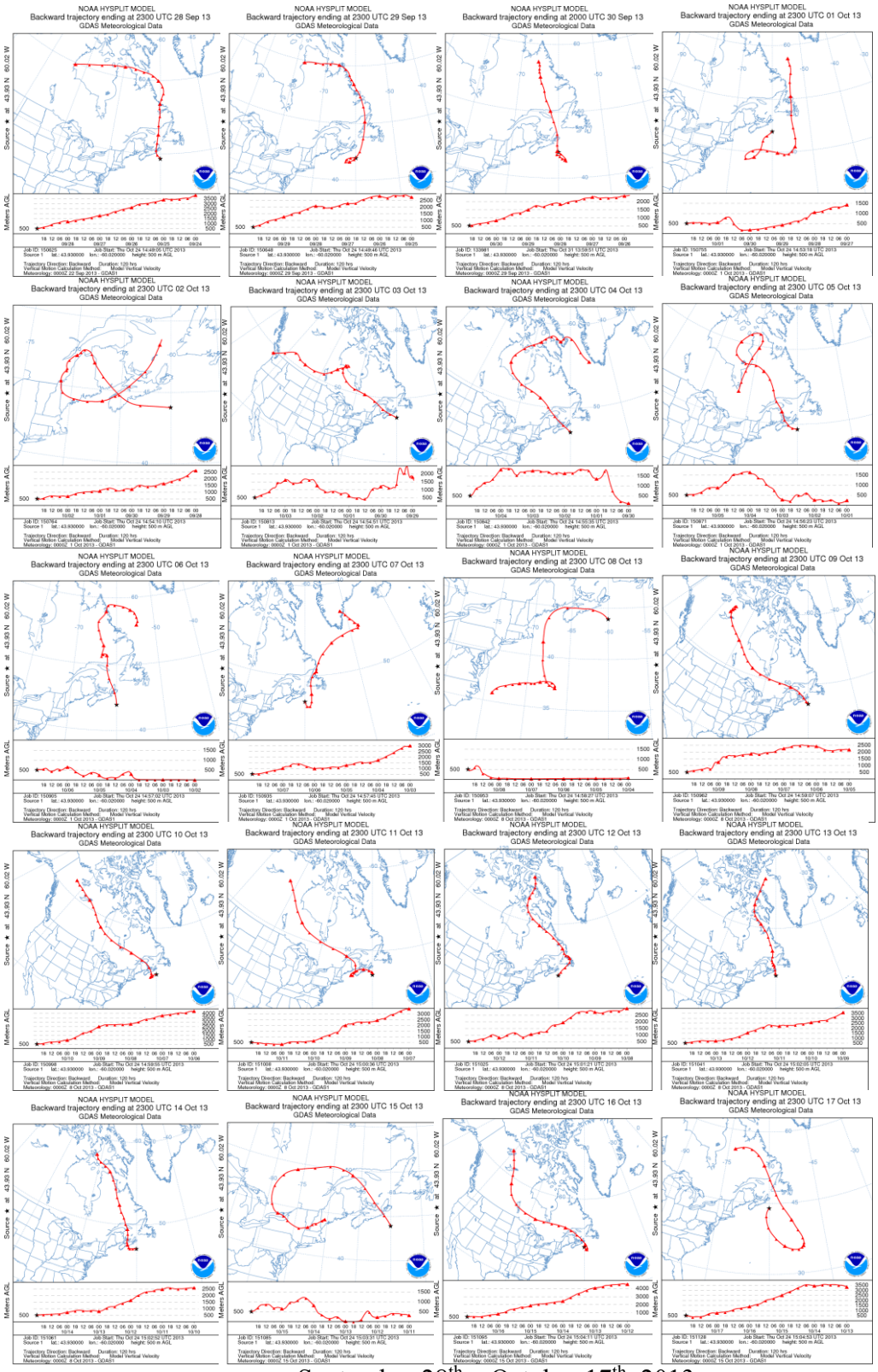

September 28th – October 17th, 2013

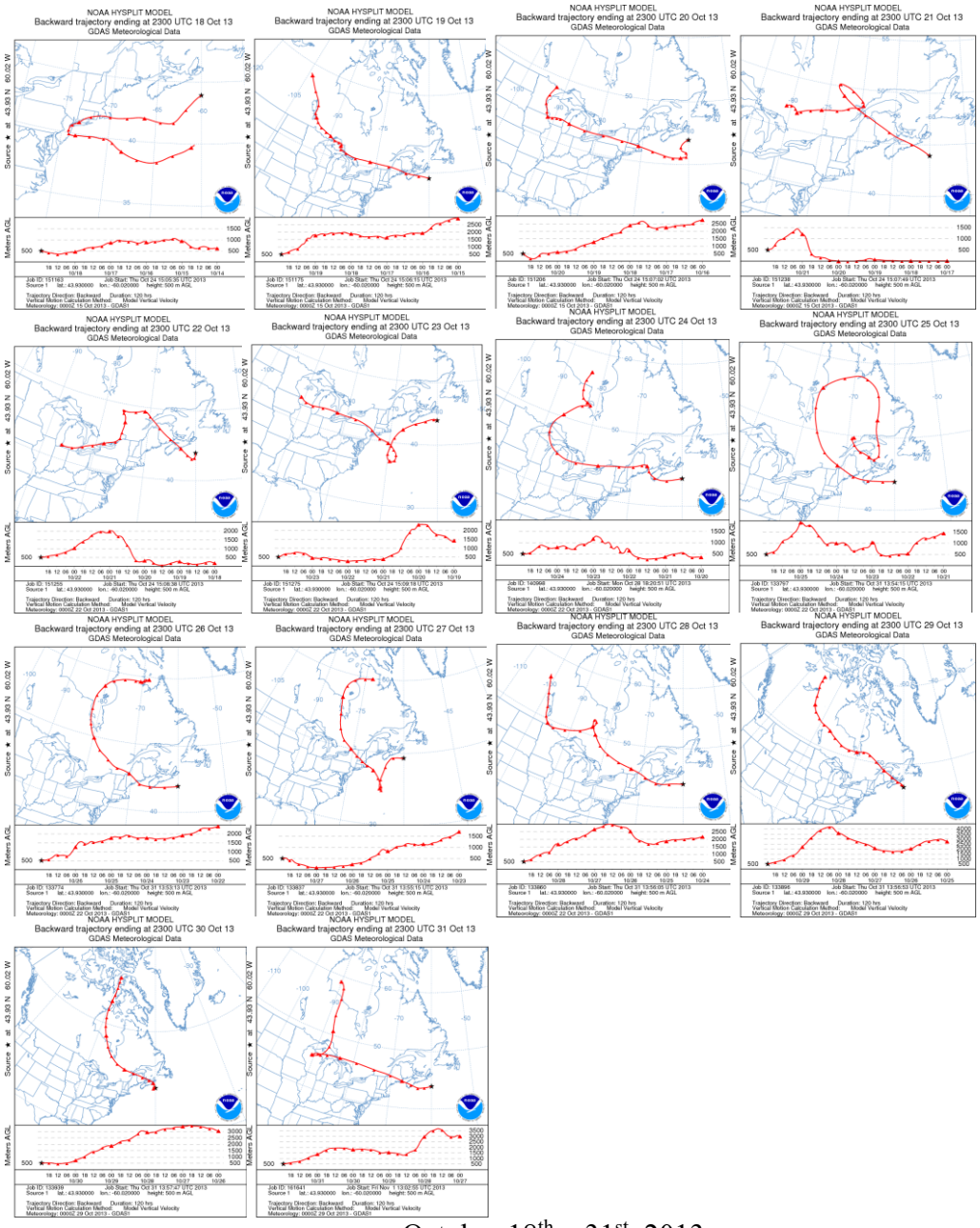

October 18th – 31st, 2013

Figure 61. Daily HYSPLIT back trajectories.

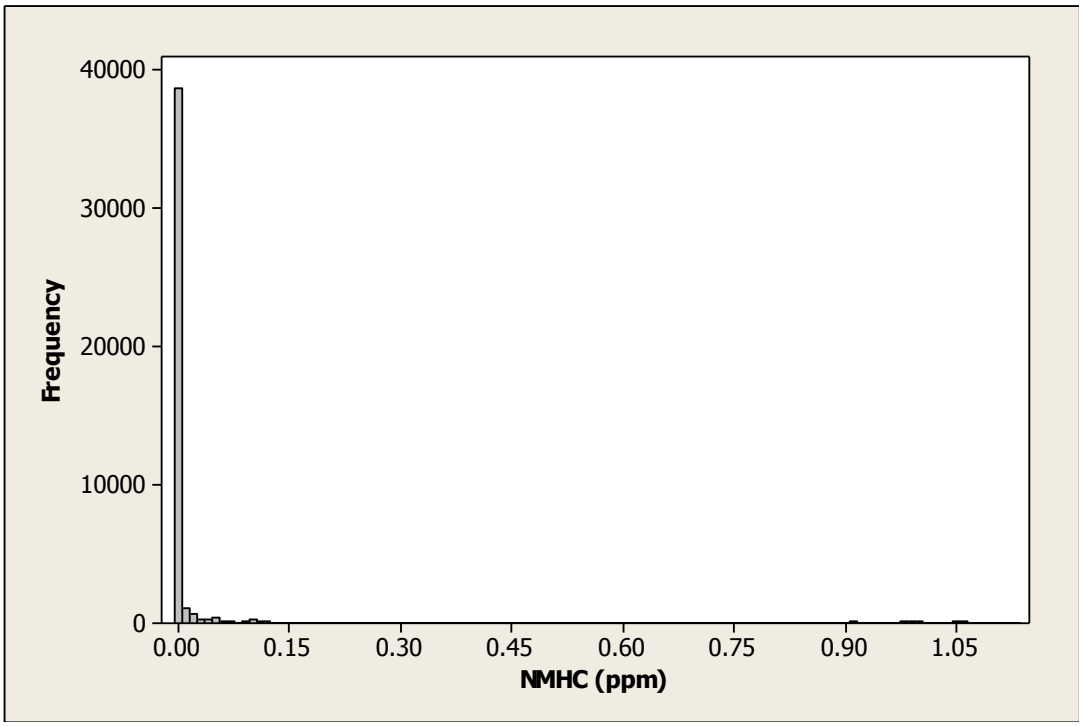

Figure 62. Histogram of NMHC data.

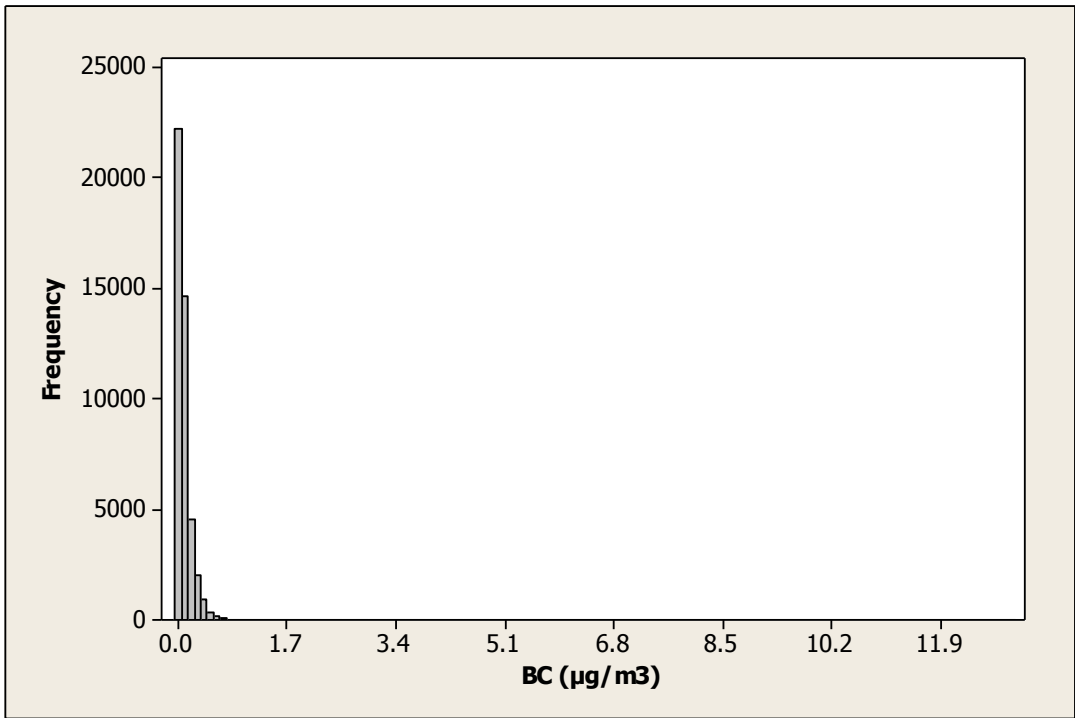

Figure 63. Histogram of BC data.

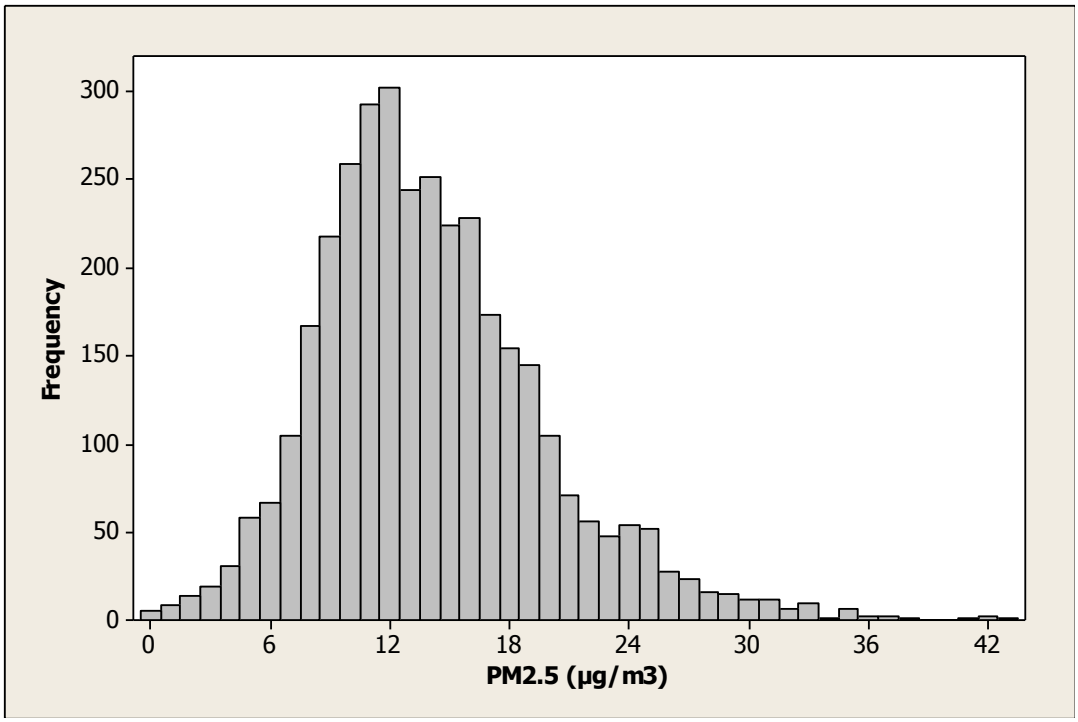

Figure 64. Histogram of $PM_{2.5}$ data.

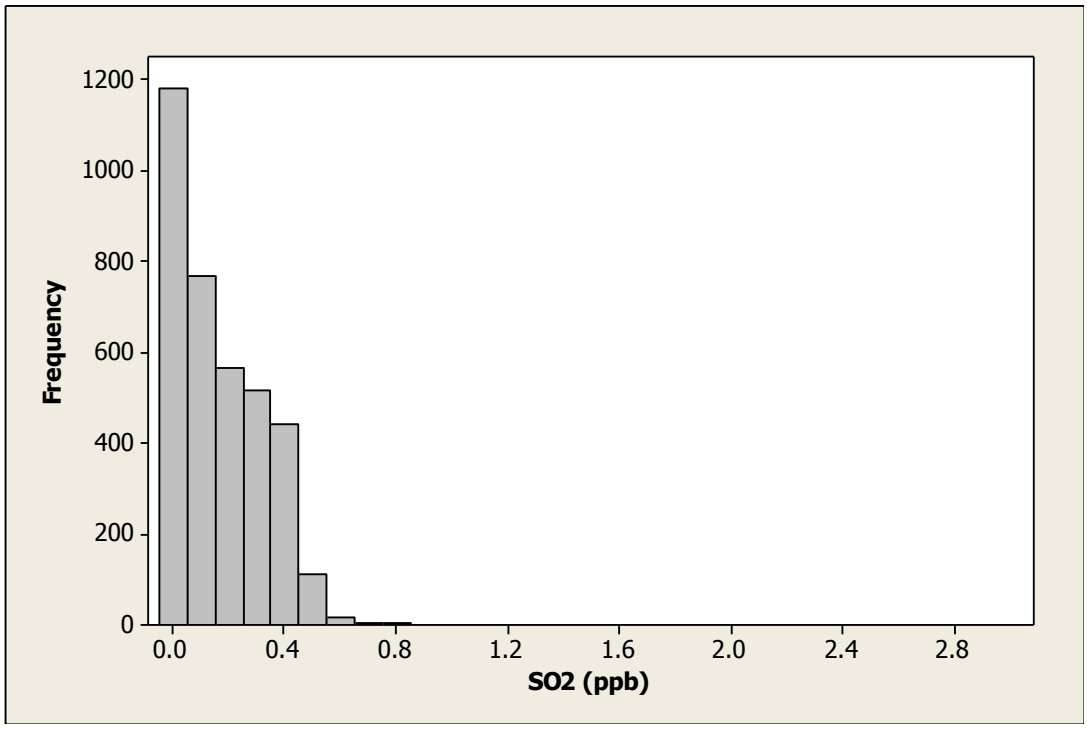

Figure 65. Histogram of SO_2 data.

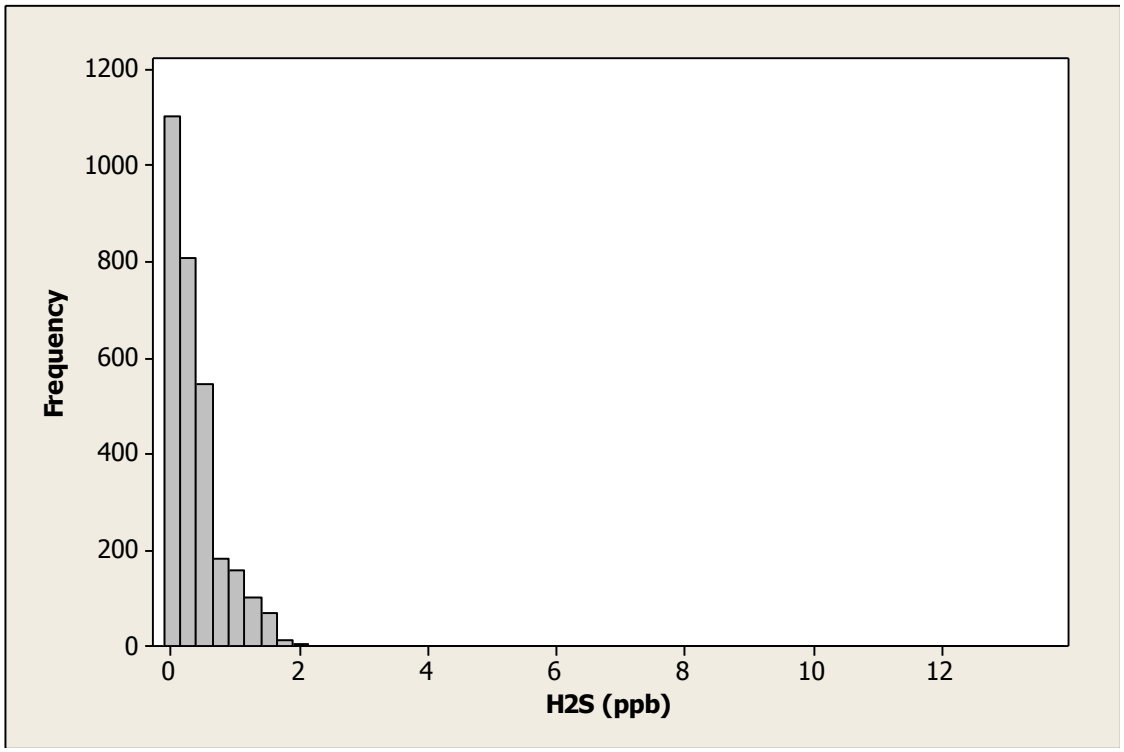

Figure 66. Histogram of H_2S data.

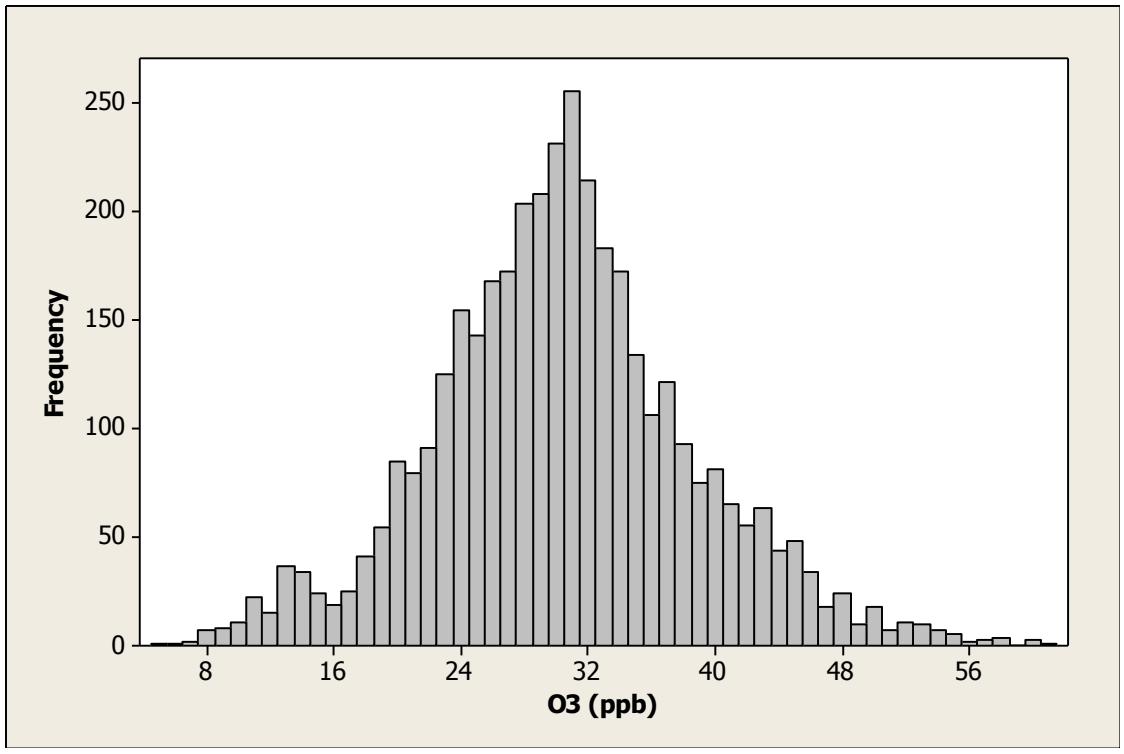

Figure 67. Histogram of O_3 data.

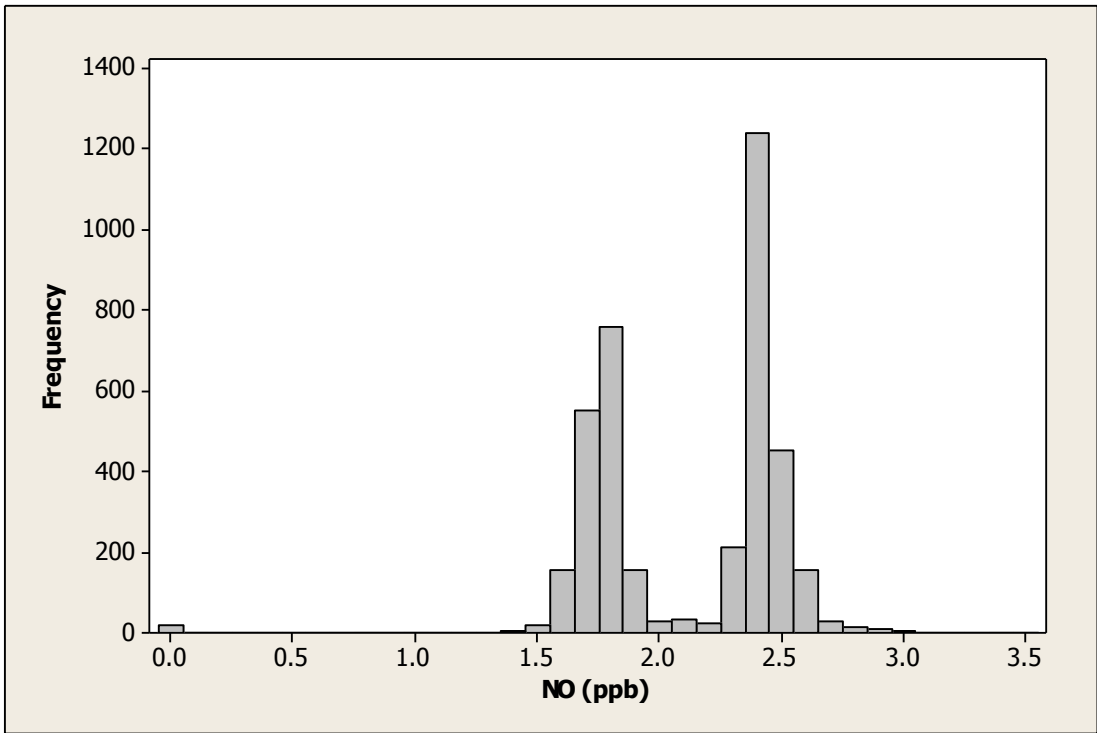

Figure 68. Histogram of NO data.

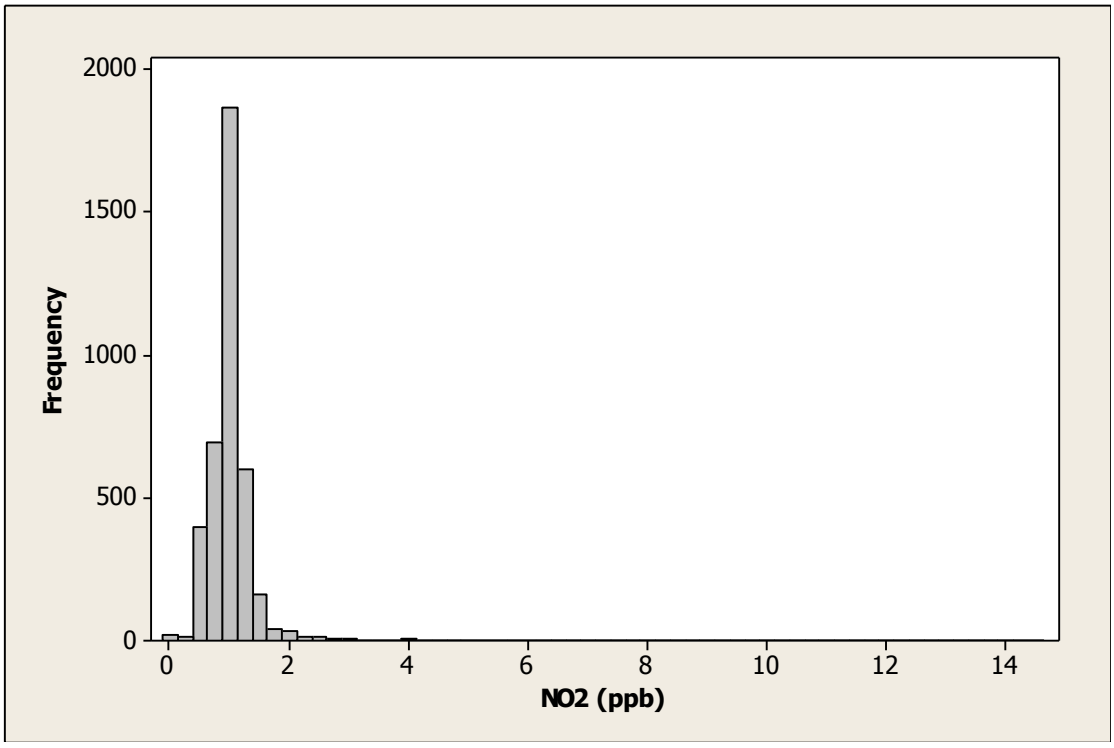

Figure 69. Histogram of NO_2 data.

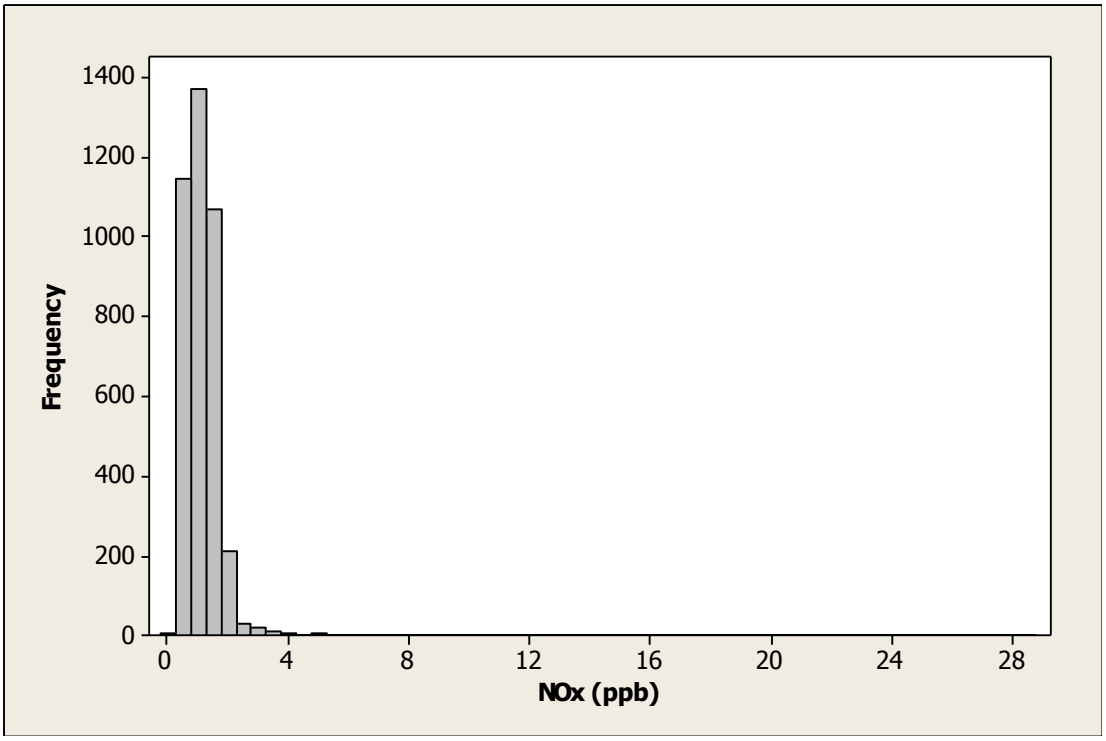

Figure 70. Histogram of NO_x data.

Table 10. Descriptive statistics for hourly wind speed and direction.

	Wind Direction (degrees)	Wind Speed (km/h)
Mean	206.4923	20.16667
Standard Error	1.264784	0.137678
Median	220	19
Mode	230	19
Standard Deviation	84.04869	9.14909
Sample Variance	7064.183	83.70585
Kurtosis	0.015862	0.357089
Skewness	-0.65277	0.484321
Range	360	65
Minimum	0	0
Maximum	360	65

Mann-Whitney Test and CI: NMHC (ppm) before, NMHC (ppm) after

```
                   N   Median
NMHC (ppm)     16132  0.00000
NMHC (ppm) B   27863  0.00000


Point estimate for ETA1-ETA2 is -0.00000
95.0 Percent CI for ETA1-ETA2 is (-0.00000,0.00000)
W = 353937130.5
Test of ETA1 = ETA2 vs ETA1 not = ETA2 is significant at 0.4666
The test is significant at 0.2019 (adjusted for ties)
```

Mann-Whitney Test and CI: BC (µg/m^3) before, BC (µg/m^3) after

```
                    N   Median
BC (ug/m^3)     18589  0.06667
BC (ug/m^3) B   26455  0.04000


Point estimate for ETA1-ETA2 is 0.02167
95.0 Percent CI for ETA1-ETA2 is (0.02000,0.02333)
W = 475943105.0
Test of ETA1 = ETA2 vs ETA1 not = ETA2 is significant at 0.0000
The test is significant at 0.0000 (adjusted for ties)
```

Mann-Whitney Test and CI: $PM_{2.5}$ (µg/m^3) before, $PM_{2.5}$ (µg/m^3) after

```
                     N  Median
PM25_BAM_ugm3     1447  15.000
PM25_BAM_ugm3 B   2040  12.000


Point estimate for ETA1-ETA2 is 3.000
95.0 Percent CI for ETA1-ETA2 is (3.000,3.000)
W = 2992113.0
Test of ETA1 = ETA2 vs ETA1 not = ETA2 is significant at 0.0000
The test is significant at 0.0000 (adjusted for ties)
```

Mann-Whitney Test and CI: SO_2 (ppb) before, SO_2 (ppb) after

```
               N   Median
SO2_ppb     1454  0.10000
SO2_ppb B   2166  0.30000


Point estimate for ETA1-ETA2 is -0.20000
95.0 Percent CI for ETA1-ETA2 is (-0.20000,-0.20000)
W = 1699725.0
Test of ETA1 = ETA2 vs ETA1 not = ETA2 is significant at 0.0000
The test is significant at 0.0000 (adjusted for ties)
```

Mann-Whitney Test and CI: H_2S (ppb) before, H_2S (ppb) after

```
              N   Median
H2S_ppb    1364  0.10000
H2S_ppb B  1611  0.30000


Point estimate for ETA1-ETA2 is -0.20000
95.0 Percent CI for ETA1-ETA2 is (-0.20000,-0.20002)
W = 1586194.5
Test of ETA1 = ETA2 vs ETA1 not = ETA2 is significant at 0.0000
The test is significant at 0.0000 (adjusted for ties)
```

Mann-Whitney Test and CI: O_3 (ppb) before, O3 (ppb) after

```
             N  Median
O3_ppb    1444  29.500
O3_ppb B  2382  30.700


Point estimate for ETA1-ETA2 is -1.300
95.0 Percent CI for ETA1-ETA2 is (-1.800,-0.800)
W = 2597490.5
Test of ETA1 = ETA2 vs ETA1 not = ETA2 is significant at 0.0000
The test is significant at 0.0000 (adjusted for ties)
```

Mann-Whitney Test and CI: NO (ppb) before, NO (ppb) after

```
                       N  Median
NO_corrected_ppb    1470  2.4000
NO_corrected_ppb B  2404  1.8000


Point estimate for ETA1-ETA2 is 0.5000
95.0 Percent CI for ETA1-ETA2 is (0.5000,0.5000)
W = 3398119.5
Test of ETA1 = ETA2 vs ETA1 not = ETA2 is significant at 0.0000
The test is significant at 0.0000 (adjusted for ties)
```

Mann-Whitney Test and CI: NO_x (ppb) before, NO_x (ppb) after

```
                        N  Median
Nox_corrected_ppb    1470  1.1000
Nox_corrected_ppb B  2404  0.8000


Point estimate for ETA1-ETA2 is 0.2000
95.0 Percent CI for ETA1-ETA2 is (0.2000,0.2000)
W = 3215649.5
Test of ETA1 = ETA2 vs ETA1 not = ETA2 is significant at 0.0000
The test is significant at 0.0000 (adjusted for ties)
```

Mann-Whitney Test and CI: NO_2 (ppb) before, NO_2 (ppb) after

```
                         N  Median
NO2_corrected_ppb     1470  0.8000
NO2_corrected_ppb B   2404  1.0000


Point estimate for ETA1-ETA2 is -0.2000
95.0 Percent CI for ETA1-ETA2 is (-0.2000,-0.2000)
W = 2031513.0
Test of ETA1 = ETA2 vs ETA1 not = ETA2 is significant at 0.0000
The test is significant at 0.0000 (adjusted for ties)
```

Figure 71. Mann-Whitney statistical results comparing before and after July 22nd 2013.

Spearman Rank Order Correlation Tuesday, December 03, 2013, 11:03:37 AM

Data source: Data 1 in Sable data April to October Spearman Correlation

Cell Contents:
Correlation Coefficient
P Value
Number of Samples

	BC (ug/m^3)	**PM25 BAM (ug/m^3)**	**SO2 (ppb)**	**H2S (ppb)**
NMHC (ppm)	0.00804 0.105 40734	0.0894 0.00000109 2969	-0.146 4.441E-016 3090	0.107 0.0000000446 2598
BC (ug/m^3)		0.445 0.000000200 3064	0.0318 0.0727 3184	-0.132 9.748E-012 2646
PM25 BAM (ug/m^3)			0.0760 0.00000917 3398	-0.170 0.000000200 2900
SO2 (ppb)				0.477 0.000000200 2967
H2S (ppb)				
O3 (ppb)				
NO corrected (ppb)				
NOx corrected (ppb)				
NO2 corrected (ppb)				

	O3 (ppb)	**NO corrected (ppb)**	**NOx corrected (ppb)**	**NO2 corrected (ppb)**
NMHC (ppm)	0.139 1.332E-015 3294	0.163 0.000000200 3311	0.141 4.441E-016 3293	0.0128 0.461 3311

BC (ug/m^3)	0.211	-0.0791	0.0796	0.186
	0.000000200	0.00000410	0.00000367	0.000000200
	3374	3387	3373	3387
PM25 BAM (ug/m^3)	0.119	-0.189	-0.102	-0.0330
	2.791E-012	0.000000200	0.00000000183	0.0521
	3441	3460	3442	3458
SO2 (ppb)	0.0781	-0.696	-0.558	0.157
	0.00000273	0.000000200	0.000000200	0.000000200
	3597	3609	3592	3608
H2S (ppb)	0.283	-0.212	-0.209	0.0366
	0.000000200	0.000000200	0.000000200	0.0458
	2964	2971	2954	2970
O3 (ppb)		0.0137	-0.0448	-0.0588
		0.397	0.00568	0.000278
		3819	3802	3818
NO corrected (ppb)			0.821	0.0934
			0.000000200	0.00000000683
			3824	3840
NOx corrected (ppb)				0.529
				0.000000200
				3825
NO2 corrected (ppb)				

The pair(s) of variables with positive correlation coefficients and P values below 0.050 tend to increase together. For the pairs with negative correlation coefficients and P values below 0.050, one variable tends to decrease while the other increases. For pairs with P values greater than 0.050, there is no significant relationship between the two variables.

Figure 72. Spearman Rank Order Correlation between species.

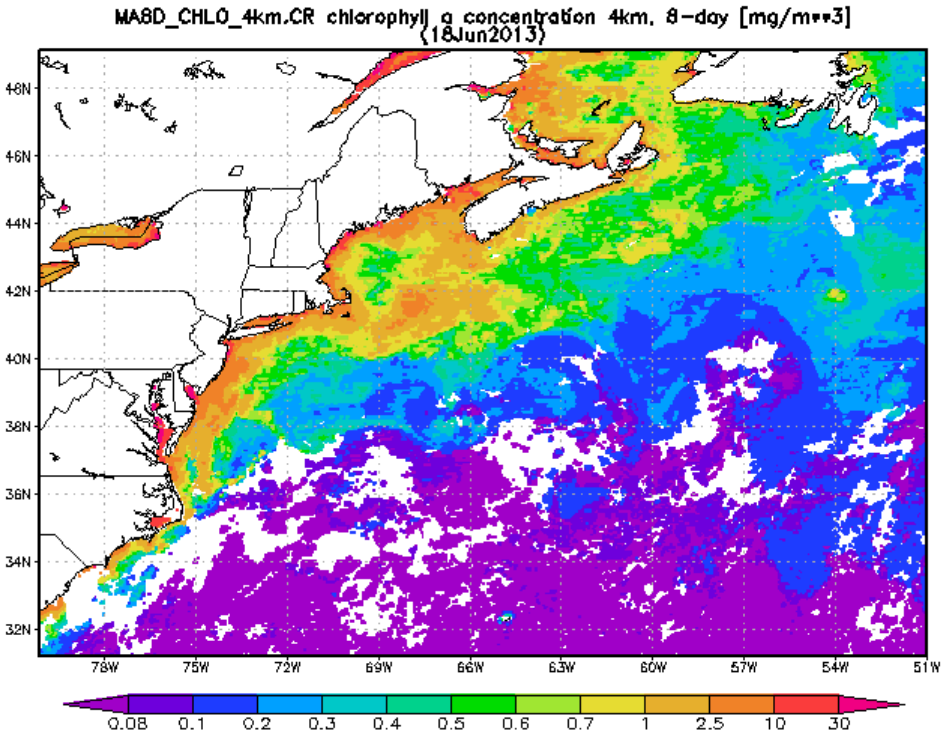

Figure 73. 8-day composite of Chlorophyll concentrations for June 18th obtained from the NASA Giovanni website.

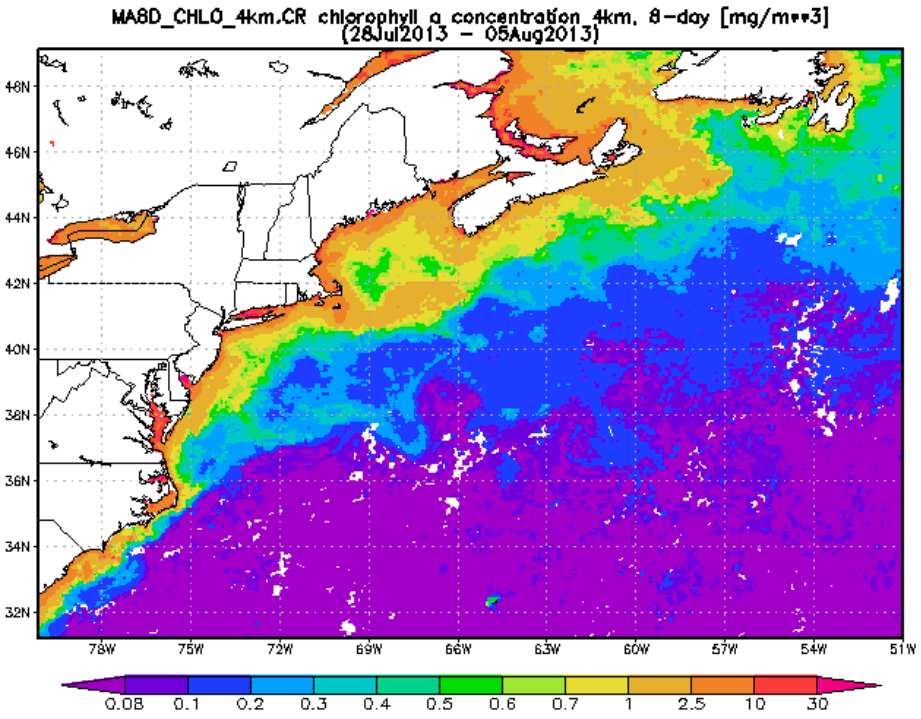

Figure 74. 8-day composite of Chlorophyll concentrations for July 28th – August 5th obtained from the NASA Giovanni website.

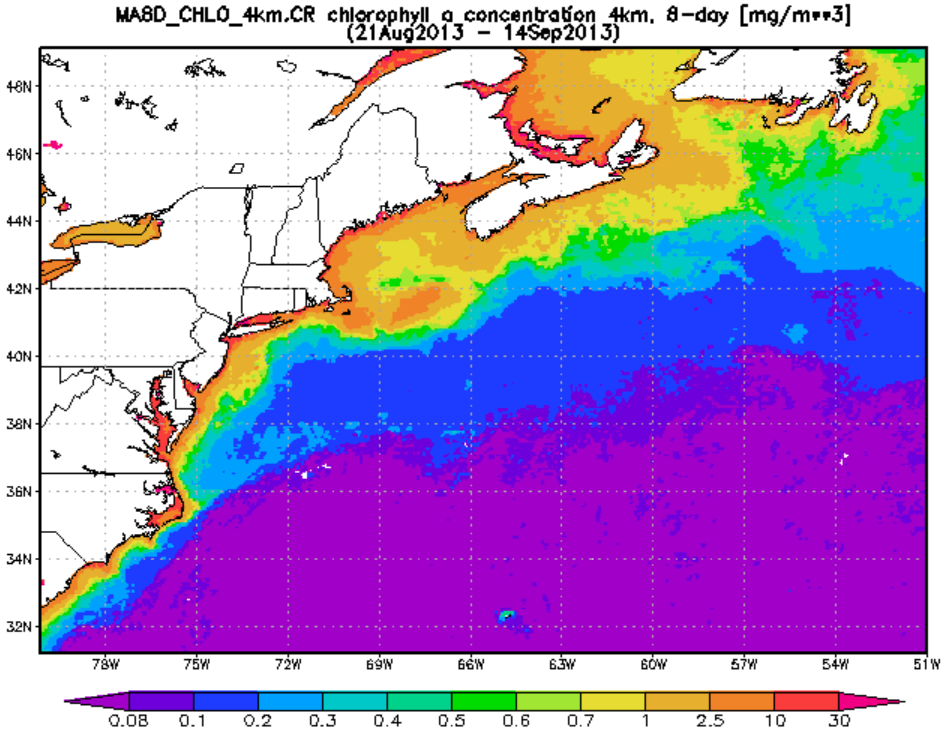

Figure 75. 8-day composite of Chlorophyll concentrations for August 21st – September 14th obtained from the NASA Giovanni website.

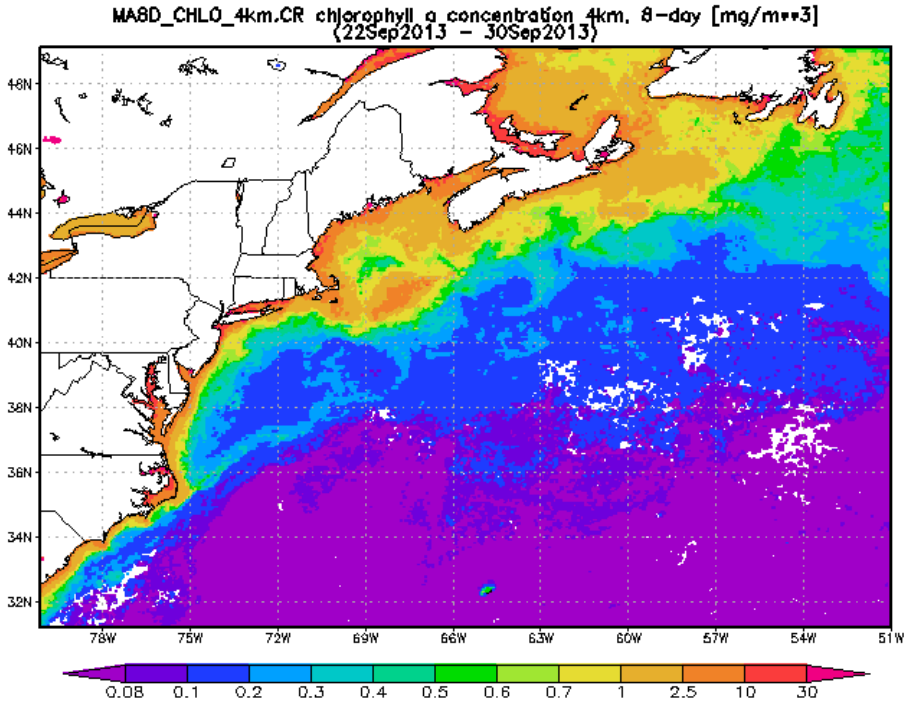

Figure 76. 8-day composite of Chlorophyll concentrations for September 22nd – September 30th obtained from the NASA Giovanni website.

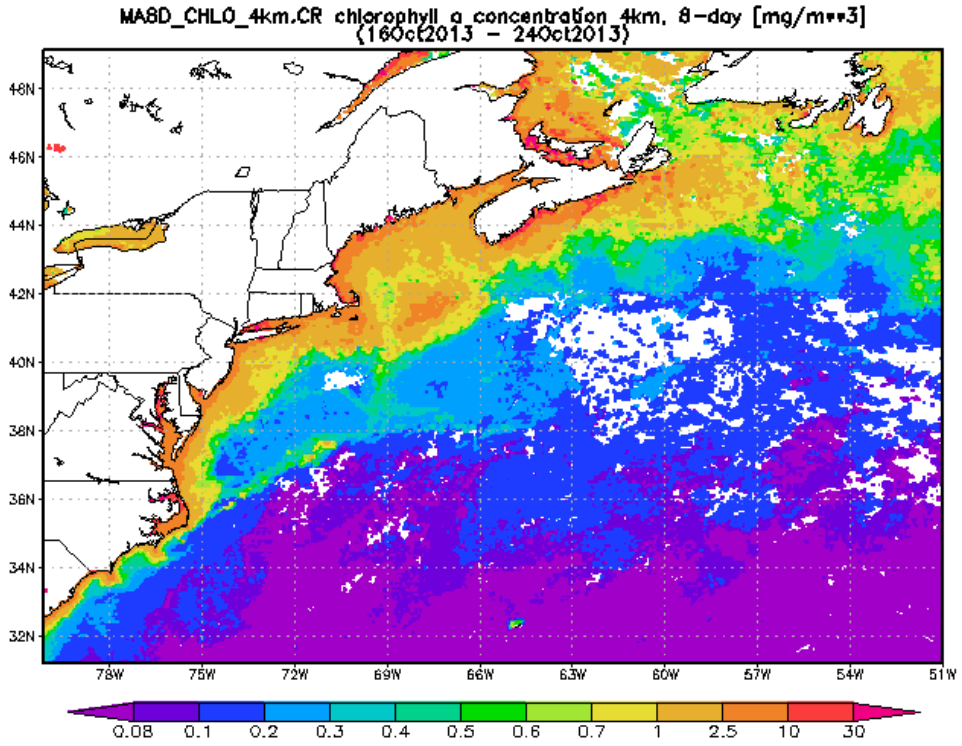

Figure 77. 8-day composite of Chlorophyll concentrations for October 16th – October 24th obtained from the NASA Giovanni website.

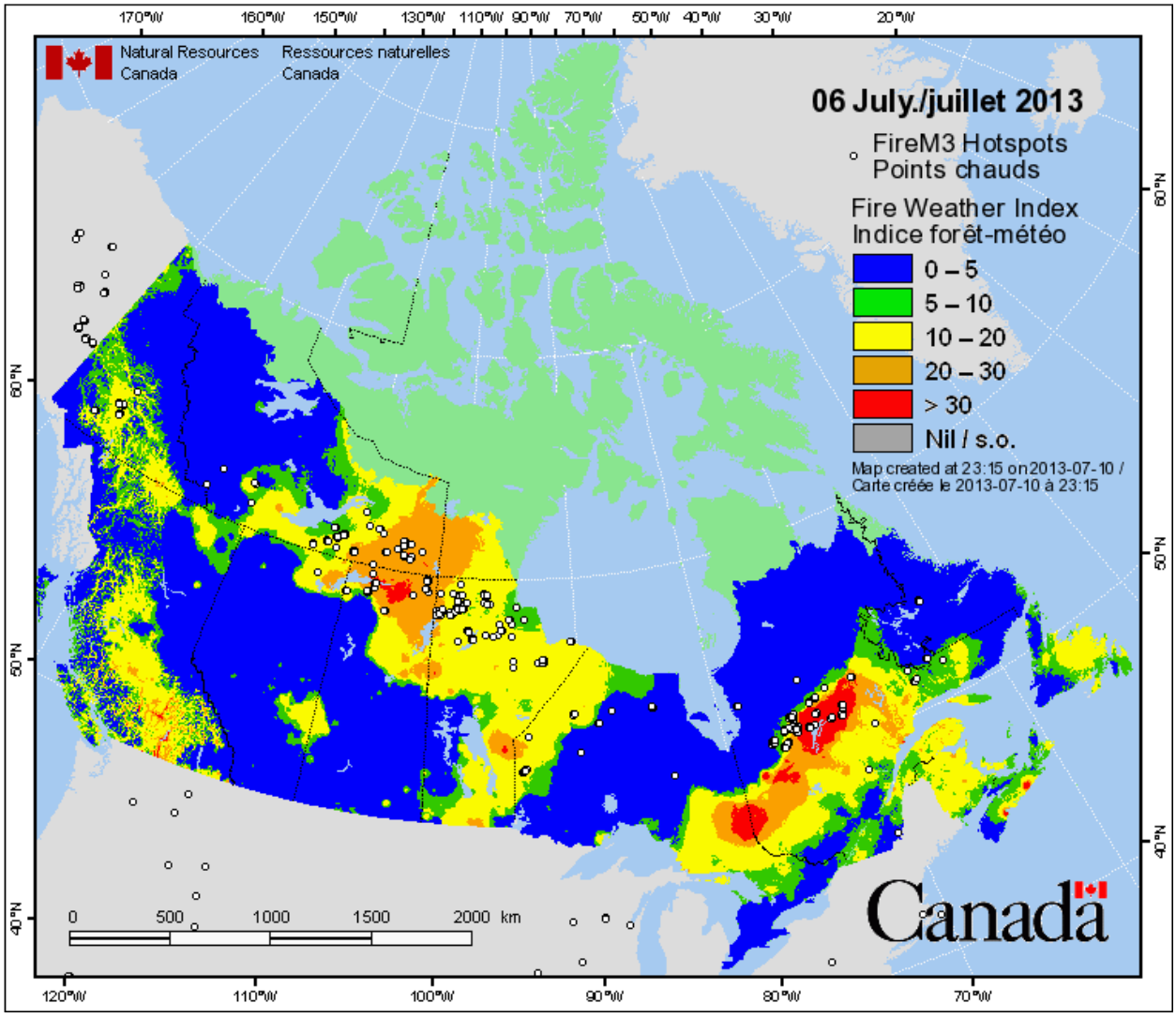

Figure 78. Fire hotspots for July 6th obtained from the Canadian Wildland Fire Information System.

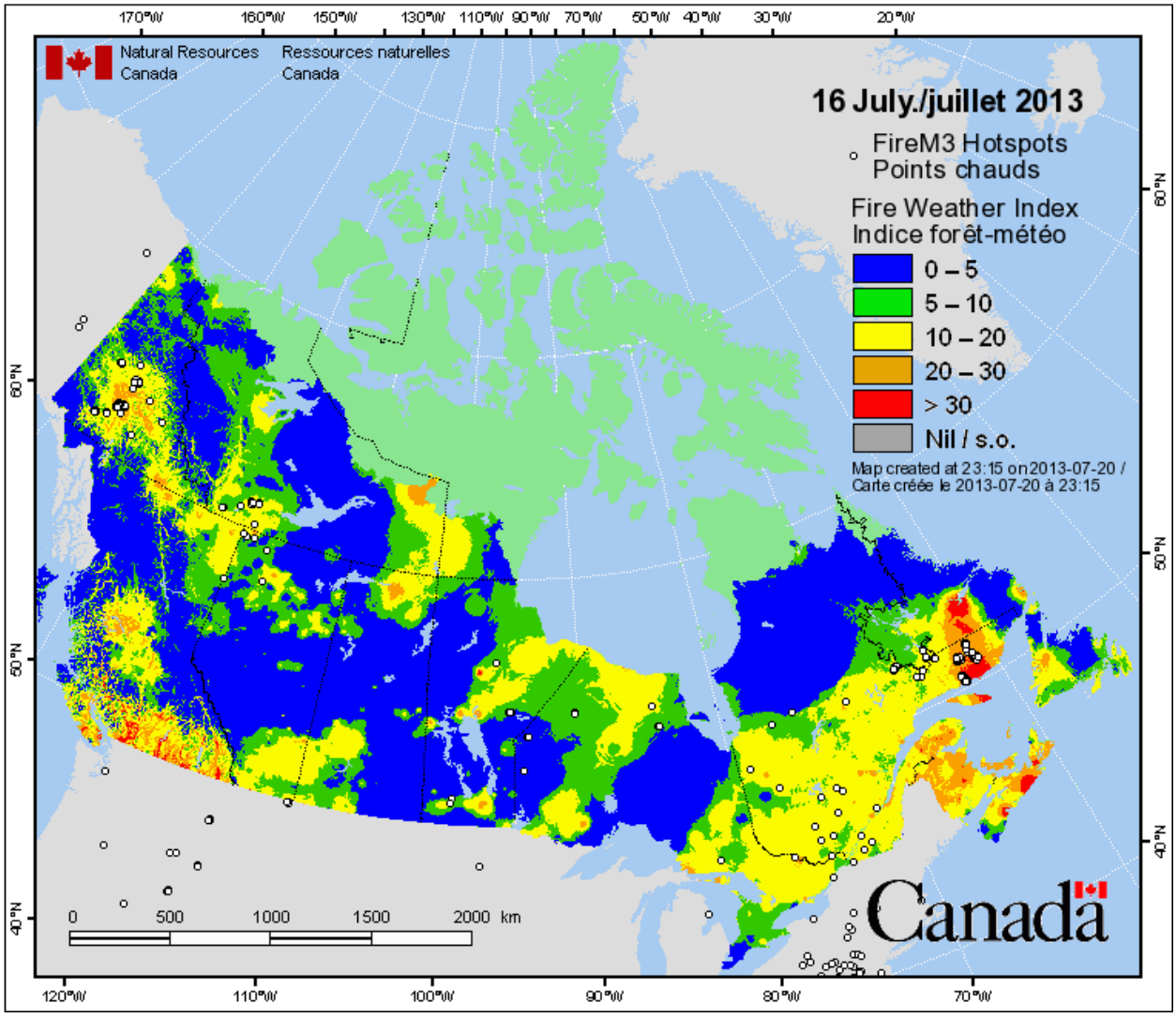

Figure 79. Fire hotspots for July 16th obtained from the Canadian Wildland Fire Information System.

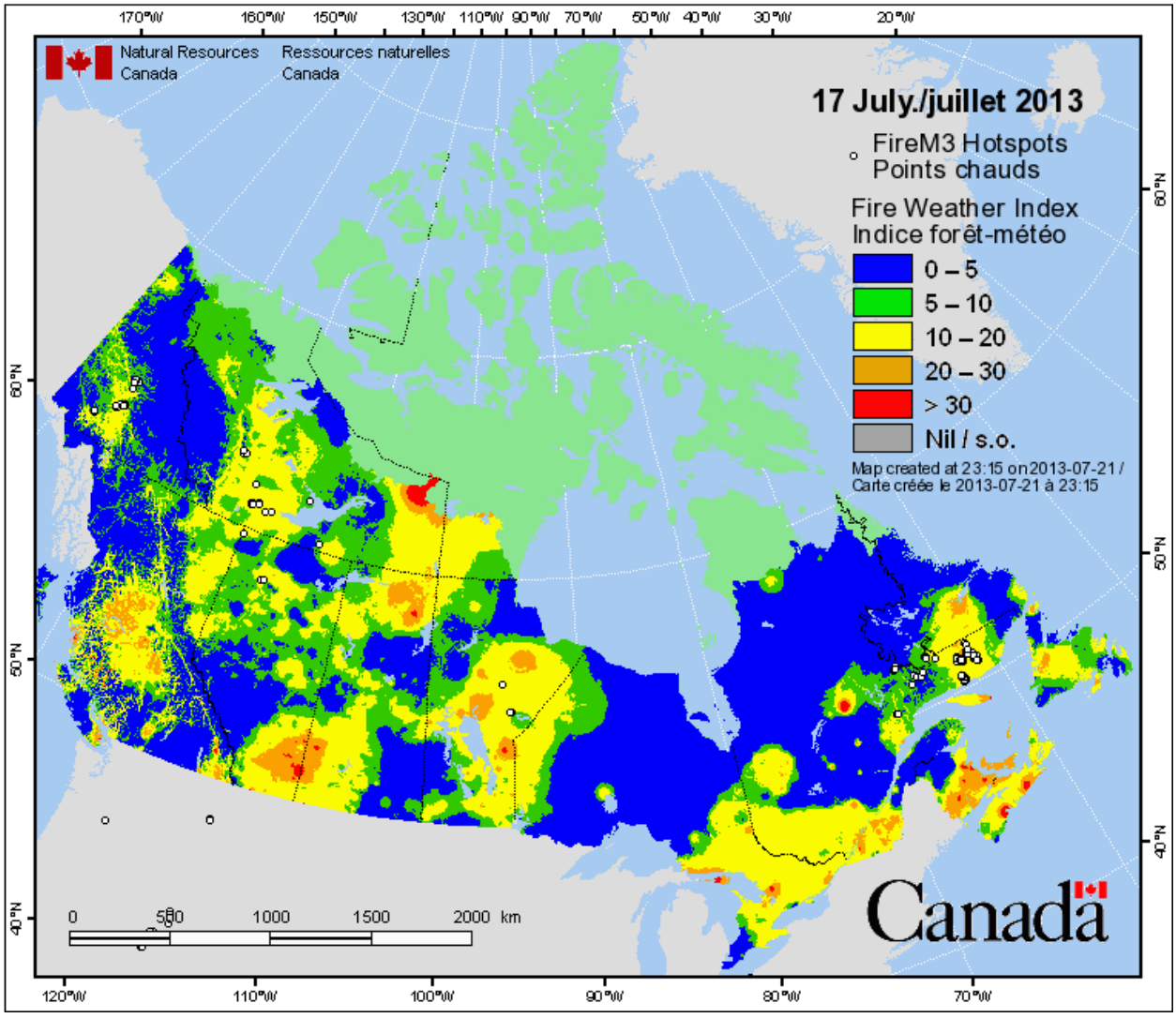

Figure 80. Fire hotspots for July 17th obtained from the Canadian Wildland Fire Information System.

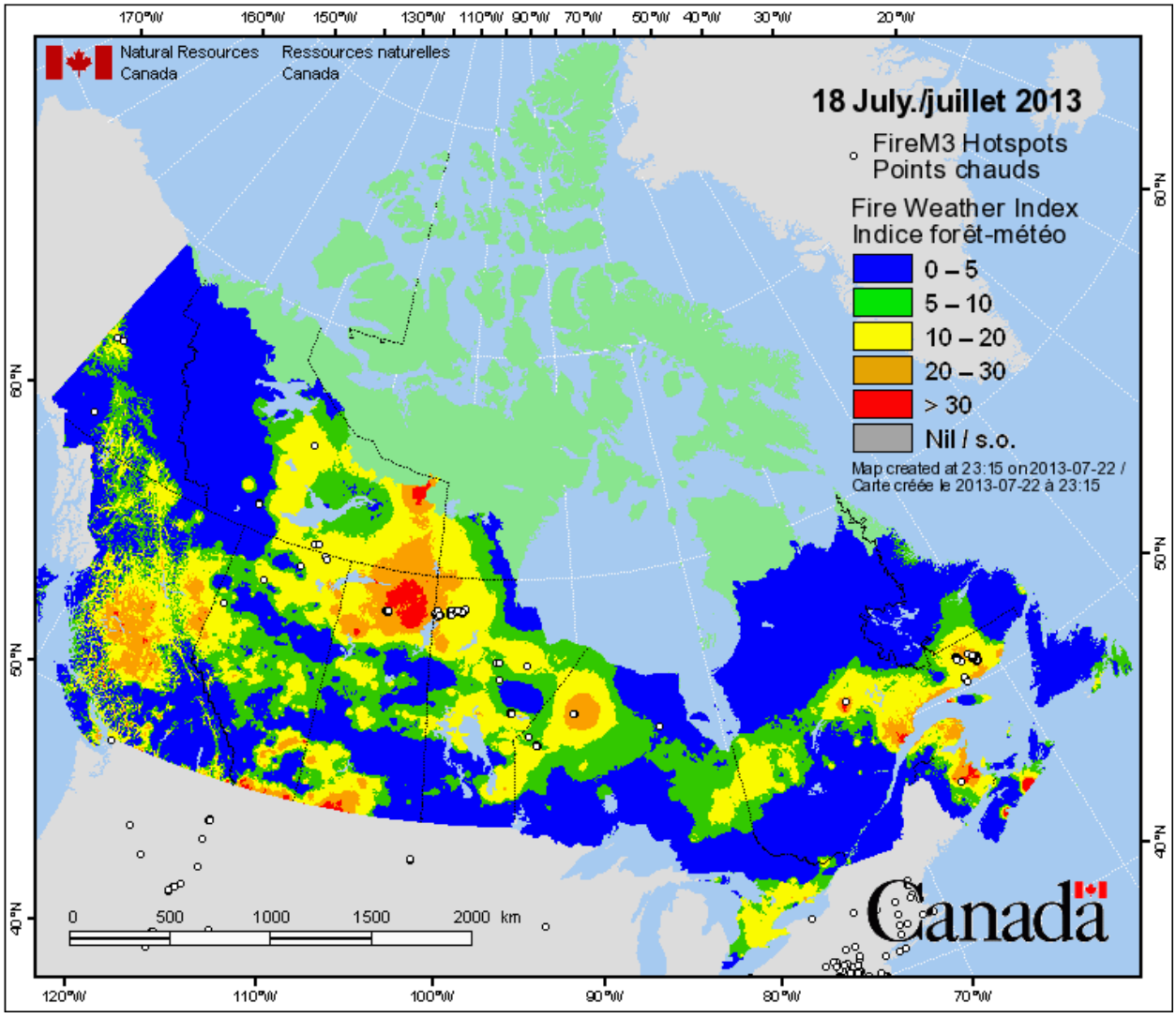

Figure 81. Fire hotspots for July 18th obtained from the Canadian Wildland Fire Information System.

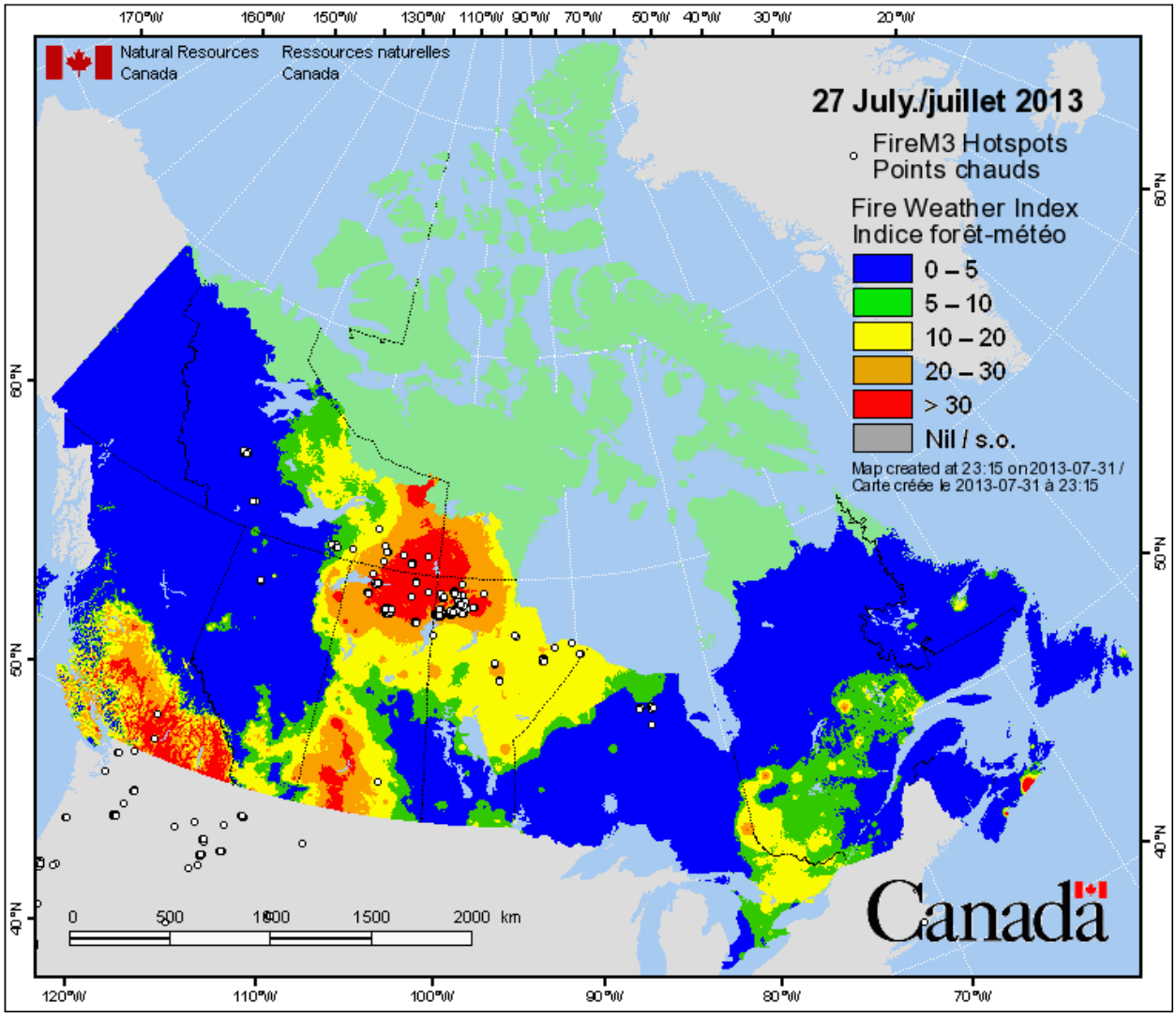

Figure 82. Fire hotspots for July 27th obtained from the Canadian Wildland Fire Information System.

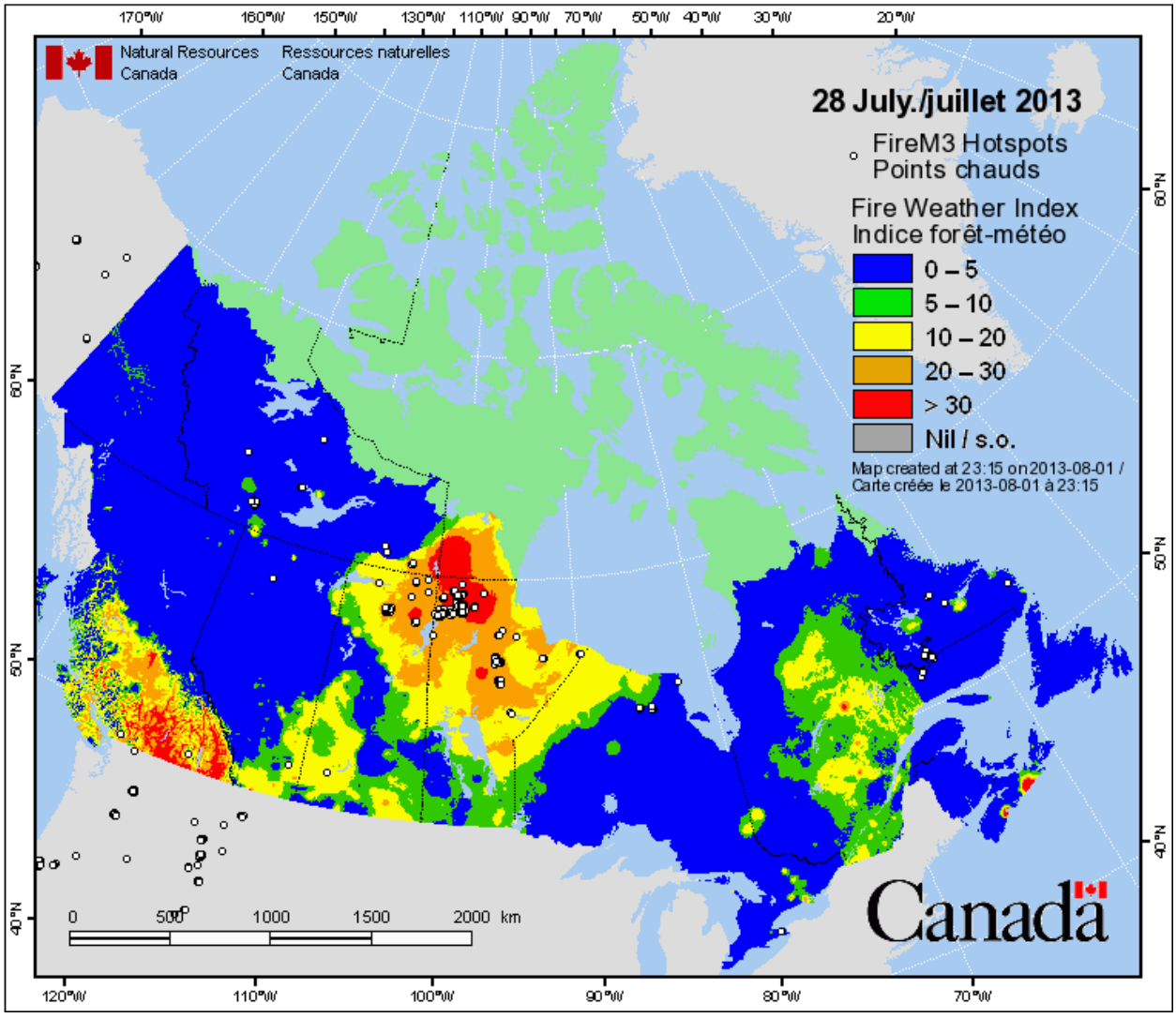

Figure 83. Fire hotspots for July 28th obtained from the Canadian Wildland Fire Information System.

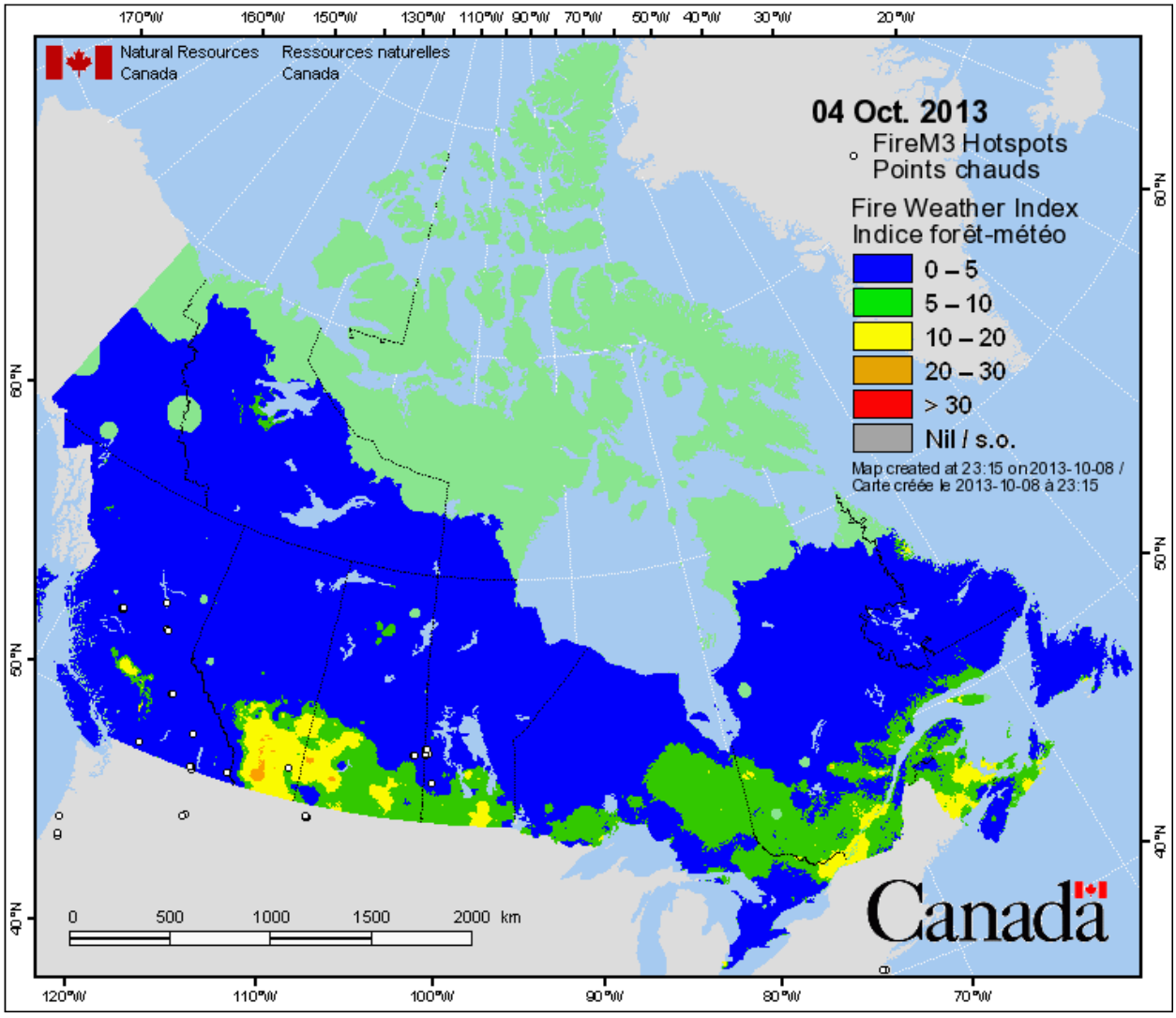

Figure 84. Fire hotspots for October 4th obtained from the Canadian Wildland Fire Information System.

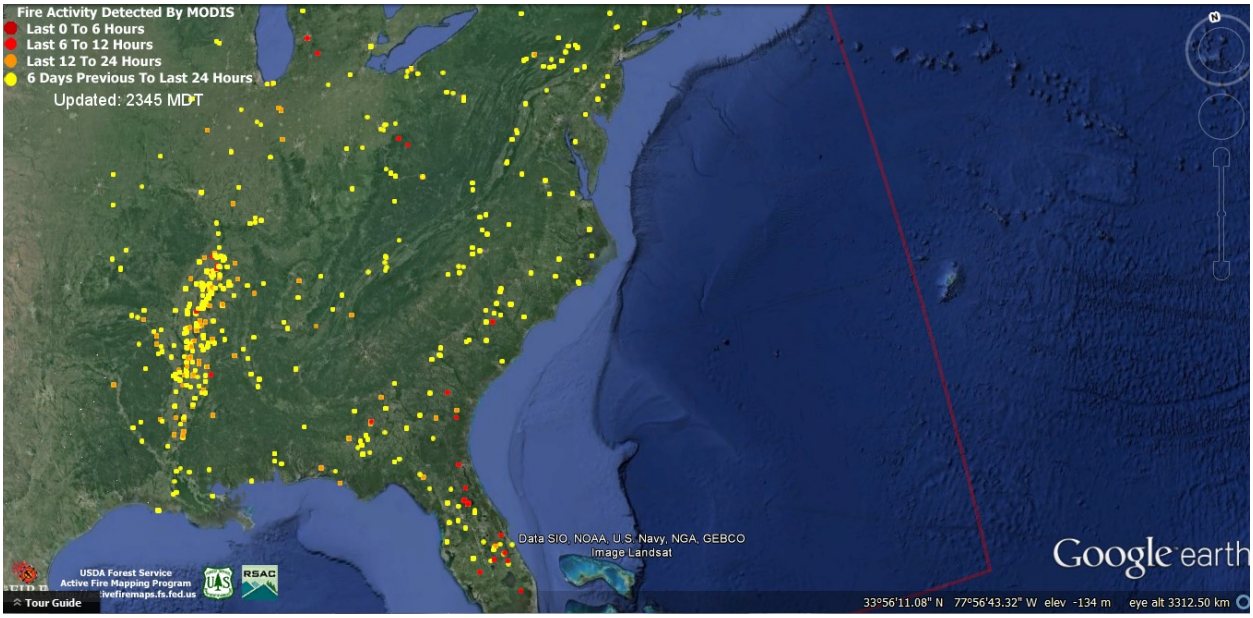

Figure 85. Fire activity detected by the MODIS satellite for June 24th as obtained from the USDA Active Fire Mapping Program.

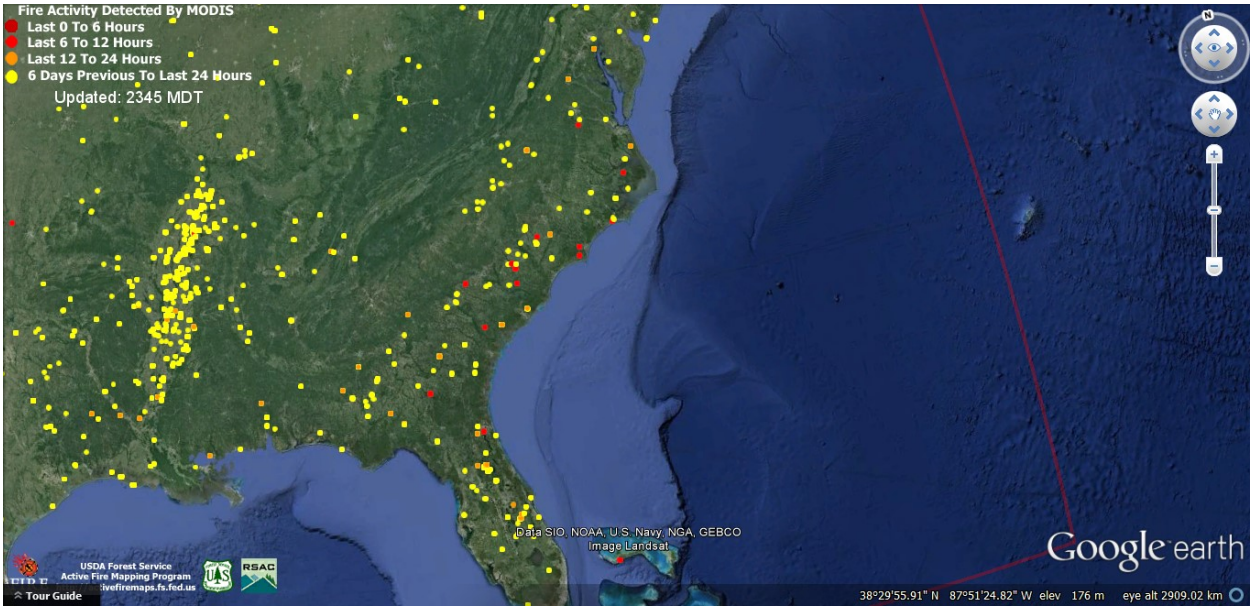

Figure 86. Fire activity detected by the MODIS satellite for June 26th as obtained from the USDA Active Fire Mapping Program.

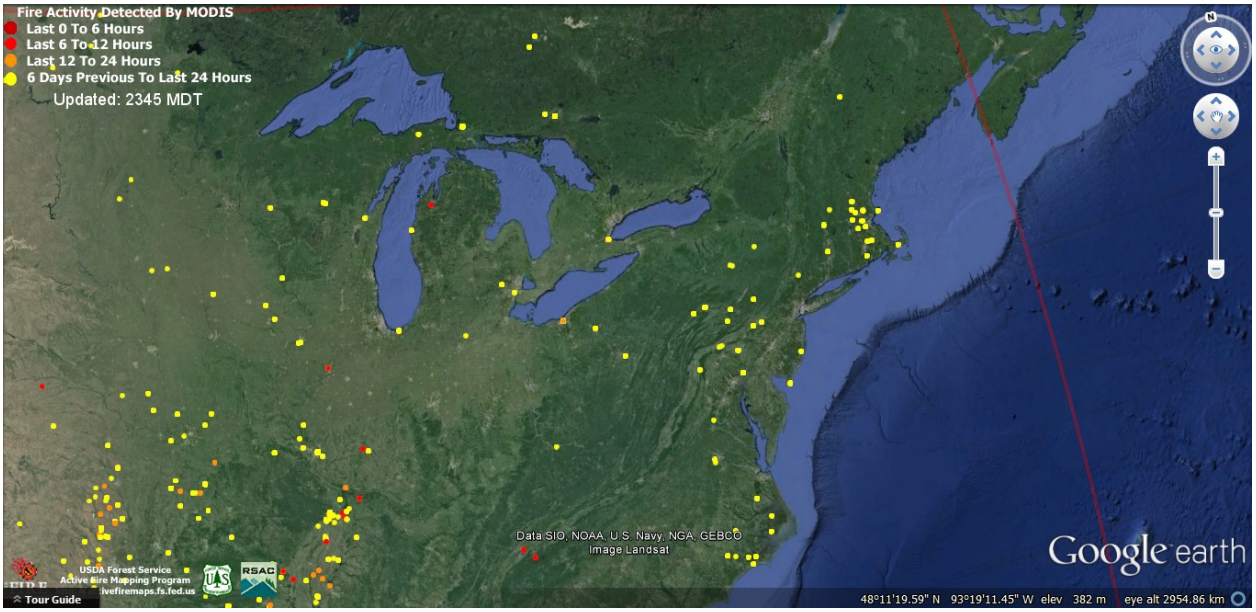

Figure 87. Fire activity detected by the MODIS satellite for July 8th as obtained from the USDA Active Fire Mapping Program.

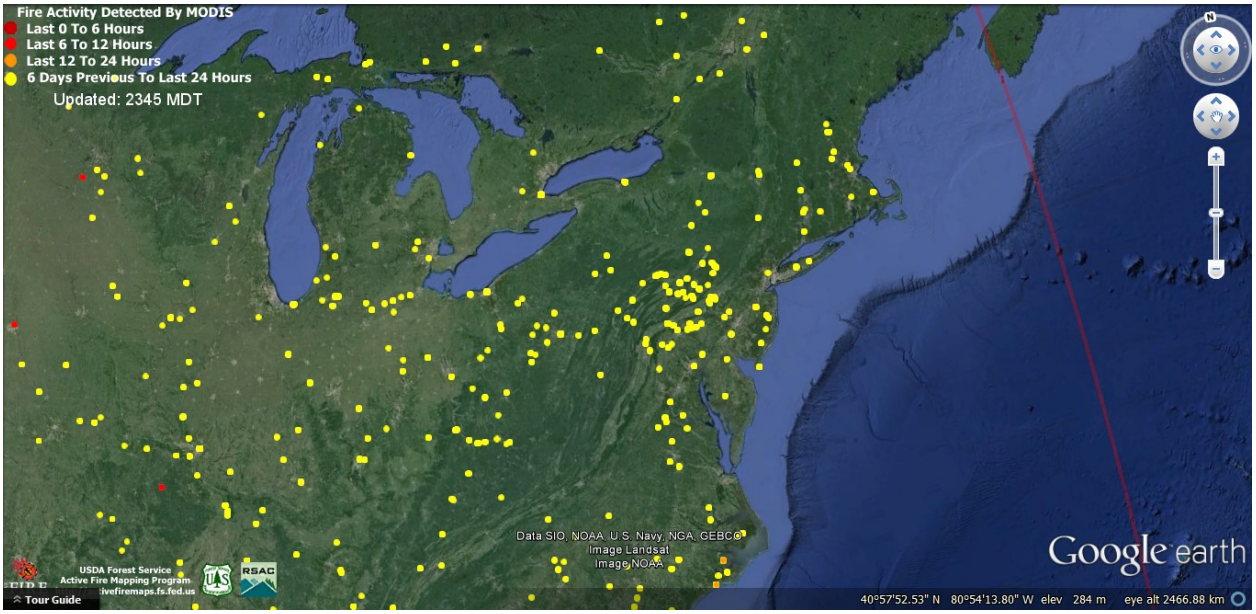

Figure 88. Fire activity detected by the MODIS satellite for July 20th as obtained from the USDA Active Fire Mapping Program.

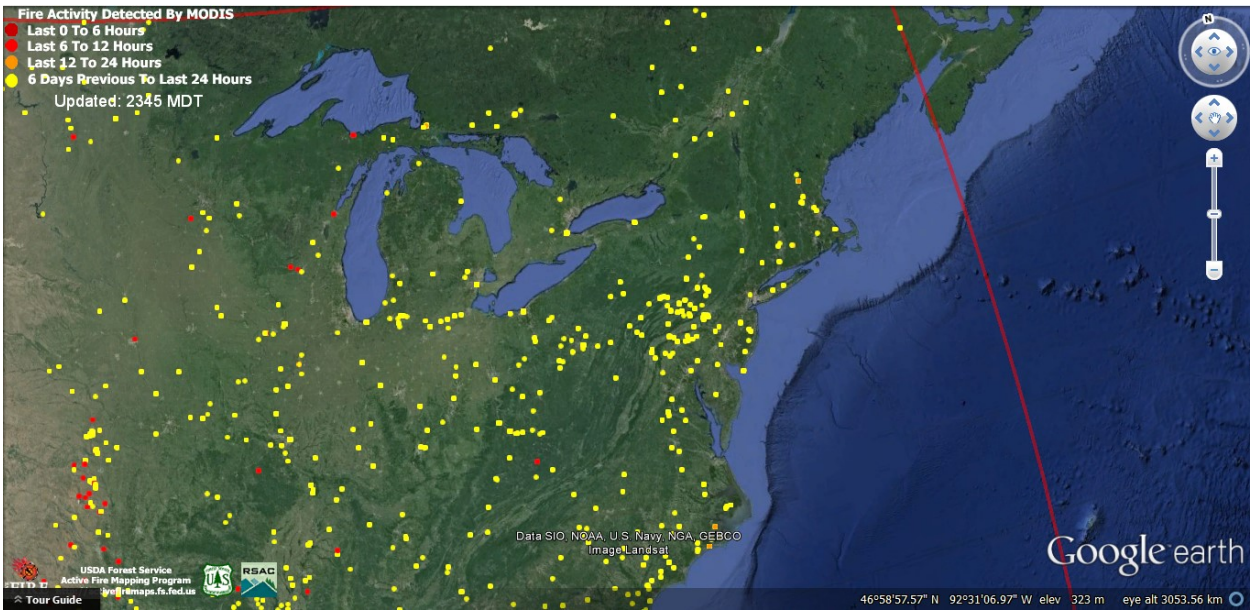

Figure 89. Fire activity detected by the MODIS satellite for August 16th as obtained from the USDA Active Fire Mapping Program.

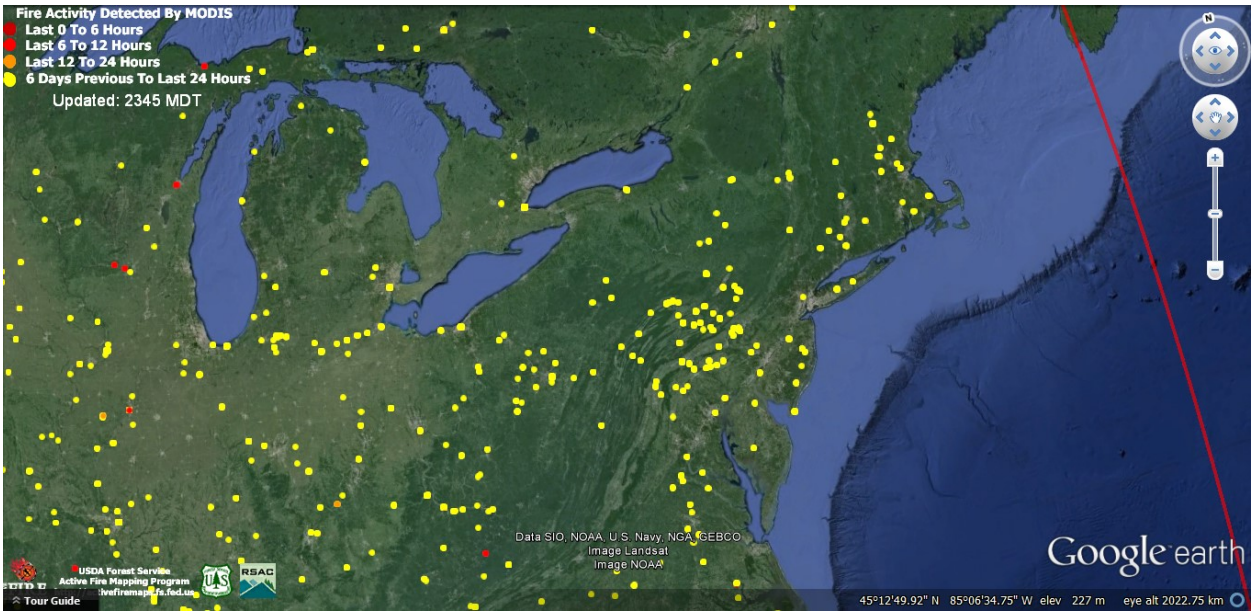

Figure 90. Fire activity detected by the MODIS satellite for August 31st as obtained from the USDA Active Fire Mapping Program.

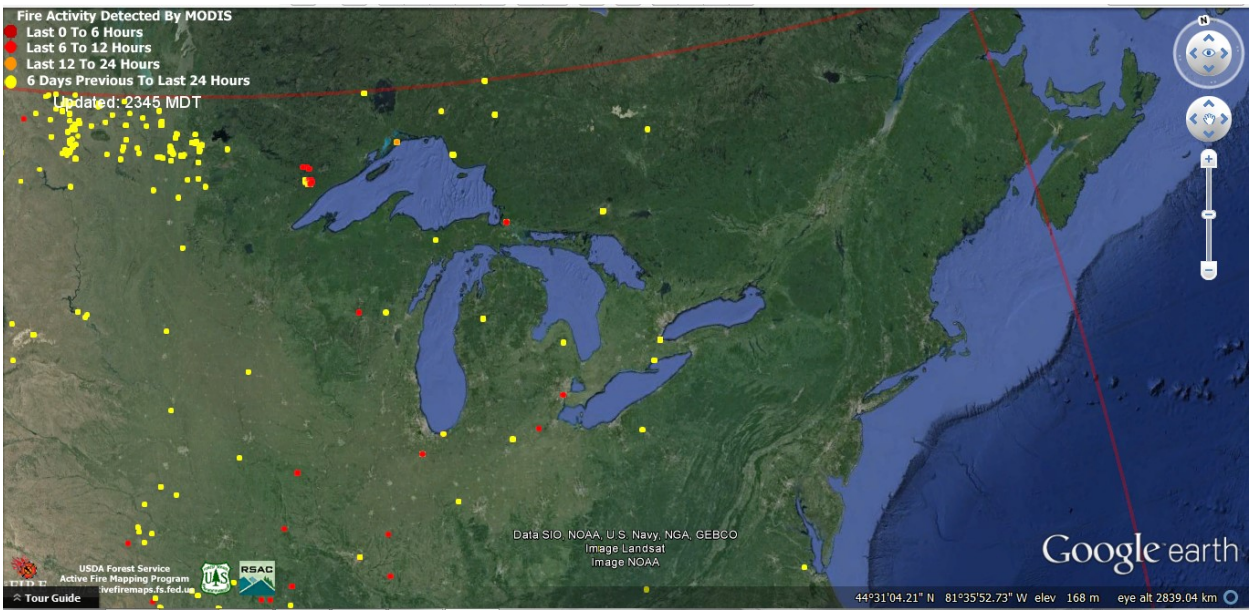

Figure 91. Fire activity detected by the MODIS satellite for September 12th as obtained from the USDA Active Fire Mapping Program.